Title
Feeding state sculpts a circuit for sensory valence

Author
Rengarajan, Sophie

Publication Date
2017

Peer reviewed|Thesis/dissertation

UNIVERSITY OF CALIFORNIA

Los Angeles

Feeding state sculpts a circuit for sensory valence

A dissertation submitted in partial satisfaction

of the requirements for the degree of Doctor of Philosophy

in Neuroscience

by

Sophie Rengarajan

2017

ABSTRACT OF THE DISSERTATION

Feeding state sculpts a circuit for sensory valence

by

Sophie Rengarajan

Doctor of Philosophy in Neuroscience

University of California, Los Angeles

Professor Elissa A. Hallem, Chair

The valence of sensory stimuli (i.e. a measure of attractiveness or aversiveness that an animal attaches to a stimulus) is flexible and determined by a combination of factors including environment, behavioral state, and experience. Together, these factors prime the nervous system in order to drive appropriate behaviors. In this dissertation I investigate how environmental context and behavioral state regulate the valence of the chemosensory cue carbon dioxide (CO_2) in the free-living nematode *Caenorhabditis elegans*. CO_2 can signify the presence of food, conspecifics, and predators. When raised in standard laboratory conditions *C. elegans* avoids CO_2, but this response is flexible. Whereas oxygen, salt, and food all promote CO_2 avoidance, food-deprivation shifts CO_2-response valence from avoidance to attraction. We have identified two sets of neurons, RIG and AIY, that contribute to the starvation-dependent shift. We have demonstrated that dopamine signaling enhances the CO_2-evoked responses in both of these neurons in order to drive avoidance in fed worms. All animals must make ecologically relevant decisions to survive, and our results provide fundamental insights into how neural circuits are dynamically sculpted by internal state and context to drive behavior.

The dissertation of Sophie Rengarajan is approved

David E Krantz

Alison Renee Frand

Kelsey C. Martin

Stephen Lawrence Zipursky

Elissa A Hallem, Committee Chair

University of California, Los Angeles

2017

to my parents for their endless encouragement and unwavering confidence

தாயும் தகப்பனும் தவிர சகலமும் வாங்கலாம்

TABLE OF CONTENTS

LIST OF FIGURES

Chapter 1:

Chapter 2:

Chapter 3:

LIST OF TABLES

Chapter 1

Chapter 3

ACKNOWLEDGEMENTS

First and foremost, thank you to my advisor, Professor Elissa Hallem. By far, my favorite part of graduate school has been meetings with you where we come up with exciting new theories together to explain our results and devise new experiments. These theories change on a pretty rapid timescale, but what remains constant is your enthusiasm and passion for science. I always leave our meetings feeling delighted and eager to do experiments. You are a role model for me on both academic and personal levels, and I am very grateful that I have had the privilege of training with you.

I would also like to acknowledge members of my lab who made valuable contributions to the work in this thesis: Wendy Fung, Manon Guillermin, Mayra Carrillo and Kristen Yankura, and Ryo Okubo. Thanks to Tiffany Mao for making many types of media for me that rapidly enabled our salt-context studies. Finally, thanks to the rest of the Hallem Lab for insights, concerted April Fools' jokes, and a plethora of gluten-free snacks.

Thank you to my incredible committee: Professors Larry Zipursky, Kelsey Martin, David Krantz and Alison Frand. Thank you for your feedback and for advising me at many points over the past few years. I have been extremely fortunate to have such an intelligent and inspirational group of people so invested in my training, and I really appreciate your help.

Thank you to the UCLA-Caltech Medical Scientist Training Program, especially to the directors, Professors Carlos Portera-Cailliau and Leanne Jones, and to Josie Alviar, Susie Esquivel and Judy Cervantes. Thanks also to the Neuroscience Interdepartmental Program and especially to Professor Felix Schweizer and Jenny Lee for supporting my graduate training.

It has also been a great privilege to be supported by the Neural Microcircuits Training Grant, which not only provided financial support but also expanded my knowledge of neural microcircuits and helped me broaden my results to higher-level systems in neuroscience. Thanks especially to Jack Feldman, who has been a great mentor. Thank you also to the NIH for supporting me financially with a predoctoral training grant from the NIGMS, and to Lana Song and Chenda Seng for managing this grant.

Finally, I would like to acknowledge my friends and family. I am so grateful that I had the opportunity to train with such incredibly intelligent and compassionate people throughout college, medical school and graduate school. Many of you have become family, and I'm excited for us to train together in the future. And last but certainly not least, thank you to my family, a group of extraordinarily hard-working, passionate, and bright people. Reese, Mom, Dad and Michelle: I am continually amazed and inspired by all of you. Thank you for constantly encouraging me. I wouldn't be here if it weren't for you.

Chapter 1 is a version of: Rengarajan S. and Hallem E.A. (2016) Olfactory circuits and behaviors of nematodes. *Curr Opin Neurobiol* 41:136-148. It was part of a special issue on "Microcircuit computation and evolution.," and was written by Elissa Hallem and me.

Chapter 2 is a version of: Carrillo M.A., Guillermin M.L., Rengarajan S., Okubo R.P., and Hallem E. A. (2013) O_2-sensing neurons control CO_2 response in *C. elegans*. *J Neurosci* 33, 9675–9683. I contributed to this project by performing *npr-1* rescue studies and laser ablation experiments. Based on these results, I formulated an initial

hypothesis that the neuropeptide receptor NPR-1 acts in the oxygen-sensing URX neurons and limits the URX-mediated suppression of CO_2 avoidance. Graduate students Mayra Carrillo and Manon Guillermin and technician Ryo Okubo followed up on these results and explored the role of oxygen environment on CO_2 response to complete the study.

Chapter 3 is a draft of a manuscript for submission to be entitled, “Feeding state sculpts a circuit for sensory valence.” I wrote this draft with feedback from Professor Elissa Hallem. Elissa Hallem and I designed the study, and analyzed and interpreted experiments. I performed all types of experiments. Wendy Fung performed behavioral experiments. Manon Guillermin generated interneuron ablation strains and made findings (in submission) that influenced our work. Kristen Yankura made findings (in preparation) that influenced our work.

VITA

Education:

M.D. in Medicine, University of California Los Angeles, Los Angeles, CA (2011-present)

Ph.D. in Neuroscience, University of California Los Angeles, Los Angeles, CA (2011-present)

A.B. in Neurobiology Cum Laude, Harvard University, Cambridge, MA (2006-2010)

Academic Honors and Awards:

2015-present	NIH NIGMS F30 Individual Predoctoral Training Grant (F30GM116810)
2014-2015	NIH NINDS T32 Neural Microcircuits Training Grant (T32NS058280)
2010	High Honors in Neurobiology, Harvard College
2009	Mary Gordon Roberts Summer Mind, Brain and Behavior Fellowship
2008-2010	Harvard Allston Science Mentor Award
2008	Herchel Smith Fellowship
2008	Program in Research in Science and Engineering Fellow
2007	Caltech Summer Undergraduate Research Fellowship
2006	Salutatorian, Westridge School for Girls
2006	Semifinalist, Intel Science Talent Search
2005	Caltech Signature Award
2005	Rensselaer Medal Award

Publications:

Rengarajan S. and Hallem E.A. (2016) Olfactory circuits and behaviors of nematodes. Curr Opin Neurobiol 41:136-148.

Carrillo M.A., Guillermin M.L., Rengarajan S., Okubo R.P., and Hallem E. A. (2013) O_2-sensing neurons control CO_2 response in *C. elegans*. J Neurosci 33, 9675–9683.

Selected presentations:

1. Rengarajan S. Feeding state modulates CO_2 response through dopamine signaling in *C. elegans.* Presented at the UCLA-Caltech Medical Scientist Training Program Annual Research Conference, Los Angeles, CA, September, 2016.

2. Rengarajan S. Dopaminergic modulation of CO_2 response during starvation in *C. elegans.* Presented at the UCLA-Caltech Tutorial Series, Los Angeles, CA, November, 2015.

3. Rengarajan S. Dopaminergic modulation of CO_2 response during starvation in *C. elegans*. Presented at the UCLA Synapse to Circuit Affinity Group, Los Angeles, CA, January, 2015.

4. Rengarajan S, Portugues R, and Engert F. Characterization of the Neuronal Basis of Habituation to Electrical Shocks in Zebrafish Larvae. Presented at the Harvard Undergraduate Research Symposium, Cambridge, MA, November, 2008 [Plenary Speaker].

Chapter 1

Introduction: Olfactory circuits and behaviors of nematodes

Olfactory circuits and behaviors of nematodes

Sophie Rengarajan and Elissa A Hallem

Over one billion people worldwide are infected with parasitic nematodes. Many parasitic nematodes actively search for hosts to infect using volatile chemical cues, so understanding the olfactory signals that drive host seeking may elucidate new pathways for preventing infections. The free-living nematode *Caenorhabditis elegans* is a powerful model for parasitic nematodes: because sensory neuroanatomy is conserved across nematode species, an understanding of the microcircuits that mediate olfaction in *C. elegans* may inform studies of olfaction in parasitic nematodes. Here we review circuit mechanisms that allow *C. elegans* to respond to odorants, gases, and pheromones. We also highlight work on the olfactory behaviors of parasitic nematodes that lays the groundwork for future studies of their olfactory microcircuits.

Address
Department of Microbiology, Immunology, and Molecular Genetics University of California, Los Angeles, Los Angeles, CA 90095, United States

Corresponding author: Hallem, Elissa A (ehallem@ucla.edu)

Current Opinion in Neurobiology 2016, **41**:136–148

This review comes from a themed issue on **Microcircuit computation and evolution**

Edited by **Thomas R Clandinin** and **Eve Marder**

For a complete overview see the Issue and the Editorial

Available online 23rd September 2016

http://dx.doi.org/10.1016/j.conb.2016.09.002

Introduction

Nematodes comprise a large and diverse phylum of roundworms that includes both free-living and parasitic species. Parasitic nematodes of humans, livestock, and plants cause extensive disease and economic loss worldwide. The free-living nematode *C. elegans* has emerged as a model for the study of sensory neurobiology. *C. elegans* offers many advantages as a model system: it has a small and transparent body, making it possible to image neural activity in real time and to use behavior as a readout of circuit function. Its small nervous system consists of 302 neurons in the adult hermaphrodite and 385 in the adult male [1,2]. The connections among these neurons have been mapped, facilitating the identification of functional microcircuits [1,2,3]. Studies of the *C. elegans* connectome have shown that similar connectivity motifs are found in both *C. elegans* and the mammalian cortex [3], suggesting that similar computational units operate across diverse taxa. Recent technical advances have made probing neural circuit function in intact animals feasible with the ability to reversibly manipulate neural activity through genetics, pharmacology, light, and sound [4,5,6,7]. These advances have greatly expanded our knowledge of how olfactory microcircuits drive behavior and how these circuits are contextually modulated.

Different nematode species share conserved positional sensory neuroanatomy [8,9], and thus understanding how *C. elegans* microcircuits generate olfactory behaviors may have direct implications for how analogous microcircuits operate in parasitic nematodes. Although the microcircuits underlying olfactory preferences in parasitic nematodes are poorly understood, recent studies have elucidated the divergent olfactory preferences of different parasitic nematode species. Here we review the olfactory behaviors of free-living and parasitic nematodes, and highlight some of the microcircuit computations underlying olfactory behaviors in *C. elegans*.

Olfaction in *C. elegans*

Olfaction is an important sensory modality for *C. elegans*that enables it to sense food, pathogens, predators, and conspecifics. Proliferating populations of *C. elegans* are found primarily in fallen rotting fruits, where oxygen (O_2) concentrations are low [10]. When environmental conditions are unfavorable or food is scarce, *C. elegans* enters a developmentally arrested, alternative larval stage called the dauer. Dauers disperse into the soil to search for more favorable environments. Dauers are also phoretic, meaning that they associate with insect vectors that can transport them to more favorable environments [10]. These ecological niches inhabited by *C. elegans* inform the olfactory and gas-sensing strategies of the worm. Like other animals, *C. elegans* responds flexibly to odors and gases, modulating its behavior based on both internal and external contexts. The contextual modulation of olfactory behaviors allows worms to make appropriate behavioral decisions in their current environment.

The olfactory circuit of *C. elegans* consists of a small number of highly interconnected neurons, with an average of 3.5 synapses separating sensory neuron input from motor neuron output [2,3,11••]. Using this circuit, *C. elegans* can sense and respond to at least 50 odorants [12]. *C. elegans* expands its coding capacity through dynamic modulation of neurons and microcircuits, including the use of neuromodulators and neuropeptides to create extrasynaptic functional connections between neurons [13]. The computations performed by the *C. elegans*

olfactory circuit involve fundamental circuit motifs of neural networks and control systems (e.g. feedback inhibition and reciprocal inhibition), suggesting that the mechanisms by which *C. elegans* microcircuits functionally process sensory information and drive contextually appropriate behaviors may be conserved in other nervous systems [14].

Organization of the olfactory system

The primarily olfactory organs of *C. elegans* are the bilaterally symmetric amphid sensilla in the head. Eleven chemosensory neurons extend anterior processes with ciliated endings into each amphid sensillum [12]. In contrast to the olfactory sensory neurons of insects and mammals, those of *C. elegans* each express many different olfactory receptors. As in mammals, most of the olfactory receptors are seven transmembrane domain G protein-coupled receptors [12]. Different pairs of olfactory sensory neurons generally drive attraction or avoidance: odor sensing by the AWA and AWC neurons promotes attraction, whereas odor sensing by the ASH, ADL, and AWB neurons promotes repulsion (Box 1) [12].

The AWA olfactory neurons are 'on-cells' that depolarize in the presence of odors, whereas the AWC olfactory neurons are 'off-cells' that hyperpolarize in the presence of odors and depolarize upon odor removal [11••,15,16••,17]. AWB neurons show both 'off' and 'on' responses [11••,16••,17,18]. Each of these neurons has synaptic connections with other sensory neurons as well as downstream interneurons [3]. Whereas insect and mammalian sensory neurons are generally dedicated to one sensory modality, most *C. elegans* sensory neurons are polymodal as a consequence of the worm's compact and highly interconnected nervous system. For example, the AWC neurons sense odors, temperature, salt, pH, CO_2, and osmotic stress [11••,19,20,21,22••].

Box 1 Summary of functional properties of selected *C. elegans* chemosensory neurons.

Neuron:	AWC	AWA	ASH	BAG	ADL
Senses:	odors, temperature, CO_2, salt, osmotic stress, pH	odors	odors, soluble chemicals, mechanical and osmotic stimuli	CO_2, O_2	odors, pheromones
Schematic of activity: (neural activity, time)	isoamyl alcohol* 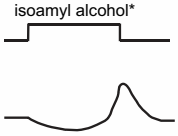 *low concentrations	diacetyl 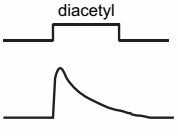	isoamyl alcohol** 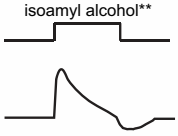 **high concentrations	5% CO_2 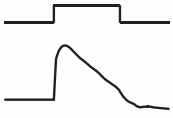	ascarosides 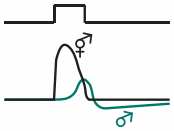
Valence promoted:	**attraction**	**attraction**	**avoidance**	**avoidance** (adults) **attraction** (dauers)	**avoidance**
Highlighted interactions:	• AIB, AIA and AIY (odor attraction) • AIA (feedback inhibition) • RIA (learned odor avoidance) • AIB, RIM and AVA (network variability) • HSN (CO_2 modulation of egg laying)	• AIA (attraction/gain control) • NSM (reciprocal inhibition circuit)	• RIM/RIC (reciprocal inhibition circuit)	• URX (O_2 modulation of CO_2 response) • HSN (CO_2 modulation of egg laying)	• RMG (hub and spoke circuit) • ASK (push/pull circuit)

Current Opinion in Neurobiology

A circuit for olfactory attraction

The microcircuit that mediates olfactory attraction via the glutamatergic AWC neurons is the most well-characterized and involves at least three downstream interneurons — AIY, AIA, and AIB [15,23]. In response to the removal of an attractive odorant, AWC inhibits AIY and AIA via glutamate-gated chloride channels, and activates AIB via AMPA-type glutamate receptors. This organization of the olfactory microcircuit into parallel pathways with inverted polarities resembles that of the vertebrate retina, where photoreceptors synapse onto opposing ON and OFF bipolar cells [15]. The temporal dynamics of AWC neuron responses to on/off patterns of olfactory stimuli correspond to the timescales of AWC-mediated odor-evoked behaviors, suggesting that sensory neuron temporal dynamics instruct behavioral dynamics [24•].

Navigational strategies for odor responses

To navigate through odor gradients, *C. elegans* primarily uses klinokinesis, also called a biased random walk, to modulate its turning rate and forward locomotion in response to its changing perception of odor concentration [12]. Worms either increase turns and decrease linear forward motion to reorient themselves away from their last (unfavorable) position, or suppress turns and increase forward motion to continue moving in the same (favorable) direction [12]. Manipulating the activity of first-order interneurons can mimic chemoattraction, suggesting that navigational strategy is determined at the level of the first-order interneurons [6]. By changing the polarity of klinokinesis in response to increasing and decreasing odor gradients, worms can shift their behavior from odor attraction to odor avoidance.

Mechanisms that determine odor valence

A number of mechanisms operate within the olfactory circuit to encode odor valence, i.e. whether an odor is attractive or repulsive. One mechanism involves a guanylate cyclase signaling pathway mediated by the receptor guanylate cyclase GCY-28, which acts in AWC sensory neurons to promote attraction to odors that AWC senses. Loss of *gcy-28* switches AWC from a neuron that mediates attraction to one that mediates repulsion [25]. A similar switch from attraction to repulsion occurs in wild-type animals that are exposed to an odor that is initially attractive for a prolonged period in the absence of food [12,25], raising the possibility that *gcy-28* signaling is part of a normal mechanism that flexibly alters odor valence based on environmental context. This study suggests that *C. elegans* olfactory sensory neurons are not irreversibly hard-wired for attraction or repulsion, but may in fact be more flexible in their responses than previously thought.

The valence of an odor stimulus can depend on its concentration. For example, low concentrations of the food-associated odorant isoamyl alcohol are attractive to *C. elegans*, while high concentrations are less attractive or even repulsive [18]. This valence change occurs because different sensory neurons mediate the response at different concentrations. At low concentrations the response is mediated primarily by the AWC olfactory neurons, while at high concentrations the response is mediated primarily by the ASH polymodal avoidance neurons (Box 1). The AWC response is blocked at high concentrations due to synaptic inhibition from other neurons [18]. A similar mechanism operates in the fruit fly *Drosophila melanogaster*, where the behavioral response to apple cider vinegar shifts from attraction at low concentrations to repulsion at high concentrations due to the recruitment of additional glomeruli [26]. In both of these cases, odor valence is determined by which sensory neurons respond to the odor at a given concentration.

The valence of an odor stimulus can also depend on the presence of other sensory stimuli. First-order interneurons can modulate odor valence by integrating information about odor stimuli with information about other sensory stimuli to generate appropriate behaviors. For example, the AIA interneurons have been implicated in multisensory decision-making for behavioral cues with conflicting valences, such as the attractive odorant diacetyl and the aversive stimulus Cu^{2+} [27]. Multisensory decision-making is an important computation for evolutionarily stable nervous systems but occurs much earlier in *C. elegans* microcircuits (i.e. within one synapse of sensory input) than those of insects and mammals because the worm nervous system is so small and shallow. However, how first-order interneurons in worms integrate olfactory stimuli with other types of stimuli to drive appropriate behaviors remains poorly understood and is an active area of research.

Mechanisms of gain control and olfactory adaptation

Like other animals, *C. elegans* is capable of maintaining a dynamic range for sensing odors across concentrations that span several orders of magnitude. One mechanism for this involves rapidly attenuating sensory neuron responses and normalizing first-order interneuron responses [28••]. Attenuation of the sensory neuron response prevents saturation, while normalization of the interneuron response results in a relatively concentration-invariant odor representation. The result is a microcircuit specialized for detecting small increases in odor concentration regardless of the absolute odor concentration. Similar mechanisms of odor coding operate in insects and vertebrates, where first-order interneurons in the olfactory circuit show normalized odor responses that encode odor identity regardless of concentration [29,30].

Another mechanism that may contribute to gain control is feedback inhibition from interneurons onto olfactory sensory neurons. For example, neuropeptide signaling between the AWC olfactory neurons and the AIA interneurons creates a feedback loop that promotes adaption to

Figure 1

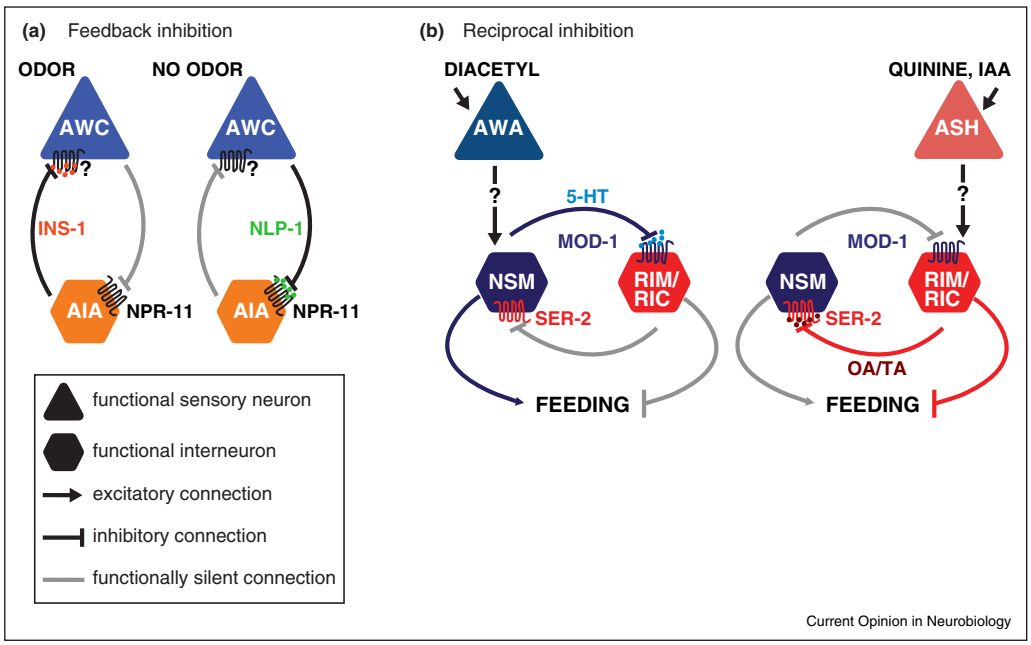

Models of microcircuit motifs present in the *C. elegans* olfactory system. (a) A feedback inhibition motif promotes odor adaptation and possibly gain control [23]. The AWC olfactory neurons release NLP-1, which binds NPR-11 on AIA interneurons to inhibit their activity. In the presence of an odor, AWC activity is suppressed. The resulting decrease in NLP-1 signaling permits AIA to release INS-1, which inhibits AWC through an unknown receptor [23]. **(b)** Odor environment modulates feeding through a reciprocal inhibition motif [39]. The presence of attractive odors increases feeding, while the presence of repulsive odors decreases feeding. The attractive odorant diacetyl is sensed by the AWA neurons and causes serotonin (5-HT) release from the NSM neurons. 5-HT binds the serotonin-gated chloride channel MOD-1 on the RIM and RIC interneurons, which inhibits them and increases feeding. Repellents such as quinine or high concentrations of isoamyl alcohol (IAA) are sensed by the ASH neurons and promote release of octopamine (OA) and tyramine (TA) from RIM/RIC. OA/TA binds the SER-2 receptor on the NSM neurons and inhibits serotonin release [39].

prolonged odor exposure and may also function as a gain control mechanism by dampening responses to strong odor stimuli (Figure 1a) [23]. Thus, both intracellular and circuit-level mechanisms are used to maintain odor responses across concentrations and promote adaption to prolonged odor exposures.

Mechanisms that contribute to behavioral flexibility and variability

Olfactory responses in *C. elegans* are modulated by external and internal context, memory, sex, and life stage [12,16••,31••,32]. Multiple circuit mechanisms contribute to this behavioral flexibility. One mechanism involves modulation of chemoreceptor expression levels [31••,32]. For example, sex, developmental stage, and feeding status alter expression of ODR-10, an odorant receptor in the AWA sensory neurons that detects the food-associated odor diacetyl [31••]. Developing larvae of both sexes and starved adults express high levels of ODR-10, allowing them to find and remain in food. In contrast, adult males express low levels of ODR-10, allowing them to forego food in favor of locating mates [31••]. By modulating the response properties of its sensory neurons, the worm can prioritize either food finding or mating in a context-appropriate manner.

In addition to showing context-dependent modulation of behavior, *C. elegans* shows stochasticity in its olfactory behavior. This behavioral variability stems at least in part from variability in interneuron responses: while sensory neuron responses are stereotyped, first-order interneuron responses are variable [33•]. Interneuron response variability arises from the stochastic activity of multiple regulatory interneurons in the circuit; silencing these interneurons increases the reliability of first-order interneuron responses and reduces behavioral variability [33•]. From an ecological perspective, behavioral variability is presumably advantageous at a population level: olfactory stimuli are often unpredictable, and behavioral variability increases the likelihood that at least some members of the population generate an appropriate behavioral response and survive.

Variability also occurs across populations as a result of genetic polymorphisms. For example, polymorphisms in the tyramine receptor TYRA-3, the neuropeptide Y receptor NPR-1, and the globin GLB-5 all cause population differences in foraging behavior and other chemosensory behaviors [32,34,35,36,37,38]. The behavioral differences that result from these polymorphisms demonstrate that the same olfactory circuit can drive a wide range of behaviors.

Interactions between the olfactory circuit and other sensory circuits

Olfactory signals can be integrated with other sensory stimuli to enhance or suppress behavioral responses. For example, pairing food with an attractive odor causes worms to eat more, whereas pairing it with an aversive odor causes worms to eat less [39]. Odors modulate feeding through a mutual inhibition circuit motif that relies on extrasynaptic neuromodulator signaling (Figure 1b). The increased feeding caused by attractive odors requires serotonin release from the NSM neurons. In contrast, the decreased feeding caused by aversive odors requires release of the neuromodulators octopamine and tyramine from the RIC and RIM interneurons. Serotonin and octopamine/tyramine bind receptors on RIC/RIM and NSM, respectively, and reciprocally block release of the other neuromodulator [39]. This reciprocal inhibition motif permits a bistable 'winner take all' output from the circuit that either enhances or suppresses eating [39]. As a result, food intake in *C. elegans* is modulated based on the valence of associated olfactory stimuli, as it is in humans.

Olfactory sensory neurons can also participate directly in other sensory circuits to modulate non-olfactory behaviors. For example, in the presence of high salt concentrations one of the two AWC neurons is recruited as an interneuron into the gustatory circuit by the release of neuropeptides from the salt-sensing ASEL neuron and enhances attraction to salt [21]. By both responding to multiple types of stimuli and modulating behavioral responses to non-olfactory stimuli, olfactory neurons participate in multiple functional microcircuits. Dynamic regulation of these microcircuits through neuropeptide signaling expands the coding capacity of the *C. elegans* nervous system and allows the same neurons to be used for multiple functional microcircuits.

Circuits for learned avoidance of pathogenic bacteria

C. elegans displays associative olfactory learning: naïve worms that have never ingested the pathogenic bacterium *Pseudomonas aeruginosa* strain PA14 show either mild attraction or no preference for its odor, whereas worms that have ingested PA14 avoid it [17,40]. Learned avoidance of PA14 involves the RIA interneurons and two insulin-like peptides [41]. INS-7 released from the gas-sensing URX neurons increases the RIA response to PA14 and prevents worms from avoiding PA14. Antagonistically, INS-6 release from the ASI chemosensory neurons promotes learning by silencing signaling from URX onto RIA through the inhibition of *ins-7* expression [41]. The ethological contexts in which insulin peptides regulate learning in wild-type animals remain to be determined.

Recently it was discovered that if *C. elegans* is exposed to PA14 early in development, olfactory imprinting occurs: worms form an aversive memory of the pathogenic bacteria that lasts into adulthood [42••]. Separate microcircuits create and retrieve the memory, and transfer of the aversive memory from the formation microcircuit to the retrieval microcircuit involves tyraminergic signaling between the two circuits [42••]. These examples of learned PA14 avoidance and aversive imprinting demonstrate that *C. elegans* is capable of learning on multiple timescales, and that learning on different timescales involves distinct circuit computations.

Microcircuits for gas-sensing behaviors

In addition to sensing volatile organic compounds, *C. elegans* senses oxygen (O_2) and carbon dioxide (CO_2). The natural habitat of *C. elegans* is fallen rotting fruit, where O_2 levels are low [10]. Consistent with this, wild isolates of *C. elegans* prefer low O_2 environments [43]. O_2 is sensed primarily by the dedicated gas-sensing URX, AQR, PQR, and BAG neurons via soluble guanylate cyclases [43,44,45,46]. Variation in O_2-evoked behaviors among *C. elegans* strains is due in part to polymorphisms in NPR-1 and GLB-5 [12,34,35]. The downstream circuitry for O_2 response involves multiple interneurons, including RMG, AIY, AIA, AVB, and AVA [36,47••]. High O_2 environments are unfavorable and induce a global arousal state that is driven by the URX neurons and translated to other neurons in the circuit via the RMG interneurons [47••]. This circuit architecture generates a long-lasting behavioral state in response to aversive high O_2 environments that promotes rapid escape.

CO_2 is a complex cue for *C. elegans* that may signal the presence of predators, conspecifics, or food. Well-fed *C. elegans* adults avoid CO_2 both in the presence and absence of food [48,49]. However, CO_2-evoked behavior is modulated by feeding status, O_2 environment, and temperature [37,38,48,49,50]. For example, CO_2 response in adults is regulated by O_2 environment through the O_2-sensing URX neurons and NPR-1, such that the level of ambient O_2 determines whether CO_2 is perceived as aversive or neutral [37,38,48,49,50]. CO_2 response also varies across life stages, with developmentally arrested dauer larvae showing CO_2 attraction (Figure 2a) [51].

The microcircuits underlying CO_2 response are incompletely understood. CO_2 exposure alters the activity of many sensory neurons, although CO_2 chemotaxis appears to be primarily mediated by the BAG and AFD neurons

Figure 2

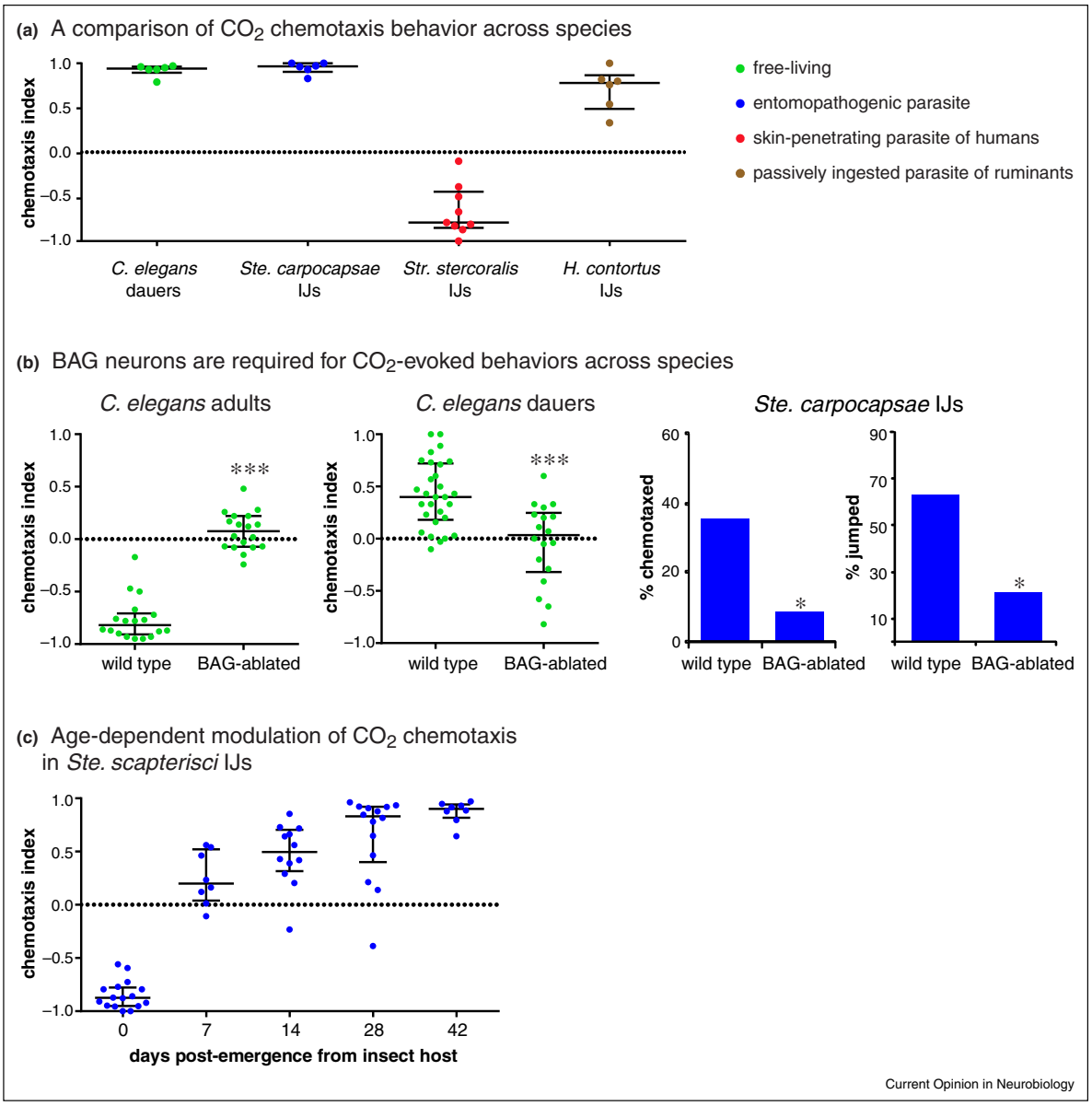

Diverse responses to CO_2 across nematode species. (a) CO_2 chemotaxis behavior varies across nematode species [51,65,84••]. Phoretic *C. elegans* dauers, which seek insect vectors, entomopathogenic *Ste. carpocapsae* IJs, and passively ingested *H. contortus* IJs are attracted to CO_2, while skin-penetrating *Str. stercoralis* IJs are repelled by CO_2 [51,65,84••]. Dauers and IJs were tested in a chemotaxis assay with 10% CO_2, in which the animals were given 1 h to migrate in a CO_2 gradient. A positive chemotaxis index (CI) indicates attraction and a negative CI indicates repulsion. **(b)** The BAG neurons are required for multiple CO_2-evoked behaviors across species. Left, BAG neurons are required for CO_2 chemotaxis in *C. elegans* adults and dauers regardless of whether CO_2 is attractive or repulsive [37,51]. BAG-ablated *C. elegans* adults were tested in a 20 min assay [37], whereas dauers were tested in a 10 min assay [51]. Right, BAG neurons are required for both CO_2 chemotaxis and CO_2-evoked jumping in *Ste. carpocapsae* IJs [51]. The BAG neurons in IJs were laser-ablated; wild-type animals were mock-ablated. IJs were tested in either a 1 h chemotaxis assay or a jumping assay in which IJs were given 8 s to jump in response to a 10% CO_2 puff [51]. **(c)** The response of *Ste. scapterisci* IJs to CO_2 shifts from repulsion to attraction as the IJs age [90•]. IJs were tested in a 1 h chemotaxis assay with 1% CO_2. Data are from Hallem *et al.* [51], Dillman *et al.* [65], and Castelletto *et al.* [84••] (a); Carrillo *et al.* [37] and Hallem *et al.* [51] (b); and Lee *et al.* [90•] (c).

[22••,37,38,48,50,51,52]. The BAG neurons are depolarized primarily by molecular CO_2 rather than bicarbonate or low pH (Box 1) [53], and this response is mediated by the receptor guanylate cyclase GCY-9 [52,53]. The mechanisms of CO_2 detection that operate in AFD and other CO_2-sensing neurons have not been elucidated. The downstream circuitry that mediates CO_2 chemotaxis is poorly understood, but both the RIA and AIA interneurons display CO_2-evoked activity, implicating them in the CO_2 microcircuit [22••,38].

CO_2 not only stimulates chemotaxis, but also inhibits egg-laying [22••]. The CO_2-induced inhibition of egg laying is mediated in part by the BAG and AWC sensory neurons [22••,54]. This circuit presumably functions to prevent deposition of eggs in unfavorable environments. Through extensive modulation of the O_2 and CO_2 microcircuits, and interactions of these circuits with those driving related behaviors such as egg laying, *C. elegans* can efficiently position itself in favorable environments for feeding and reproduction.

Microcircuits for pheromone-sensing behaviors

The *C. elegans* population consists of both hermaphrodites and males, and *C. elegans* males display mating behaviors toward hermaphrodites. The attraction of males to hermaphrodites is an essential aspect of mating behavior, and involves both volatile pheromones of unknown molecular identity [55] and soluble small-molecule pheromones in the ascaroside family that also mediate dauer formation [56,57]. Male attraction to hermaphrodites is driven by a combination of ascarosides that synergistically promote attraction [56]. Different free-living and parasitic species release different blends of ascarosides, and the behavioral responses to ascarosides are species-specific [58].

Detection of ascarosides by *C. elegans* males is mediated by both male-specific and shared sensory neurons: the four male-specific CEM sensory neurons, as well as the shared ASK and ADL sensory neurons, contribute to pheromone response [36,56,59]. The CEM neurons are unusual in that they show stochastic functional heterogeneity in their ascaroside responses both within and between animals, which may contribute to their encoding of ascaroside concentration [60••]. The AIA interneurons act downstream of the ASK sensory neurons to mediate ascaroside attraction [36,57].

While males are attracted to ascarosides released by hermaphrodites, other hermaphrodites are repelled. This sexual dimorphism is regulated by a push-pull circuit motif involving the ADL and ASK sensory neurons [59]. In hermaphrodites the ADL neurons promote ascaroside avoidance (Box 1), whereas in males the ADL neuron response is smaller and eclipsed by the ASK neuron response, which antagonizes ADL-mediated avoidance to promote attraction. This push-pull arrangement can generate opposite behavioral responses depending on the balance of activity between the attractive and repulsive arms of the microcircuit [59], thereby enabling sex-specific responses to the same pheromone.

In wild isolates of *C. elegans*, pheromones are not only important for mating but also promote aggregation behavior, in which worms cluster together in the low O_2 environment found at the edges of a bacterial lawn. Aggregation is regulated by both O_2 and pheromone environments [36]. Responses to O_2 and pheromones are coordinated by a hub-and-spoke microcircuit motif. The RMG interneurons form the hub and sensory neurons form the spokes. RMG is connected to the spoke sensory neurons, including the O_2-sensing URX neurons and the pheromone-sensing ASK neurons, by gap junctions. This hub-and-spoke arrangement enables a single interneuron to regulate a complex behavior involving multiple sensory modalities by coordinately modulating the activity of many different sensory neurons [36].

In summary, *C. elegans* has a small nervous system but expands its coding capacity through the use of neuropeptides and neuromodulators that dynamically alter microcircuit function and composition. These neuropeptides and neuromodulators complement the highly interconnected nature of the nervous system and allow neurons to simultaneously participate in multiple orthogonal microcircuits that all coordinately converge on motor neurons to produce contextually appropriate behaviors. Many of the computational mechanisms found in *C. elegans* are likely used by parasitic nematodes in the context of host-seeking behavior, as discussed below.

Olfaction in parasitic nematodes

Human–parasitic nematodes infect over one billion people globally and cause some of the most neglected tropical diseases [61]. These diseases occur predominantly in low-resource settings and result in reduced work productivity and decreased cognitive performance as a result of chronic morbidity [61]. In addition, parasitic nematodes of livestock and plants result in billions of dollars in economic and food losses each year [62]. Many parasitic nematodes have an environmental infective stage, called the infective juvenile (IJ) or infective third-stage larva (L3i) in the case of insect-parasitic and mammalian-parasitic nematodes, that actively searches for hosts to infect using olfaction in combination with other sensory modalities [9]. A better understanding of olfaction in parasitic nematodes could therefore lead to new strategies for preventing parasitic nematode infections.

A unique aspect of nematode neurobiology is conserved neuroanatomy: electron microscopy studies of anterior

sensory anatomy have demonstrated that even distantly related species have approximately the same number of neurons located in roughly the same positions within the body [8,9]. In addition, laser ablation studies have demonstrated that sensory neuron function is often conserved across free-living and parasitic nematode species [9]. For this reason, studies of *C. elegans* olfaction can directly inform studies of olfaction in parasitic worms.

A number of recent technical advances with skin-penetrating nematodes in the genera *Strongyloides* and *Parastrongyloides* promise to greatly facilitate the study of parasitic nematode sensory neurobiology. These include the ability to generate transgenic nematodes by gonadal microinjection and the ability to conduct genome editing using the CRISPR/Cas9 system [63]. In addition, RNAi has been used successfully with some parasitic nematodes [63,64]. These techniques will enable studies of the neurons and circuits underlying the host-seeking behaviors of parasitic nematodes.

Olfactory behaviors of entomopathogenic nematodes

Entomopathogenic nematodes (EPNs) in the genera *Heterorhabditis* and *Steinernema* are parasitic nematodes that infect and kill insects. They are sometimes referred to as 'beneficial nematodes' due to their utility for insect biocontrol. EPN-infection of insects is also of interest as a model for harmful parasitic nematodes that infect humans. Like *C. elegans*, EPNs respond to a diverse array of insect odorants, plant odorants, and CO_2 [51,65,66,67,68,69,70,71]. Attraction to plant odorants serves to draw EPNs to locations where their insect hosts feed, and in fact some of the plant odorants that attract EPNs are emitted in response to insect-mediated damage [71,72,73,74].

CO_2 is a strong attractant for EPNs and is used in combination with both insect- and plant-emitted odorants to locate insect hosts (Figure 2a) [51,65,66,71]. Attraction of EPNs to the odors of live insects is greatly reduced or eliminated when CO_2 is chemically removed, suggesting that CO_2 is a critical host cue [65,67]. However, the relative importance of CO_2 versus insect-specific odorants varies for different EPN species and different insect species [65].

The attractive response of EPN IJs to CO_2 resembles that of *C. elegans* dauer larvae (Figure 2a) [51,65]. Parasitic IJs and *C. elegans* dauers are developmentally analogous life stages [75] that may also be behaviorally analogous: whereas IJs seek out hosts to infect, dauers seek out invertebrate carriers [10]. CO_2 attraction by both IJs and dauers may serve the similar purpose of facilitating interactions with insects and other invertebrates. CO_2 also stimulates jumping, a specialized host-finding behavior exhibited by some EPN species in which the IJs propel themselves into the air [51,65]. Thus the same chemosensory cue, CO_2, can stimulate both general and species-specific behavioral responses. As in *C. elegans*, the BAG neurons mediate CO_2-evoked behaviors (Figure 2b), indicating that the neural basis of CO_2 response is at least partly conserved across species regardless of whether CO_2 is an attractive or repulsive cue [51].

Olfactory behaviors of plant–parasitic nematodes

Soil-dwelling plant–parasitic nematodes (PPNs) use the general cue CO_2 in combination with plant-specific odorants to specifically target the roots of host plants [70,76,77]. For at least some species, the attractive response to CO_2 may in fact be a response to low pH resulting from dissolved CO_2 rather than to the CO_2 itself [78]. Some of the plant root volatiles produced in response to insect damage attract PPNs as well as EPNs, suggesting that there is an ecological cost for the plant associated with the production of these volatiles [79].

Plants also release volatiles such as ethylene that modulate attraction of PPNs to their roots [80]. In addition, volatiles from nearby plants can modulate attraction of PPNs to host plants. For example, when intercropped with crown daisy, the tomato plant is protected from parasitism by the root-knot nematode *Meloidogyne incognita* [81••]. Crown daisy roots produce lauric acid, which is attractive for PPNs at low concentrations but repulsive at high concentrations [81••], reminiscent of the concentration-dependent effects of isoamyl alcohol on *C. elegans* [18]. After attracting *M. incognita* to crown daisy root, lauric acid appears to disrupt chemotaxis behavior and infectivity by regulating expression of the FMRFamide-related neuropeptide FLP-18 [81••]. The intercropping of certain plants may be a nonhazardous alternative to artificial pesticides: intercropping can decrease PPN-induced crop damage through the modulation of PPN chemotaxis behavior.

Olfactory behaviors of mammalian-parasitic nematodes

Mammalian-parasitic nematodes also respond to a chemically diverse array of odorants. The olfactory behaviors of the human-parasitic threadworm *Strongyloides stercoralis* are the most well-studied. *Str. stercoralis* infects approximately 100 million people worldwide and leads to chronic gastrointestinal distress; infections can be fatal for immunocompromised individuals [82]. *Str. stercoralis* is a soil-dwelling worm that infects primarily by penetrating the skin of the feet. As such, *Str. stercoralis* IJs are attracted to a number of human skin and sweat odorants [83,84••]. For example, *Str. stercoralis* IJs are attracted to urocanic acid, a histidine metabolite found in mammalian skin that is enriched in the skin of the feet [83]. Many of the odorants that attract *Str. stercoralis* are also known mosquito attractants, suggesting that human-parasitic nematodes and mosquitoes may target humans using some of the same olfactory cues [84••]. An exception is CO_2, which is generally attractive for mosquitoes but repulsive for

Str. stercoralis and other skin-penetrating nematodes (Figure 2a) [84••,85]. CO_2 is presumably not an effective long-range host cue for *Str. stercoralis* due to its route of infection since only very low levels of CO_2 are emitted from human skin [84••].

The only passively ingested mammalian-parasitic nematode whose olfactory behavior has been characterized in detail is *Haemonchus contortus*, a parasite of ruminants that is a major cause of livestock disease worldwide [86]. *H. contortus* IJs respond robustly to olfactory cues, but unlike skin-penetrating IJs, they are attracted to CO_2 (Figure 2a) [84••]. *H. contortus* is also attracted to grass odor [84••]. Attraction to CO_2 and grass may serve to direct *H. contortus* IJs toward the mouths of grazing animals, where they are more likely to be ingested.

Olfactory behaviors of the necromenic nematode *Pristionchus pacificus*

Olfactory behavior has also been studied in *Pristionchus pacificus*, a necromenic species that associates with beetles [87]. Necromenic nematodes do not kill their host, but rather wait for their host to die and then propagate on the host cadaver. As such, necromeny is often considered an evolutionary intermediate between free-living and parasitic lifestyles. *P. pacificus* is attracted to live beetles as well as beetle odorants, beetle pheromone, and plant odorants [87,88]. Olfactory preferences differ among wild *P. pacificus* strains and among closely related *Pristionchus* species, perhaps reflecting differences in their host preferences [87,88]. Natural variation in the responses of different *P. pacificus* strains to beetle pheromone is associated with the cGMP-dependent protein kinase gene *egl-4* [89], raising the possibility that cGMP signaling contributes to host seeking in parasitic nematodes.

Parasite olfactory preferences exhibit context-dependent modulation

As is the case for *C. elegans*, the olfactory preferences of parasitic nematodes are context-dependent and flexible. For example, both EPN IJs and skin-penetrating IJs exhibit temperature-dependent olfactory plasticity: culturing IJs at different temperatures changes their odor preferences [90•]. In the case of the EPN *Steinernema carpocapsae*, the response to 80% of the tested odorants changed as a function of their previous cultivation temperature. IJs are long-lived and can survive in the soil through multiple seasons. The volatiles emitted by both animals and plants change seasonally, and thus temperature-dependent modulation of olfactory behavior may enable IJs to locate hosts despite seasonal changes in volatile emissions [90•].

Some parasitic nematodes also show age-dependent changes in their olfactory preferences [90•]. For example, the EPN *Steinernema scapterisci* is initially repelled by CO_2 but becomes attracted to CO_2 as the IJs age (Figure 2c). This change in CO_2-evoked behavior may reflect a change in host-seeking strategy: CO_2 avoidance by younger IJs may cause them to disperse into the environment in search of new host niches with more available resources (a high cost but potentially high reward behavior), whereas CO_2 attraction by older IJs may cause them to remain in the proximity of existing host niches (a low cost but lower reward behavior) [90•].

Odor preferences of parasitic nematodes are shaped by host specificity and mode of infection

A comparison of olfactory behavior across parasitic nematode species revealed that parasite olfactory preferences reflect host specificity and infection strategy rather than genetic relatedness, and that these parasite-specific preferences have evolved multiple times (Figure 3) [84••]. For example, the skin-penetrating rat parasites *Str. ratti* and *Nippostrongylus brasiliensis* share similar odor preferences but are not closely related [84••]. That odor preferences reflect parasite lifestyle rather than phylogeny suggests that olfaction plays an important role in the ability of parasitic nematodes to find and infect their hosts.

In summary, parasitic nematodes show species-specific olfactory behaviors despite the fact that sensory neuroanatomy is roughly conserved across nematode species [8,9]. Efforts to study olfactory neural circuits in parasitic nematodes are ongoing. Existing knowledge of sensory neuron function is based exclusively on laser ablation studies; the dynamics of sensory neural activity in parasitic nematodes have not been examined. Although the BAG neurons are the only olfactory neurons shown to have conserved function in parasitic and free-living worms [51], conserved sensory neurons also drive salt chemotaxis, thermotaxis, and changes in developmental stage in *C. elegans* and mammalian-parasitic worms [8,9]. Based on these studies, sensory neuron function appears to be broadly conserved across free-living and parasitic nematodes. In addition, the RIA interneurons play a role in thermotaxis in both *C. elegans* and *H. contortus* [91], suggesting that interneuron function may be conserved in at least some cases. Nervous system connectivity has not yet been examined in parasitic nematodes. However, a recent study of the *P. pacificus* pharynx found that although *P. pacificus* and *C. elegans* share a set of 20 homologous pharyngeal neurons, the connectivity of these neurons differs in the two species [92]. Thus, behavioral differences among species may arise from a combination of altered connectivity of the nervous system, the actions of neuromodulators and neuropeptides, and species-specific differences in the functional properties of neurons. Future studies of olfactory circuits in parasitic nematodes should clarify the relative contribution of each of these factors to the evolution of olfactory neural circuits and odor-driven behaviors.

Figure 3

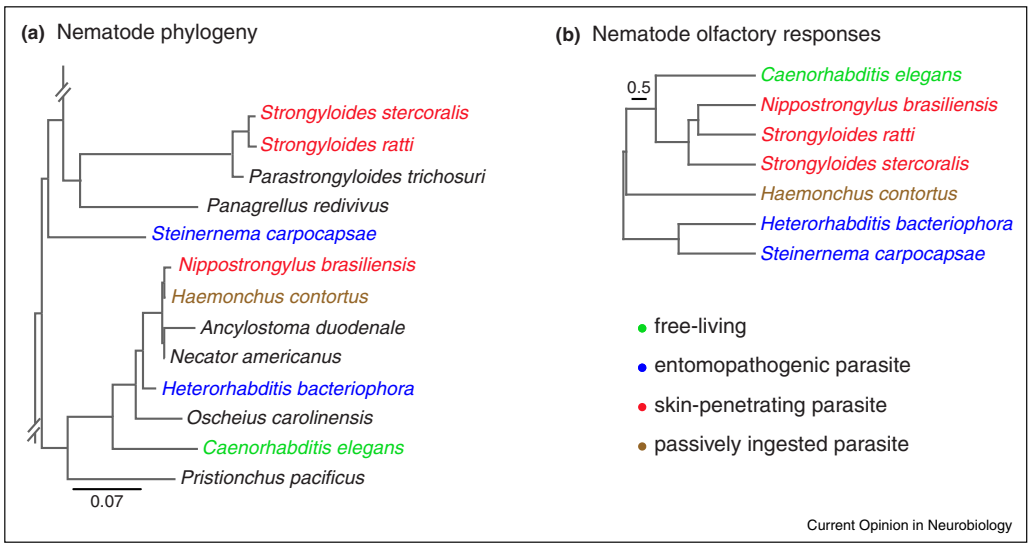

Olfactory responses of parasitic nematodes reflect their host ranges and infection modes rather than their genetic relatedness. (a) Schematic of phylogenetic relationships among nematode species [65,84••]. Phylogenetic analysis is based on Castelletto *et al.* [84••] and Dillman *et al.* [65]. **(b)** A behavioral dendrogram of odor preferences among nematode species [84••]. Species cluster based on the hosts they infect and their modes of infection, rather than their genetic relationships. For example, the skin-penetrating rat parasites *Str. ratti* and *N. brasiliensis* show similar odor preferences, even though they are not closely related genetically [84••].

Conclusion

Recent studies of olfactory microcircuits in *C. elegans* have elucidated how the worm responds to odorants across a wide range of concentrations, and how these responses are modulated by environmental stimuli, internal behavioral state, and genotype. With new technical advances that enable nearly whole-brain imaging with single-neuron resolution in freely moving *C. elegans* [93,94,95,96], it should now be possible to determine how global changes in brain state alter olfactory microcircuits and to clarify the dynamics of how neurons are recruited into or omitted from these microcircuits.

Studies of olfactory behavior in parasitic nematodes have demonstrated how these parasites use olfactory cues to find and infect hosts, with implications for nematode control. Since molecular and genetic tools are now available for some parasitic worms, the microcircuits that drive these behaviors are at the cusp of discovery. Future studies comparing microcircuit function in *C. elegans* and parasitic nematodes should provide insight into how analogous microcircuits operate in free-living versus parasitic species to support parasite-specific olfactory behaviors.

Conflict of interest statement

Nothing declared.

Acknowledgements

We thank Astra Bryant, Michelle Castelletto, Albert Kao, Joon Ha Lee, Michelle Rengarajan, Sara Wasserman, and Kristen Yankura for insightful comments on the manuscript. This work was supported by the UCLA-Caltech Medical Scientist Training Program [T32GM008042], the UCLA Neural Microcircuit Training Grant [T32NS058280], and a predoctoral NRSA fellowship [1F30GM116810] to S.R.; and a MacArthur Fellowship, McKnight Scholar Award, NIH New Innovator Award [1DP2DC014596], and NSF grant [NSF IOS-1456064] to E.A.H.

References and recommended reading

Papers of particular interest, published within the period of review, have been highlighted as:

- • of special interest
- •• of outstanding interest

1. Emmons SW: **Connectomics, the Final Frontier**. *Curr Top Dev Biol* 2016, **116**:315-330.
2. White JG, Southgate E, Thomson JN, Brenner S: **The structure of the nervous system of the nematode *Caenorhabditis elegans***. *Phil Trans Royal Soc London B* 1986, **314**:1-340.
3. Varshney LR, Chen BL, Paniagua E, Hall DH, Chklovskii DB: **Structural properties of the *Caenorhabditis elegans* neuronal network**. *PLoS Comput Biol* 2011, **7**:e1001066.
4. Ibsen S, Tong A, Schutt C, Esener S, Chalasani SH: **Sonogenetics is a non-invasive approach to activating neurons in *Caenorhabditis elegans***. *Nat Commun* 2015, **6**:8264.
5. Fang-Yen C, Alkema MJ, Samuel AD: **Illuminating neural circuits and behaviour in *Caenorhabditis elegans* with optogenetics**. *Philos Trans R Soc Lond B Biol Sci* 2015, **370**:20140212.

6. Kocabas A, Shen CH, Guo ZV, Ramanathan S: **Controlling interneuron activity in *Caenorhabditis elegans* to evoke chemotactic behaviour**. *Nature* 2012, **490**:273-277.

7. Pokala N, Liu Q, Gordus A, Bargmann CI: **Inducible and titratable silencing of *Caenorhabditis elegans* neurons in vivo with histamine-gated chloride channels**. *Proc Natl Acad Sci USA* 2014, **111**:2770-2775.

8. Ashton FT, Li J, Schad GA: **Chemo- and thermosensory neurons: structure and function in animal parasitic nematodes**. *Vet Parasitol* 1999, **84**:297-316.

9. Gang SS, Hallem EA: **Mechanisms of host seeking by parasitic nematodes**. *Mol Biochem Parasitol* 2016, **208**:23-32.

10. Felix MA, Duveau F: **Population dynamics and habitat sharing of natural populations of *Caenorhabditis elegans* and *C. briggsae***. *BMC Biol* 2012, **10**:59.

11. •• Zaslaver A, Liani I, Shtangel O, Ginzburg S, Yee L, Sternberg PW: **Hierarchical sparse coding in the sensory system of *Caenorhabditis elegans***. *Proc Natl Acad Sci USA* 2015, **112**:1185-1189.

In this study, the authors survey the responses of sensory neurons to a large panel of sensory stimuli and find that the *C. elegans* nervous system exhibits sparse coding (i.e. many stimuli only activate a few neurons) and functional hierarchy (i.e. some neurons respond to many more stimuli than others). This circuit organization may have evolved to expand the coding capacity of the worm's small nervous system.

12. Hart AC, Chao MY: **From odors to behaviors in *Caenorhabditis elegans***. In *The Neurobiology of Olfaction, edn 2011/09/02.* Edited by Menini A, Boca Raton FL. CRC Press; 2010.

13. Bargmann CI: **Beyond the connectome: How neuromodulators shape neural circuits**. *Bioessays* 2012.

14. Milo R, Shen-Orr S, Itzkovitz S, Kashtan N, Chklovskii D, Alon U: **Network motifs: simple building blocks of complex networks**. *Science* 2002, **298**:824-827.

15. Chalasani SH, Chronis N, Tsunozaki M, Gray JM, Ramot D, Goodman MB, Bargmann CI: **Dissecting a circuit for olfactory behaviour in *Caenorhabditis elegans***. *Nature* 2007, **450**:63-70.

16. •• Leinwand SG, Yang CJ, Bazopoulou D, Chronis N, Srinivasan J, Chalasani SH: **Circuit mechanisms encoding odors and driving aging-associated behavioral declines in *Caenorhabditis elegans***. *Elife* 2015, **4**:e10181.

The response of adult *C. elegans* to the attractive odorant benzaldehyde declines with age. This study implicates four neurons in benzaldehyde attraction: two primary sensory neurons and two secondary neurons that receive input from the primary neurons. The authors elucidate a mechanism for the age-dependent decay in benzaldehyde attraction involving decreased responsiveness of the secondary but not primary neurons. The age-related behavioral decline was rescued by increasing synaptic output from the primary neurons, suggesting that age-related olfactory decline results from reduced neurotransmission in the circuit.

17. Ha HI, Hendricks M, Shen Y, Gabel CV, Fang-Yen C, Qin Y, Colon-Ramos D, Shen K, Samuel AD, Zhang Y: **Functional organization of a neural network for aversive olfactory learning in *Caenorhabditis elegans***. *Neuron* 2010, **68**:1173-1186.

18. Yoshida K, Hirotsu T, Tagawa T, Oda S, Wakabayashi T, Iino Y, Ishihara T: **Odour concentration-dependent olfactory preference change in *C. elegans***. *Nat Commun* 2012, **3**:739.

19. Biron D, Wasserman S, Thomas JH, Samuel AD, Sengupta P: **An olfactory neuron responds stochastically to temperature and modulates *Caenorhabditis elegans* thermotactic behavior**. *Proc Natl Acad Sci USA* 2008, **105**:11002-11007.

20. Kuhara A, Okumura M, Kimata T, Tanizawa Y, Takano R, Kimura KD, Inada H, Matsumoto K, Mori I: **Temperature sensing by an olfactory neuron in a circuit controlling behavior of *C. elegans***. *Science* 2008, **320**:803-807.

21. Leinwand SG, Chalasani SH: **Neuropeptide signaling remodels chemosensory circuit composition in *Caenorhabditis elegans***. *Nat Neurosci* 2013, **16**:1461-1467.

22. •• Fenk LA, de Bono M: **Environmental CO_2 inhibits *Caenorhabditis elegans* egg-laying by modulating olfactory neurons and evokes widespread changes in neural activity**. *Proc Natl Acad Sci USA* 2015, **112**:E3525-E3534.

This study shows that the polymodal AWC neurons are CO_2 sensors that modulate the egg-laying behavior of worms as a function of ambient CO_2 levels. In high CO_2 environments, which may be unfavorable to developing larvae, the AWC neurons are activated and suppress activity of the hermaphrodite-specific neurons (HSNs), preventing deposition of eggs. These results demonstrate a mechanism for context-dependent modulation of behavior that may enhance reproductive fitness.

23. Chalasani SH, Kato S, Albrecht DR, Nakagawa T, Abbott LF, Bargmann CI: **Neuropeptide feedback modifies odor-evoked dynamics in *Caenorhabditis elegans* olfactory neurons**. *Nat Neurosci* 2010, **13**:615-621.

24. • Kato S, Xu Y, Cho CE, Abbott LF, Bargmann CI: **Temporal responses of *C. elegans* chemosensory neurons are preserved in behavioral dynamics**. *Neuron* 2014, **81**:616-628.

By imaging the calcium activity of olfactory sensory neurons to fluctuating on/off sequences of odorants, the authors determine that the odor-evoked activity of these neurons acts on similar timescales to the behaviors the odors evoke. Disrupting the temporal dynamics of the olfactory sensory neuron responses disrupts behavioral dynamics. Thus, the behavioral responses to complex odor stimuli are guided by the temporal dynamics of the olfactory sensory neuron responses.

25. Tsunozaki M, Chalasani SH, Bargmann CI: **A behavioral switch: cGMP and PKC signaling in olfactory neurons reverses odor preference in *C. elegans***. *Neuron* 2008, **59**:959-971.

26. Semmelhack JL, Wang JW: **Select *Drosophila* glomeruli mediate innate olfactory attraction and aversion**. *Nature* 2009, **459**:218-223.

27. Shinkai Y, Yamamoto Y, Fujiwara M, Tabata T, Murayama T, Hirotsu T, Ikeda DD, Tsunozaki M, Iino Y, Bargmann CI *et al.*: **Behavioral choice between conflicting alternatives is regulated by a receptor guanylyl cyclase, GCY-28, and a receptor tyrosine kinase, SCD-2, in AIA interneurons of *Caenorhabditis elegans***. *J Neurosci* 2011, **31**:3007-3015.

28. •• Larsch J, Flavell SW, Liu Q, Gordus A, Albrecht DR, Bargmann CI: **A circuit for gradient climbing in *C. elegans* chemotaxis**. *Cell Rep* 2015, **12**:1748-1760.

This study identifies a mechanism for gain control that enables *C. elegans* to migrate toward attractive odorants across a wide range of concentrations. As odorant concentration increases, the olfactory sensory neuron attenuates its response, allowing it to remain sensitive to small increases in concentration. At the same time, the downstream interneuron normalizes its response to generate a mostly concentration-invariant signal. The result is a microcircuit capable of detecting small increases in odorant concentration across a wide range of absolute concentrations. This enables the worm to efficiently ascend an odor gradient.

29. Olsen SR, Bhandawat V, Wilson RI: **Divisive normalization in olfactory population codes**. *Neuron* 2010, **66**:287-299.

30. Zhu P, Frank T, Friedrich RW: **Equalization of odor representations by a network of electrically coupled inhibitory interneurons**. *Nat Neurosci* 2013, **16**:1678-1686.

31. •• Ryan DA, Miller RM, Lee K, Neal SJ, Fagan KA, Sengupta P, Portman DS: **Sex, age, and hunger regulate behavioral prioritization through dynamic modulation of chemoreceptor expression**. *Curr Biol* 2014, **24**:2509-2517.

This study demonstrates that modulation of odorant receptor expression contributes to context-dependent olfactory plasticity. The odorant receptor ODR-10, which detects the food odorant diacetyl, is expressed at lower levels in males than hermaphrodites, allowing males to forego food sources in favor of finding hermaphrodites. When males are starved, ODR-10 expression increases, allowing males to search for food. This mechanism enables males to prioritize either finding food or finding mates depending on current internal and external conditions.

32. Gruner M, Nelson D, Winbush A, Hintz R, Ryu L, Chung SH, Kim K, Gabel CV, van der Linden AM: **Feeding state, insulin and NPR-1 modulate chemoreceptor gene expression via integration of sensory and circuit inputs**. *PLoS Genet* 2014, **10**:e1004707.

33. • Gordus A, Pokala N, Levy S, Flavell SW, Bargmann CI: **Feedback from network states generates variability in a probabilistic olfactory circuit**. *Cell* 2015, **161**:215-227.

This study identifies a network mechanism that generates behavioral

variability to an odorant despite reliable sensory neuron responses. Three interneurons are connected to each other through synaptic and electrical connections, resulting in the emergence of a network state. Although one of the interneurons has reliable odorant responses in isolation, feedback from the other interneurons promotes probabilistic odorant responses and a probabilistic behavioral output. Behavioral variability is presumably adaptive given the complex and ambiguous nature of many olfactory stimuli.

34. Persson A, Gross E, Laurent P, Busch KE, Bretes H, de Bono M: **Natural variation in a neural globin tunes oxygen sensing in wild *Caenorhabditis elegans***. *Nature* 2009, **458**:1030-1033.

35. McGrath PT, Rockman MV, Zimmer M, Jang H, Macosko EZ, Kruglyak L, Bargmann CI: **Quantitative mapping of a digenic behavioral trait implicates globin variation in *C. elegans* sensory behaviors**. *Neuron* 2009, **61**:692-699.

36. Macosko EZ, Pokala N, Feinberg EH, Chalasani SH, Butcher RA, Clardy J, Bargmann CI: **A hub-and-spoke circuit drives pheromone attraction and social behaviour in *C. elegans***. *Nature* 2009, **458**:1171-1175.

37. Carrillo MA, Guillermin ML, Rengarajan S, Okubo R, Hallem EA: **O_2-sensing neurons control CO_2 response in *C. elegans***. *J Neurosci* 2013, **33**:9675-9683.

38. Kodama-Namba E, Fenk LA, Bretscher AJ, Gross E, Busch KE, de Bono M: **Cross-modulation of homeostatic responses to temperature, oxygen and carbon dioxide in *C. elegans***. *PLoS Genet* 2013, **9**:e1004011.

39. Li Z, Li Y, Yi Y, Huang W, Yang S, Niu W, Zhang L, Xu Z, Qu A, Wu Z *et al.*: **Dissecting a central flip-flop circuit that integrates contradictory sensory cues in *C. elegans* feeding regulation**. *Nat Commun* 2012, **3**:776.

40. Harris G, Shen Y, Ha H, Donato A, Wallis S, Zhang X, Zhang Y: **Dissecting the signaling mechanisms underlying recognition and preference of food odors**. *J Neurosci* 2014, **34**:9389-9403.

41. Chen Z, Hendricks M, Cornils A, Maier W, Alcedo J, Zhang Y: **Two insulin-like peptides antagonistically regulate aversive olfactory learning in *C. elegans***. *Neuron* 2013, **77**:572-585.

42. •• Jin X, Pokala N, Bargmann CI: **Distinct circuits for the formation and retrieval of an imprinted olfactory memory**. *Cell* 2016, **164**:632-643.

This study demonstrates that first-stage *C. elegans* larvae exposed to pathogenic bacteria undergo imprinted aversion, resulting in long-lasting avoidance of the bactera. The authors show that different microcircuits underlie the formation and retrieval of this memory, and they implicate the biogenic amine tyramine in the transfer of learning from the formation to the retrieval microcircuit.

43. Gray JM, Karow DS, Lu H, Chang AJ, Chang JS, Ellis RE, Marletta MA, Bargmann CI: **Oxygen sensation and social feeding mediated by a *C. elegans* guanylate cyclase homologue**. *Nature* 2004, **430**:317-322.

44. Zimmer M, Gray JM, Pokala N, Chang AJ, Karow DS, Marletta MA, Hudson ML, Morton DB, Chronis N, Bargmann CI: **Neurons detect increases and decreases in oxygen levels using distinct guanylate cyclases**. *Neuron* 2009, **61**:865-879.

45. Couto A, Oda S, Nikolaev VO, Soltesz Z, de Bono M: **In vivo genetic dissection of O_2-evoked cGMP dynamics in a *Caenorhabditis elegans* gas sensor**. *Proc Natl Acad Sci USA* 2013, **110**:E3301-E3310.

46. Cheung BH, Arellano-Carbajal F, Rybicki I, de Bono M: **Soluble guanylate cyclases act in neurons exposed to the body fluid to promote *C. elegans* aggregation behavior**. *Curr Biol* 2004, **14**:1105-1111.

47. •• Laurent P, Soltesz Z, Nelson GM, Chen C, Arellano-Carbajal F, Levy E, de Bono M: **Decoding a neural circuit controlling global animal state in *C. elegans***. *Elife* 2015:4.

This study finds that high ambient oxygen levels promote a global arousal state that enhances efficient avoidance of the unfavorable environment. The oxygen-sensing URX neurons initiate this arousal state by stimulating neurpeptide release from the downstream RMG interneurons.

48. Hallem EA, Sternberg PW: **Acute carbon dioxide avoidance in *Caenorhabditis elegans***. *Proc Natl Acad Sci USA* 2008, **105**:8038-8043.

49. Bretscher AJ, Busch KE, de Bono M: **A carbon dioxide avoidance behavior is integrated with responses to ambient oxygen and food in *Caenorhabditis elegans***. *Proc Natl Acad Sci USA* 2008, **105**:8044-8049.

50. Bretscher AJ, Kodama-Namba E, Busch KE, Murphy RJ, Soltesz Z, Laurent P, de Bono M: **Temperature, oxygen, and salt-sensing neurons in *C. elegans* are carbon dioxide sensors that control avoidance behavior**. *Neuron* 2011, **69**:1099-1113.

51. Hallem EA, Dillman AR, Hong AV, Zhang Y, Yano JM, DeMarco SF, Sternberg PW: **A sensory code for host seeking in parasitic nematodes**. *Curr Biol* 2011, **21**:377-383.

52. Hallem EA, Spencer WC, McWhirter RD, Zeller G, Henz SR, Ratsch G, Miller DM, Horvitz HR, Sternberg PW, Ringstad N: **Receptor-type guanylate cyclase is required for carbon dioxide sensation by *Caenorhabditis elegans***. *Proc Natl Acad Sci USA* 2011, **108**:254-259.

53. Smith ES, Martinez-Velazquez L, Ringstad N: **A chemoreceptor that detects molecular carbon dioxide**. *J Biol Chem* 2013, **288**:37071-37081.

54. Ringstad N, Horvitz HR: **FMRFamide neuropeptides and acetylcholine synergistically inhibit egg-laying by *C. elegans***. *Nat Neurosci* 2008, **11**:1168-1176.

55. Leighton DH, Choe A, Wu SY, Sternberg PW: **Communication between oocytes and somatic cells regulates volatile pheromone production in *Caenorhabditis elegans***. *Proc Natl Acad Sci USA* 2014, **111**:17905-17910.

56. Srinivasan J, Kaplan F, Ajredini R, Zachariah C, Alborn HT, Teal PE, Malik RU, Edison AS, Sternberg PW, Schroeder FC: **A blend of small molecules regulates both mating and development in *Caenorhabditis elegans***. *Nature* 2008, **454**:1115-1118.

57. Srinivasan J, von Reuss SH, Bose N, Zaslaver A, Mahanti P, Ho MC, O'Doherty OG, Edison AS, Sternberg PW, Schroeder FC: **A modular library of small molecule signals regulates social behaviors in *Caenorhabditis elegans***. *PLoS Biol* 2012, **10**:e1001237.

58. Choe A, von Reuss SH, Kogan D, Gasser RB, Platzer EG, Schroeder FC, Sternberg PW: **Ascaroside signaling is widely conserved among nematodes**. *Curr Biol* 2012, **22**:772-780.

59. Jang H, Kim K, Neal SJ, Macosko E, Kim D, Butcher RA, Zeiger DM, Bargmann CI, Sengupta P: **Neuromodulatory state and sex specify alternative behaviors through antagonistic synaptic pathways in *C. elegans***. *Neuron* 2012, **75**:585-592.

60. •• Narayan A, Venkatachalam V, Durak O, Reilly DK, Bose N, Schroeder FC, Samuel AD, Srinivasan J, Sternberg PW: **Contrasting responses within a single neuron class enable sex-specific attraction in *Caenorhabditis elegans***. *Proc Natl Acad Sci USA* 2016, **113**:E1392-E1401.

The CEM neurons are a male-specific class of sensory neurons in *C. elegans* that detect ascaroside pheromones and are involved in the attraction of males to hermaphrodites for the purpose of mating. Although the CEM neurons were previously thought to be functionally equivalent, the authors demonstrate stochastic functional heterogeneity of CEM neurons. Variation in the ascaroside responses of the CEM neurons of a single worm may arise from feedback inhibition between CEM neurons and may enable the worm to better encode ascaroside concentration.

61. Boatin BA, Basanez MG, Prichard RK, Awadzi K, Barakat RM, Garcia HH, Gazzinelli A, Grant WN, McCarthy JS, N'Goran EK *et al.*: **A research agenda for helminth diseases of humans: towards control and elimination**. *PLoS Negl Trop Dis* 2012, **6**:e1547.

62. Jasmer DP, Goverse A, Smant G: **Parasitic nematode interactions with mammals and plants**. *Annu Rev Phytopathol* 2003, **41**:245-270.

63. Lok JB, Shao H, Massey HC, Li X: **Transgenesis in *Strongyloides* and related parasitic nematodes: historical perspectives, current functional genomic applications and progress towards gene disruption and editing**. *Parasitology* 2016:1-16.

64. Ratnappan R, Vadnal J, Keaney M, Eleftherianos I, O'Halloran D, Hawdon JM: **RNAi-mediated gene knockdown by microinjection in the model entomopathogenic nematode *Heterorhabditis bacteriophora***. *Parasit Vectors* 2016, **9**:160.

65. Dillman AR, Guillermin ML, Lee JH, Kim B, Sternberg PW, Hallem EA: **Olfaction shapes host-parasite interactions in parasitic nematodes**. *Proc Natl Acad Sci USA* 2012, **109**:E2324-E2333.

66. O'Halloran DM, Burnell AM: **An investigation of chemotaxis in the insect parasitic nematode *Heterorhabditis bacteriophora***. *Parasitol* 2003, **127**:375-385.

67. Gaugler R, Campbell JF, Gupta P: **Characterization and basis of enhanced host-finding in a genetically improved strain of *Steinernema carpocapsae***. *J Invert Pathol* 1991, **57**:234-241.

68. Robinson AF: **Optimal release rates for attracting *Meloidogyne incognita*, *Rotylenchulus reniformis*, and other nematodes to carbon dioxide in sand**. *J Nematol* 1995, **27**:42-50.

69. Koppenhofer AM, Fuzy EM: **Attraction of four entomopathogenic nematodes to four white grub species**. *J Invert Path* 2008, **99**:227-234.

70. Rasmann S, Ali JG, Helder J, van der Putten WH: **Ecology and evolution of soil nematode chemotaxis**. *J Chem Ecol* 2012, **38**:615-628.

71. Turlings TC, Hiltpold I, Rasmann S: **The importance of root-produced volatiles as foraging cues for entomopathogenic nematodes**. *Plant Soil* 2012, **358**:51-60.

72. Rasmann S, Kollner TG, Degenhardt J, Hiltpold I, Toepfer S, Kuhlmann U, Gershenzon J, Turlings TC: **Recruitment of entomopathogenic nematodes by insect-damaged maize roots**. *Nature* 2005, **434**:732-737.

73. Ali JG, Alborn HT, Stelinski LL: **Subterranean herbivore-induced volatiles released by citrus roots upon feeding by *Diaprepes abbreviatus* recruit entomopathogenic nematodes**. *J Chem Ecol* 2010, **36**:361-368.

74. Li C, Wang Y, Hua Y, Hua C, Wang C: **Three dimensional study of wounded plant roots recruiting entomopathogenic nematodes with Pluronic gel as a medium**. *Biol Control* 2015, **89**:68-74.

75. Crook M: **The dauer hypothesis and the evolution of parasitism: 20 years on and still going strong**. *Int J Parasitol* 2014, **44**:1-8.

76. Farnier K, Bengtsson M, Becher PG, Witzell J, Witzgall P, Manduric S: **Novel bioassay demonstrates attraction of the white potato cyst nematode *Globodera pallida* (Stone) to non-volatile and volatile host plant cues**. *J Chem Ecol* 2012, **38**:795-801.

77. Reynolds AM, Dutta TK, Curtis RH, Powers SJ, Gaur HS, Kerry BR: **Chemotaxis can take plant-parasitic nematodes to the source of a chemo-attractant via the shortest possible routes**. *J R Soc Interface* 2011, **8**:568-577.

78. Wang C, Bruening G, Williamson VM: **Determination of preferred pH for root-knot nematode aggregation using pluronic F-127 gel**. *J Chem Ecol* 2009, **35**:1242-1251.

79. Ali JG, Alborn HT, Stelinski LL: **Constitutive and induced subterranean plant volatiles attract both entomopathogenic and plant parasitic nematodes**. *J Ecol* 2011, **99**:26-35.

80. Fudali SL, Wang C, Williamson VM: **Ethylene signaling pathway modulates attractiveness of host roots to the root-knot nematode *Meloidogyne hapla***. *Mol Plant Microbe Interact* 2013, **26**:75-86.

81. •• Dong L, Li X, Huang L, Gao Y, Zhong L, Zheng Y, Zuo Y: **Lauric acid in crown daisy root exudate potently regulates root-knot nematode chemotaxis and disrupts *Mi-flp-18* expression to block infection**. *J Exp Bot* 2014, **65**:131-141.
Previous studies have shown that when tomato plants are intercropped with the crown daisy plant, the tomato plant is protected from parasitism by the root-knot nematode *Meloidogyne incognita*. This study identifies a compound, lauric acid, in the crown daisy plant that attracts *M. incognita* at low concentrations and interferes with FMRFamide signaling to alter the parasite's behavior and infectivity. By enhancing our understanding of how intercropping protects against plant-parasitic nematodes, these results could lead to new strategies for protecting crops without the use of pesticides.

82. Mejia R, Nutman TB: **Screening, prevention, and treatment for hyperinfection syndrome and disseminated infections caused by *Strongyloides stercoralis***. *Curr Opin Infect Dis* 2012, **25**:458-463.

83. Safer D, Brenes M, Dunipace S, Schad G: **Urocanic acid is a major chemoattractant for the skin-penetrating parasitic nematode *Strongyloides stercoralis***. *Proc Natl Acad Sci USA* 2007, **104**:1627-1630.

84. •• Castelletto ML, Gang SS, Okubo RP, Tselikova AA, Nolan TJ, Platzer EG, Lok JB, Hallem EA: **Diverse host-seeking behaviors of skin-penetrating nematodes**. *PLoS Pathog* 2014, **10**:e1004305.
This study shows that mammalian-parasitic nematodes respond to many odorants found in human skin and sweat. The study also shows that the odor preferences of parasitic nematodes are shaped by their host preferences and infection routes rather than their phylogeny, suggesting that odor preferences have evolved to complement parasitic behavior.

85. Chaisson KE, Hallem EA: **Chemosensory behaviors of parasites**. *Trends Parasitol* 2012, **28**:427-436.

86. O'Connor LJ, Walkden-Brown SW, Kahn LP: **Ecology of the free-living stages of major trichostrongylid parasites of sheep**. *Vet Parasitol* 2006, **142**:1-15.

87. McGaughran A, Morgan K, Sommer RJ: **Natural variation in chemosensation: lessons from an island nematode**. *Ecol Evol* 2013, **3**:5209-5224.

88. Hong RL, Sommer RJ: **Chemoattraction in *Pristionchus nematodes* and implications for insect recognition**. *Curr Biol* 2006, **16**:2359-2365.

89. Hong RL, Witte H, Sommer RJ: **Natural variation in *Pristionchus pacificus* insect pheromone attraction involves the protein kinase EGL-4**. *Proc Natl Acad Sci USA* 2008, **105**:7779-7784.

90. • Lee J, Dillman AR, Hallem EA: **Temperature-dependent changes in the host-seeking behaviors of parasitic nematodes**. *BMC Biol* 2016, **14**:36.
This study demonstrates that the odor preferences of parasitic nematodes are plastic and are shaped by age and cultivation temperature. These changes in olfactory behavior may enable the long-lived parasitic infective larvae to efficiently locate hosts despite seasonal changes in host-emitted or host-associated odors.

91. Li J, Zhu X, Boston R, Ashton FT, Gamble HR, Schad GA: **Thermotaxis and thermosensory neurons in infective larvae of *Haemonchus contortus*, a passively ingested nematode parasite**. *J Comp Neurol* 2000, **424**:58-73.

92. Bumbarger DJ, Riebesell M, Rodelsperger C, Sommer RJ: **System-wide rewiring underlies behavioral differences in predatory and bacterial-feeding nematodes**. *Cell* 2013, **152**:109-119.

93. Venkatachalam V, Ji N, Wang X, Clark C, Mitchell JK, Klein M, Tabone CJ, Florman J, Ji H, Greenwood J *et al.*: **Pan-neuronal imaging in roaming *Caenorhabditis elegans***. *Proc Natl Acad Sci USA* 2016, **113**:E1082-E1088.

94. Prevedel R, Yoon YG, Hoffmann M, Pak N, Wetzstein G, Kato S, Schrodel T, Raskar R, Zimmer M, Boyden ES *et al.*: **Simultaneous whole-animal 3D imaging of neuronal activity using light-field microscopy**. *Nat Methods* 2014, **11**:727-730.

95. Schrodel T, Prevedel R, Aumayr K, Zimmer M, Vaziri A: **Brain-wide 3D imaging of neuronal activity in *Caenorhabditis elegans* with sculpted light**. *Nat Methods* 2013, **10**:1013-1020.

96. Nguyen JP, Shipley FB, Linder AN, Plummer GS, Liu M, Setru SU, Shaevitz JW, Leifer AM: **Whole-brain calcium imaging with cellular resolution in freely behaving *Caenorhabditis elegans***. *Proc Natl Acad Sci USA* 2016, **113**:E1074-E1081.

Chapter 2

O_2-sensing neurons control CO_2 response in *C. elegans*

Cellular/Molecular

O_2-Sensing Neurons Control CO_2 Response in *C. elegans*

Mayra A. Carrillo,* Manon L. Guillermin,* Sophie Rengarajan, Ryo P. Okubo, and Elissa A. Hallem
Department of Microbiology, Immunology, and Molecular Genetics, University of California, Los Angeles, Los Angeles, California 90095

Sensory behaviors are often flexible, allowing animals to generate context-appropriate responses to changing environmental conditions. To investigate the neural basis of behavioral flexibility, we examined the regulation of carbon dioxide (CO_2) response in the nematode *Caenorhabditis elegans*. CO_2 is a critical sensory cue for many animals, mediating responses to food, conspecifics, predators, and hosts (Scott, 2011; Buehlmann et al., 2012; Chaisson and Hallem, 2012). In *C. elegans*, CO_2 response is regulated by the polymorphic neuropeptide receptor NPR-1: animals with the N2 allele of *npr-1* avoid CO_2, whereas animals with the Hawaiian (HW) allele or an *npr-1* loss-of-function (*lf*) mutation appear virtually insensitive to CO_2 (Hallem and Sternberg, 2008; McGrath et al., 2009). Here we show that ablating the oxygen (O_2)-sensing URX neurons in *npr-1*(*lf*) mutants restores CO_2 avoidance, suggesting that NPR-1 enables CO_2 avoidance by inhibiting URX neurons. URX was previously shown to be activated by increases in ambient O_2 (Persson et al., 2009; Zimmer et al., 2009; Busch et al., 2012). We find that, in *npr-1*(*lf*) mutants, O_2-induced activation of URX inhibits CO_2 avoidance. Moreover, both HW and *npr-1*(*lf*) animals avoid CO_2 under low O_2 conditions, when URX is inactive. Our results demonstrate that CO_2 response is determined by the activity of O_2-sensing neurons and suggest that O_2-dependent regulation of CO_2 avoidance is likely to be an ecologically relevant mechanism by which nematodes navigate gas gradients.

Introduction

Animals from nematodes to humans respond to environmental gases, such as CO_2 and O_2. CO_2 is aversive for many free-living animals but attractive for many parasitic animals, which rely on CO_2 for host location (Luo et al., 2009; Chaisson and Hallem, 2012). O_2 increases or decreases can evoke avoidance responses in flies and nematodes (Chang et al., 2006; Morton, 2011) and alter foraging and feeding behaviors (Wingrove and O'Farrell, 1999; Cheung et al., 2005; Rogers et al., 2006; Vigne and Frelin, 2010). These responses are critical for survival: exposure to hypercapnia, hyperoxia, or hypoxia can result in reduced neural activity, cell cycle arrest, tumor formation, or death (Wingrove and O'Farrell, 1999; Harris, 2002; West, 2004; Langford, 2005).

The nematode *Caenorhabditis elegans* detects and responds to changes in environmental CO_2 and O_2 (Scott, 2011). *C. elegans* adults migrate away from a CO_2 source and toward ~10% O_2 (Gray et al., 2004; Bretscher et al., 2008; Hallem and Sternberg, 2008). However, CO_2 response can vary with developmental stage and environmental context. For example, CO_2 is repulsive for adults but attractive for dauer larvae (Hallem et al., 2011a), and the behavioral response to simultaneous changes in CO_2 and O_2 levels is indicative of an interaction between the responses to the two gases (Bretscher et al., 2008; McGrath et al., 2009).

The response of *C. elegans* to CO_2 and many other stimuli is regulated by NPR-1, a polymorphic neuropeptide receptor homologous to mammalian neuropeptide Y receptors (de Bono and Bargmann, 1998; Gray et al., 2004; Rogers et al., 2006; Bretscher et al., 2008; Hallem and Sternberg, 2008; Macosko et al., 2009; McGrath et al., 2009; Reddy et al., 2009). The N2 strain of *C. elegans* contains an *npr-1* allele that confers solitary feeding behavior, whereas the CB4856 Hawaiian (HW) strain contains an *npr-1* allele that confers social feeding behavior (de Bono and Bargmann, 1998). N2 animals respond strongly to CO_2 but weakly to O_2 on food, whereas HW animals appear relatively indifferent to CO_2 but respond strongly to O_2 on food (Gray et al., 2004; Bretscher et al., 2008; Hallem and Sternberg, 2008). NPR-1 is thought to act by repressing neural activity (Chang et al., 2006; Macosko et al., 2009).

To investigate the mechanisms of CO_2 response plasticity, we examined the regulation of CO_2 response by NPR-1. We show that HW and *npr-1*(*lf*) animals do not avoid CO_2 despite showing normal CO_2-evoked activity in BAG neurons. However, ablation of URX neurons in *npr-1*(*lf*) animals restores CO_2 avoidance, suggesting that NPR-1 enables CO_2 avoidance by decreasing URX activity. URX is activated by increases in ambient O_2 (Persson et al., 2009; Zimmer et al., 2009; Busch et al., 2012), and we show that its O_2-sensing ability is required to inhibit CO_2 avoidance. We also show that HW and *npr-1*(*lf*) animals avoid CO_2 under low O_2 conditions, when URX is inactive. Our results

Received Sept. 24, 2012; revised April 21, 2013; accepted April 27, 2013.

Author contributions: M.A.C., M.L.G., S.R., and E.A.H. designed research; M.A.C., M.L.G., S.R., R.P.O., and E.A.H. performed research; M.A.C., M.L.G., S.R., and E.A.H. analyzed data; M.A.C., M.L.G., and E.A.H. wrote the paper.

M.A.C. was supported by a National Science Foundation Graduate Research Fellowship (Grant No. DGE-0707424) and a Eugene V. Cota-Robles Fellowship. S.R. was supported by the National Institutes of Health National Institute of General Medical Sciences training Grant GM08042 and the UCLA-Cal Tech Medical Scientist Training Program. E.A.H. is a MacArthur Fellow, an Alfred P. Sloan Research Fellow, a Rita Allen Foundation Scholar, and a Searle Scholar. This work was supported by a National Institutes of Health R00 Grant to E.A.H (Grant No. R00-AI085107). We thank Cori Bargmann, Alon Zaslaver, Paul Sternberg, Jo Anne Powell-Coffman, Miriam Goodman, Maureen Barr, Ikue Mori, Mario de Bono, Shawn Lockery, Shohei Mitani, and the Caenorhabditis Genetics Center for *C. elegans* strains; Cori Bargmann, Alon Zaslaver, and Paul Sternberg for plasmids; Lars Dreier, Michelle Castelletto, Alvaro Sagasti, Doug Black, and Keely Chaisson for critical reading of this manuscript; and Joe Vanderwaart for insightful discussion of this manuscript.

The authors declare no competing financial interests.

*M.A.C. and M.L.G. contributed equally to this work.

Correspondence should be addressed to Dr. Elissa A. Hallem, University of California, Los Angeles, MIMG 237 BSRB, 615 Charles E. Young Drive East, Los Angeles, CA 90095. E-mail: ehallem@microbio.ucla.edu.

DOI:10.1523/JNEUROSCI.4541-12.2013

 0270-6474/13/339675-09$15.00/0

suggest that CO_2 avoidance is regulated by ambient O_2 via a pair of O_2-sensing neurons, allowing flexible responses to fluctuating levels of environmental gases.

Materials and Methods

Strains. C. elegans strains are listed in the order in which they appear in the figures. The following strains were used: N2 (Bristol); DA609 *npr-1(ad609);* CB4856 (Hawaiian); CX11697 *kyIs536[flp-17::p17 SL2 GFP, elt-2::mCherry]; kyIs538[glb-5::p12 SL2 GFP, elt-2::mCherry]*; EAH2 *gcy-9(tm2816)*; PS6416 *pha-1(e2123); syEx1206[gcy-33::G-CaMP3.0, pha-1(+)]*; EAH117 *npr-1(ad609); syEx1206[gcy-33::G-CaMP3.0, pha-1(+)]*; EAH119 *bruEx89[gcy-33::G-CaMP-3.0, ets-8::GFP]*; MT17148 *flp-21(ok889); flp-18(n4766)*; PR767 *ttx-1(p767)*; GN112 *pgIs2[gcy-8::caspase, unc-122::GFP]*; PR679 *che-1(p679)*; MT18636 *nIs326[gcy-33::YC3.60]; lin-15AB(n765)*; AX2047 *gcy-8::YC3.60, unc-122::dsRed*; XL115 *flp-6::YC3.60*; CX9592 *npr-1(ad609); kyEx2016[npr-1::npr-1 SL2 GFP, ofm-1::dsRed]*; CX9395 *npr-1(ad609); kyEx1965[gcy-32::npr-1 SL2 GFP, ofm-1::dsRed]*; CX9633 *npr-1(ad609); kyEx2096[flp-8::npr-1 SL2 GFP, ofm-1::dsRed]*; CX9396 *npr-1(ad609); kyEx1966[flp-21::npr-1 SL2 GFP, ofm-1::dsRed]*; CX9644 *npr-1(ad609); kyEx2107[ncs-1::npr-1 SL2 GFP, ofm-1::dsRed]*; CX7102 *lin-15(n765) qaIs2241[gcy-36::egl-1, gcy-35::GFP, lin-15(+)]*; CX7158 *npr-1(ad609) qaIs2241[gcy-36::egl-1, gcy-35::GFP, lin-15(+)]*; ZG629 *iaIs22[gcy-36::GFP, unc-119(+)]*; EAH80 *iaIs22[gcy-36::GFP, unc-119(+)]; npr-1(ad609)*; EAH106 *bruEx86[gcy-36::G-CAMP3.0, coel::RFP]*; EAH114 *npr-1(ad609)*; *bruEx86[gcy-36::G-CaMP3.0, coel::RFP]*; ZG24 *ahr-1(ia3)*; ZG624 *ahr-1(ia3); npr-1(ad609)*; CX6448 *gcy-35(ok769)*; CX7157 *gcy-35(ok769); npr-1(ad609)*; RB1902 *flp-19(ok2460)*; PT501 *flp-8(pk360)*; PT502 *flp-10(pk367)*; EAH123 *npr-1(ad609) flp-19(ok2460)*; EAH141 *npr-1(ad609) flp-8(pk360);* EAH140 *flp-10(pk367); npr-1(ad609);* PS5892 *gcy-33(ok232); gcy-31(ok296)*; EAH127 *gcy-33(ok232); gcy-31(ok296) lon-2(e678) npr-1(ad609).* In addition, CX7376 *kyIs511[gcy-36::G-CaMP, coel::GFP]* and EAH115 *kyIs511[gcy-36::G-CaMP, coel::GFP]; npr-1(ad609)* were used to confirm the results shown in Figure 5*A* with independent transgenes, and RB1903 *flp-19(ok2461)* and EAH139 *npr-1(ad609) flp-19(ok2461)* were used to confirm the results shown in Figure 5*C* with an independent deletion allele of *flp-19*. All transgenes were injected into N2, except *bruEx89*, which was injected into CB4856 to generate EAH119. EAH2 was derived from FX2816 by outcrossing to N2 for five generations. Nematodes were cultured on NGM plates containing *Escherichia coli* OP50 according to standard methods (Brenner, 1974). *C. elegans* dauer larvae were collected from the lids of plates from which the OP50 food source had been depleted ("starved plates") and stored in dH_2O at 15°C before use. All nematodes tested were hermaphrodites.

Generation of reporter transgenes and transgenic animals. To generate EAH119, the *gcy-33::G-CaMP3.0* construct from PS6416 was injected into CB4856 at 50 ng/μl along with *ets-8::GFP* at 50 ng/μl as a coinjection marker. To generate EAH106, a *gcy-36::G-CaMP3.0* transcriptional fusion construct was generated by amplifying a 1.0 kb region upstream of the start codon of the *gcy-36* gene from N2 genomic DNA using primers that included the following sequences: 5′-gatgttggtagatggggtttgga-3′ and 5′-aaattcaaacaagggctacccaaca-3′. The promoter fragment was then cloned into a modified Fire vector containing the G-CaMP3.0 coding region (Tian et al., 2009). The *gcy-36::G-CaMP3.0* construct was injected into N2 animals at a concentration of 25 ng/μl along with 50 ng/μl of *coel::RFP* as a coinjection marker.

Acute CO_2 avoidance assays. Acute CO_2 avoidance assays were performed as previously described (Hallem and Sternberg, 2008; Guillermin et al., 2011; Hallem et al., 2011b). Briefly, ~10–15 young adults were tested on 5 cm assay plates consisting of NGM agar seeded with a thin lawn of *E. coli* OP50 bacteria. Gas stimuli consisted of certified industrial mixes (Airgas or Air Liquide). CO_2 stimuli consisted of 10% CO_2, 10% O_2 (unless otherwise indicated), and the rest N_2. Control stimuli consisted of 10% O_2 (unless otherwise indicated) and the rest N_2. Two 50 ml gas-tight syringes were filled with gas: one with CO_2 and one without CO_2. The mouths of the syringes were connected to flexible PVC tubing attached to Pasteur pipettes, and gases were pumped through the Pasteur pipettes using a syringe pump at a rate of 1.5 ml/min. Worms were exposed to gases by placing the tip of the Pasteur pipette near the head of a forward-moving worm, and a response was scored if the worm reversed within 4 s. Gases were delivered blindly, and worms were scored blindly. An avoidance index was calculated by subtracting the fraction of animals that reversed to the air control from the fraction that reversed to the CO_2. Single-worm acute CO_2 avoidance assays were performed on L4 or young adult laser-ablated animals (see Fig. 3*C*) as described above, except that each animal was tested 12 times with >2 min between trials. For each animal, an avoidance index was calculated by subtracting the fraction of trials in which it reversed to the air control from the fraction of trials in which it reversed to the CO_2 stimulus. The avoidance index for each genotype or treatment was calculated as the mean avoidance index for each animal of the same genotype or treatment.

CO_2 chemotaxis assays. CO_2 chemotaxis assays were performed on young adults essentially as previously described (Bretscher et al., 2008). Briefly, animals were washed off plates and into a 65 mm Syracuse watch glass using M9 buffer. Animals were washed 3× with M9 and transferred from the watch glass to a 1 cm × 1 cm square of Whatman paper. Animals were then transferred from the filter paper to the center of a 9 cm NGM or chemotaxis plate (Bargmann et al., 1993). Gas stimuli were delivered to the plate though holes in the plate lids as previously described (Hallem et al., 2011a; Dillman et al., 2012), except at a flow rate of 2 ml/min. Assay plates were placed on a vibration-reducing platform for 20 min. The number of worms in a 2-cm-diameter circle centered under each gas inlet was then counted, except for Figures 1*B* and 2*A*, *B*, where the number of worms in an area comprising ~3/10 of the plate under each gas inlet was counted. The chemotaxis index was calculated as follows: (no. of worms at CO_2 − no. of worms at control)/(no. of worms at CO_2 + control). Two identical assays were always performed simultaneously with the CO_2 gradient in opposite directions on the two plates to control for directional bias resulting from room vibration; assays were discarded if the difference in the chemotaxis index for the two plates was ≥0.9 or if <7 worms moved into the scoring regions on one or both of the plates.

For CO_2 chemotaxis assays under different O_2 conditions, assays were performed as described above inside airtight canisters (OGGI; 13.3 cm × 10.1 cm) with four holes drilled into the lids to insert tubing for gas flow. One hole was used to establish the ambient O_2 level, two were used to establish the CO_2 gradient, and one was used as an exhaust. A gas mixture consisting of either 7% O_2 and the balance N_2, or 21% O_2 and the balance N_2, was pumped into the chamber at a rate of 2.5 L/min for 1 min and then 0.5 L/min for the duration of the assay. The CO_2 stimulus (10% CO_2, either 7% O_2 or 21% O_2, balance N_2) and control stimulus (7% O_2 or 21% O_2, balance N_2) were pumped into the chamber at a rate of 2 ml/min using a syringe pump, as described above. The assay duration was 25 min.

Dauer CO_2 chemotaxis assays were performed as previously described (Hallem et al., 2011a; Dillman et al., 2012). Briefly, assays were performed on chemotaxis plates (Bargmann et al., 1993). For each assay, ~50–150 dauers were placed in the center of the assay plate. Gas stimuli and gas delivery to the assay plate were as described above, and a chemotaxis index was calculated as described above.

Calcium imaging. Imaging was performed using the genetically encoded calcium indicators G-CaMP (Zimmer et al., 2009), G-CaMP3.0 (Tian et al., 2009), or yellow cameleon YC3.60 (Nagai et al., 2004). Young adult or L4 animals were immobilized onto a cover glass containing a 2% agarose pad made with 10 mM HEPES using Surgi-Lock 2oc instant tissue adhesive (Meridian). A custom-made gas delivery chamber was placed over the cover glass. Gases were delivered at a rate of 0.8–1 L/min. Gas delivery was controlled by a ValveBank4 controller (AutoMate Scientific). Imaging was performed on an AxioObserver A1 inverted microscope (Carl Zeiss) using a 40× EC Plan-NEOFLUAR lens, a Hamamatsu C9100 EM-CCD camera, and AxioVision software (Carl Zeiss). For YC3.60 imaging, the emission image was passed through a DV2 beam splitter (Photometrics) as previously described (Hallem et al., 2011b). Image analysis was performed using AxioVision software (Carl Zeiss) and Microsoft Excel. The mean pixel value of a background region of interest was subtracted from the mean pixel value of a region of interest containing the neuron soma. Fluorescence values were normalized to the average values obtained in the 4 s before CO_2 delivery. For YC3.60 im-

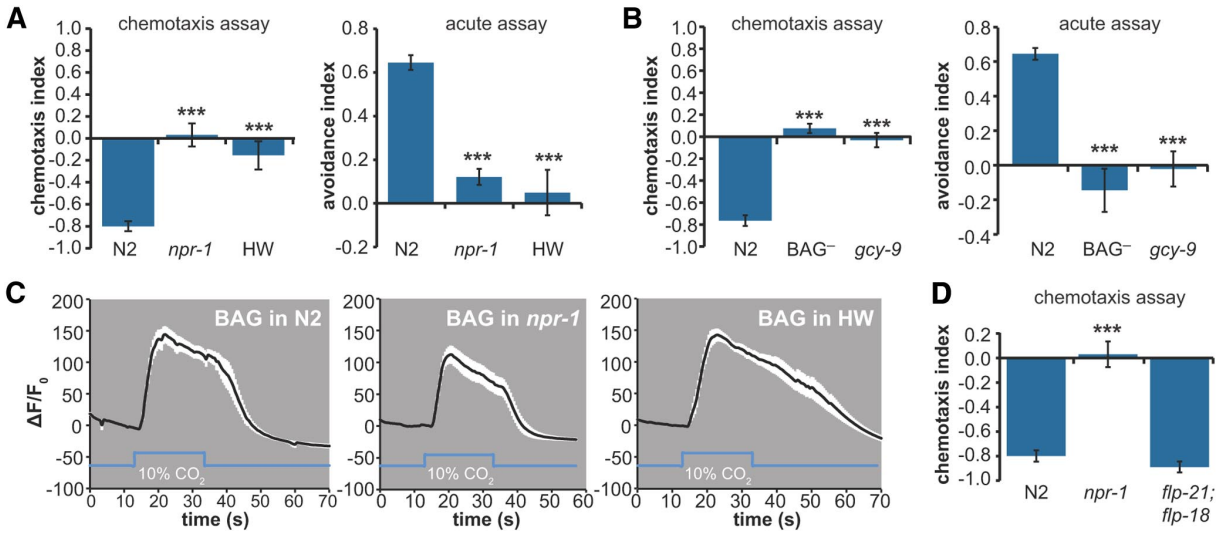

Figure 1. *npr-1* is required for CO_2 avoidance behavior but not CO_2 detection. ***A***, *npr-1* is required for CO_2 avoidance by adults. Left, CO_2 chemotaxis assay. Right, Acute CO_2 avoidance assay. *npr-1*(*lf*) and HW animals do not respond to CO_2 in either assay. ***$p < 0.001$, one-way ANOVA with Bonferroni post-test. $n = 6–9$ trials (chemotaxis assay) or 10–27 trials (acute assay) for each genotype. Error bars represent SEM. ***B***, Animals that lack BAG neurons and *gcy-9*(*tm2816*) mutant animals do not respond to CO_2. BAG-ablated animals express a transgene that specifically kills the BAG neurons (Zimmer et al., 2009; Hallem et al., 2011b). Left, CO_2 chemotaxis assay. Right, Acute CO_2 avoidance assay. The CO_2 stimulus was delivered in an airstream containing 10% O_2, which approximates the preferred O_2 concentration for *C. elegans* (Gray et al., 2004); the control airstream also contained 10% O_2. $n = 18$ or 19 trials (chemotaxis assay) or 4–27 trials (acute assay). ***$p < 0.001$, Kruskal–Wallis test with Dunn's post-test (chemotaxis assay) or one-way ANOVA with Bonferroni post-test (acute assay). Error bars represent SEM. ***C***, *npr-1* is not required for CO_2 detection by BAG neurons. BAG neuron cell bodies of N2 (left), *npr-1*(*lf*) (middle), and HW (right) animals respond to CO_2. Calcium increases were measured using the calcium indicator G-CaMP3.0. Black lines indicate average calcium responses; white shading represents SEM. Blue lines below the traces indicate the timing of the CO_2 pulse. The peak response amplitudes of all three genotypes were not significantly different (one-way ANOVA with Bonferroni post-test). The decay kinetics of all three genotypes were significantly different ($p < 0.001$ using a polynomial curve fit). However, these differences are not likely to be a result of differences at the *npr-1* locus because recordings from BAG neurons of N2 animals using G-CaMP3.0 showed different decay kinetics from BAG neurons of N2 animals using YC3.60 (Fig. 2*C*,*D*). ***D***, The NPR-1 ligands FLP-21 and FLP-18 are not required for CO_2 response. ***$p < 0.001$, one-way ANOVA with Bonferroni post-test. $n = 6–9$ animals for each genotype. Error bars represent SEM.

aging, the YFP/CFP ratio was calculated as previously described (Hallem et al., 2011b). Images were baseline corrected using a linear baseline correction. Traces with unstable baselines before the onset of the CO_2 stimulus were discarded.

Laser ablation. Ablations were performed on L2 and L3 animals as previously described (Hallem and Sternberg, 2008). Briefly, animals were mounted on glass slides for DIC microscopy on a pad consisting of 5% Noble agar in dH_2O with 5% sodium azide as anesthetic. Ablations were performed on a Zeiss AxioImager A2 microscope with an attached MicroPoint laser (Carl Zeiss). Neurons were ablated by focusing a laser microbeam on the cell. Mock-ablated animals were mounted similarly but were not subjected to a laser microbeam. Neurons were identified by both cell position and GFP expression. Loss of the ablated cell was confirmed by observing loss of fluorescence in the adult animal.

Fluorescence microscopy. Nematodes were anesthetized with 3 mM levamisole and mounted on a pad consisting of 5% Noble agar in dH_2O. Epifluorescence images were captured using a Zeiss AxioImager A2 microscope with an attached Zeiss AxioCam camera and Zeiss AxioVision software (Carl Zeiss). To quantify epifluorescence in Figure 4*D*, all images were taken with the same exposure time. Average pixel intensities in the region of interest were quantified using AxioVision software (Carl Zeiss). Relative intensities were normalized by setting the highest mean intensity value to 1.

Statistical analysis. Statistical analysis was performed using GraphPad Instat and Prism. All significance values reported are relative to the N2 control, unless otherwise indicated.

Results

NPR-1 regulates CO_2 avoidance behavior

To investigate the role of *npr-1* in mediating CO_2 response, we examined the CO_2-evoked behavior of N2, HW, and *npr-1*(*lf*) animals in both a chemotaxis assay and an acute avoidance assay. We found that N2 animals displayed robust CO_2 avoidance in both assays, whereas HW and *npr-1*(*lf*) animals were essentially unresponsive to CO_2 in both assays (Fig. 1*A*). Thus, the N2 allele of *npr-1* is required for the behavioral response to CO_2. CO_2 avoidance behavior also requires the CO_2-detecting BAG neurons and the receptor guanylate cyclase gene *gcy-9,* which encodes a putative receptor for CO_2 or a CO_2 metabolite (Fig. 1*B*) (Hallem and Sternberg, 2008; Hallem et al., 2011b; Brandt et al., 2012). To test whether *npr-1* is required for CO_2 detection, we imaged from BAG neurons using the genetically encoded calcium indicator G-CaMP3.0 (Tian et al., 2009). We found that the BAG neurons of N2, *npr-1*(*lf*), and HW animals all showed CO_2-evoked activity (Fig. 1*C*), suggesting that *npr-1* regulates the behavioral response to CO_2 downstream of the calcium response of BAG neurons. The *flp-21* and *flp-18* genes, which encode NPR-1 ligands, are not required for CO_2 avoidance, suggesting that other ligands are required for the regulation of CO_2 response by *npr-1* (Fig. 1*D*).

In addition to the BAG neurons, the salt-sensing ASE neurons and the temperature-sensing AFD neurons have been implicated in CO_2 detection and avoidance (Bretscher et al., 2011). However, we found that *che-1* mutant animals, which lack functional ASE neurons (Uchida et al., 2003), displayed normal CO_2 avoidance in both a chemotaxis assay and an acute assay (Fig. 2*A*) (Hallem and Sternberg, 2008). Both AFD-ablated animals and *ttx-1* mutant animals, which lack functional AFD neurons (Satterlee et al., 2001), showed defective CO_2 avoidance in a chemotaxis assay but not an acute assay (Fig. 2*A*) (Hallem and Sternberg, 2008). These results suggest that ASE neurons are not required for CO_2 avoidance under our assay conditions and that AFD neurons are required for some but not all CO_2-evoked be-

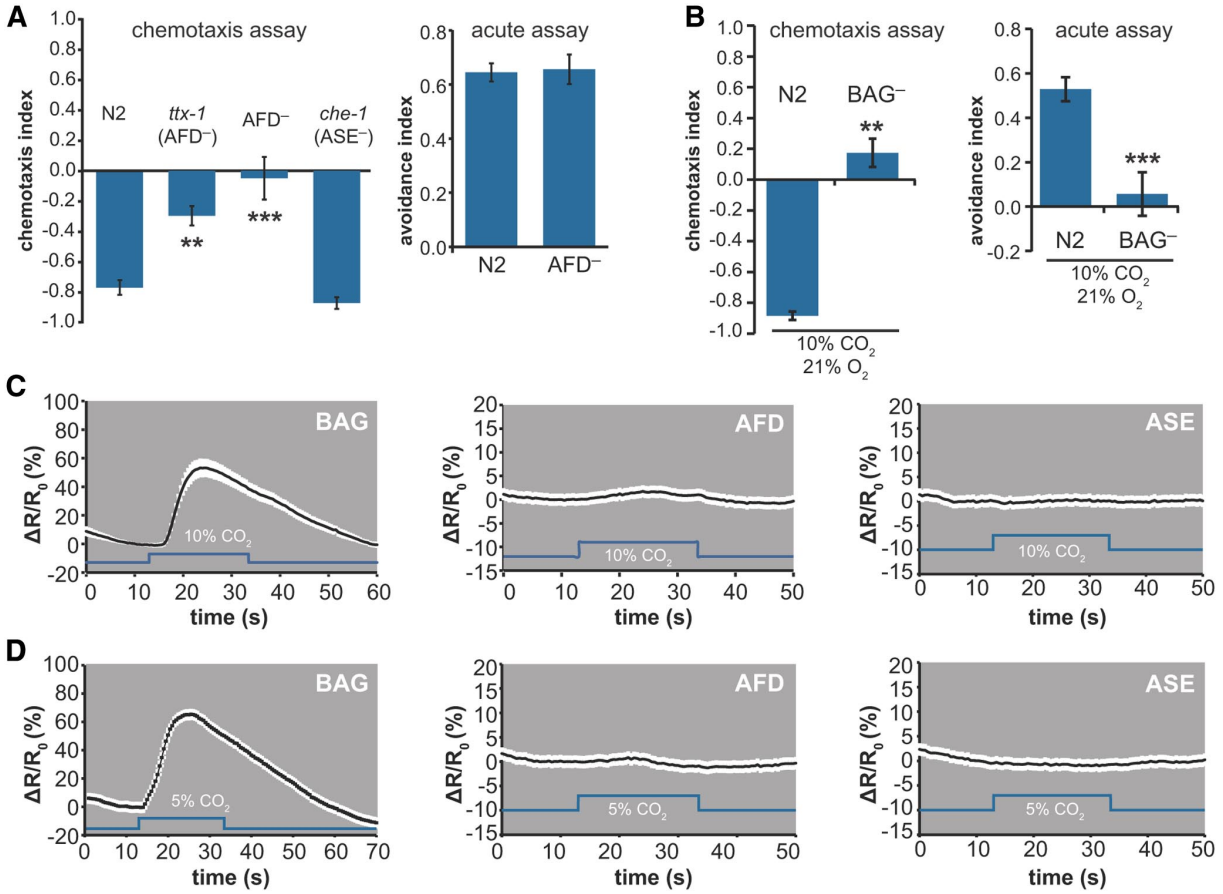

Figure 2. The role of AFD, ASE, and BAG neurons in CO_2 response. ***A***, Animals that lack functional ASE neurons respond normally to CO_2 in both a chemotaxis assay (left graph) and an acute avoidance assay (Hallem and Sternberg, 2008). Animals that lack functional AFD neurons respond normally to CO_2 in an acute avoidance assay (right) but not a chemotaxis assay (left). AFD-ablated animals (AFD^-) express a transgene that specifically kills the AFD neurons (Glauser et al., 2011). The *ttx-1* and *che-1* genes encode transcription factors that are required for normal development of the AFD and ASE neurons, respectively (Satterlee et al., 2001; Uchida et al., 2003; Hobert, 2010). $^{**}p < 0.01$, Kruskal–Wallis test with Dunn's post-test. $^{***}p < 0.001$, Kruskal–Wallis test with Dunn's post-test. $n = 10–18$ trials (chemotaxis assay) or $n = 9–27$ trials (acute assay) for each genotype. Error bars represent SEM. ***B***, Animals that lack BAG neurons do not respond to CO_2 when the CO_2 stimulus is delivered in an airstream containing 21% O_2, which approximates the atmospheric O_2 concentration. The control airstream also contained 21% O_2. $^{**}p < 0.01$, Mann–Whitney test. $^{***}p < 0.001$, one-way ANOVA with Bonferroni post-test. $n = 4–11$ trials (chemotaxis assay) or $n = 10–27$ trials (acute assay). Error bars represent SEM. ***C***, ***D***, Calcium responses of BAG, AFD, and ASE neurons to 10% CO_2 (***C***) and 5% CO_2 (***D***), measured using the ratiometric calcium indicator yellow cameleon YC3.60. Black lines indicate average calcium responses; white shading represents SEM. Blue lines below the traces indicate the timing of the CO_2 pulse. Calcium increases were observed in BAG neuron cell bodies but not AFD and ASE neuron cell bodies. $n = 5–13$ animals for each genotype.

haviors. By contrast, animals lacking BAG neurons showed a complete loss of CO_2 response in both assays, regardless of whether CO_2 was delivered in combination with 10% O_2, which approximates the preferred O_2 concentration of *C. elegans* (Gray et al., 2004), or 21% O_2, which approximates atmospheric O_2 concentration (Figs. 1*B* and 2*B*). We then imaged from BAG, ASE, and AFD neurons using the calcium indicator yellow cameleon YC3.60 (Nagai et al., 2004). We observed CO_2-evoked activity in BAG neurons but not AFD and ASE neurons in response to a 20 s pulse of either 5% or 10% CO_2 (Fig. 2*C*,*D*). Thus, BAG neurons are the primary sensory neurons that contribute to CO_2 response under our assay conditions.

NPR-1 regulates URX neuron activity to control CO_2 avoidance behavior

NPR-1 is not expressed in BAG neurons but is expressed in a number of other sensory neurons as well as some interneurons (Macosko et al., 2009). To identify the site of action for the regulation of CO_2 response by *npr-1*, we introduced the N2 allele of *npr-1* into *npr-1*(*lf*) mutants in different subsets of neurons and assayed CO_2 response. We found that expressing *npr-1* in neuronal subsets that included the O_2-sensing URX neurons (Cheung et al., 2004; Gray et al., 2004) restored CO_2 response (Fig. 3*A*). These results suggest that NPR-1 activity in URX neurons is sufficient to enable CO_2 avoidance. However, we cannot exclude the possibility that NPR-1 function in other neurons also contributes to CO_2 avoidance.

To further investigate the role of the URX neurons in regulating CO_2 response, we ablated URX neurons in both the N2 and *npr-1*(*lf*) backgrounds and assayed CO_2 avoidance behavior. We found that either genetic ablation of a neuronal subset that includes URX or specific laser ablation of URX in the N2 background had no effect on CO_2 avoidance (Fig. 3*B*,*C*). However, both genetic and laser ablation of URX in *npr-1*(*lf*) mutants restored CO_2 avoidance (Fig. 3*B*,*C*). Moreover, the response of URX-ablated *npr-1*(*lf*) animals was not significantly different from the response of URX-ablated N2 animals in our laser ablation experiment (Fig. 3*C*). Thus, in *npr-1*(*lf*) mutants, URX neu-

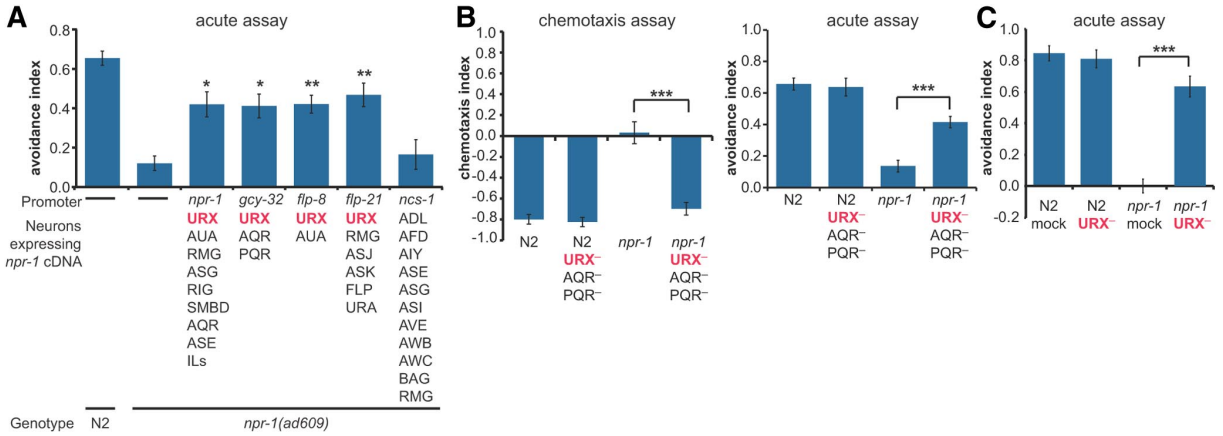

Figure 3. *npr-1* appears to act in URX neurons to regulate CO_2 avoidance. ***A***, Expression of *npr-1* cDNA from N2 animals in subsets of neurons that include URX restores CO_2 avoidance to *npr-1*(*lf*) mutants in an acute CO_2 avoidance assay. $^*p < 0.05$, relative to the *npr-1*(*lf*) mutant (one-way ANOVA with Bonferroni post-test). $^{**}p < 0.01$, relative to the *npr-1*(*lf*) mutant (one-way ANOVA with Bonferroni post-test). $n = 16–27$ trials for each genotype. Full expression patterns for each transgene were previously described (Macosko et al., 2009). ***B***, Genetic ablation of a subset of neurons that includes URX in *npr-1*(*lf*) mutants restores CO_2 avoidance. Left, CO_2 chemotaxis assay. Right, Acute CO_2 avoidance assay. $^{***}p < 0.001$, relative to the *npr-1*(*lf*) mutant (one-way ANOVA with Bonferroni post-test). $n = 7$ or 8 trials (chemotaxis assay) or 8–27 trials (acute assay) for each genotype. ***C***, Specific laser ablation of URX neurons in *npr-1*(*lf*) mutants restores CO_2 avoidance in an acute CO_2 avoidance assay. Ablations were performed on animals expressing a *gcy-36::GFP* transgene to verify the identity of the URX neurons. $^{***}p < 0.001$ (one-way ANOVA with Bonferroni post-test). The responses of mock-ablated N2 animals, URX-ablated N2 animals, and URX-ablated *npr-1* animals were not significantly different ($p > 0.05$). $n = 7–10$ trials for each treatment. For all graphs, error bars represent SEM.

rons inhibit CO_2 avoidance and removal of URX neurons is sufficient to restore CO_2 avoidance. Our results suggest a model in which CO_2 avoidance behavior is regulated by URX neuron activity. In N2 animals, NPR-1 reduces URX neuron activity, thereby enabling CO_2 avoidance. In *npr-1*(*lf*) animals, increased activity of URX neurons inhibits the CO_2 circuit, resulting in a loss of CO_2 avoidance.

URX neurons are not required for CO_2 attraction by dauers

In contrast to *C. elegans* adults and developing larvae, *C. elegans* dauer larvae are attracted to CO_2 (Fig. 4*A*) (Guillermin et al., 2011; Hallem et al., 2011a). The dauer is a developmentally arrested, alternative third larval stage that is thought to be analogous to the infective juvenile stage of parasitic nematodes (Hotez et al., 1993). The mechanism responsible for the change in CO_2 response valence that occurs at the dauer stage is not yet known. BAG neurons and the putative CO_2 receptor GCY-9 are required for CO_2 attraction by dauers (Fig. 4*A*) (Hallem et al., 2011a), suggesting that the same mechanism of CO_2 detection operates at the dauer and adult stages. However, *npr-1*(*lf*) and HW dauers are also attracted to CO_2, indicating that *npr-1* is not required for CO_2 attraction (Fig. 4*B*). The lack of requirement for *npr-1* at the dauer stage is not the result of altered *npr-1* expression in URX neurons because *npr-1* is expressed at comparable levels in N2 dauers and developing third-stage larvae (L3s) (Fig. 4*C*,*D*). To test whether URX neuron activity is required for CO_2 attraction by dauers, we tested whether dauers that lack URX neurons are still attracted to CO_2. We found that URX-ablated N2 and *npr-1*(*lf*) dauers display normal CO_2 attraction (Fig. 4*E*), indicating that URX neurons are not required to promote CO_2 attraction by dauers. Thus, URX neurons control whether CO_2 is a repulsive or neutral stimulus in adults, but other mechanisms are required to promote CO_2 attraction by dauers.

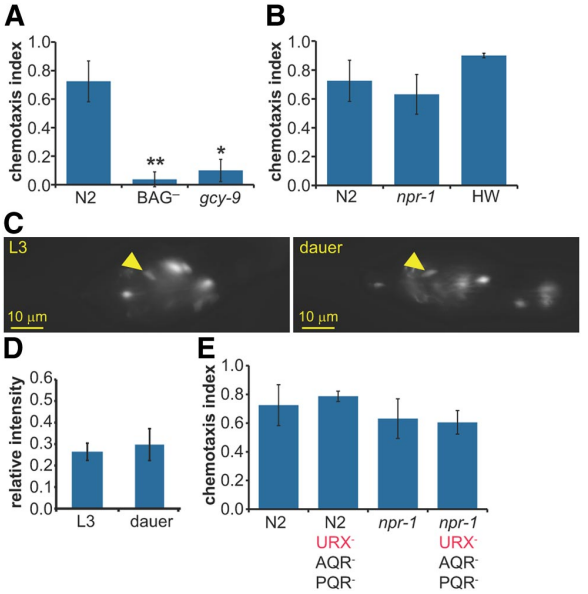

Figure 4. Mechanisms of CO_2 attraction by dauers. ***A***, BAG neurons and the receptor guanylate cyclase gene *gcy-9* are required for CO_2 attraction by dauers. $^*p < 0.05$ (Kruskal–Wallis test with Dunn's post-test). $^{**}p < 0.01$ (Kruskal–Wallis test with Dunn's post-test). $n = 4–12$ trials. ***B***, *npr-1* is not required for CO_2 attraction by dauers. $n = 4–8$ trials. ***C***, Epifluorescence images of *npr-1* expression in the URX neurons of L3 (left) and dauer (right) larvae in the N2 background. *npr-1* expression was assayed in *npr-1* animals containing an *npr-1::npr-1 SL2 GFP* transgene (Macosko et al., 2009). Arrowheads indicate the location of the URX neuron cell body. Anterior is to the left. ***D***, *npr-1* expression in the URX neurons of L3 and dauer larvae is not significantly different (unpaired *t* test). $n = 17–20$ animals. ***E***, URX neurons are not required for CO_2 attraction by dauers. Both N2 and *npr-1*(*lf*) dauers containing a genetic ablation of the URX, AQR, and PQR neurons display normal CO_2 attraction. $n = 4–8$ trials for each genotype. For all graphs, error bars represent SEM.

O_2 sensing by URX neurons is required for regulation of CO_2 avoidance

The URX neurons are O_2-sensing neurons that express O_2 receptors of the soluble guanylate cyclase (sGC) family (Cheung et al., 2004; Gray et al., 2004). Whether the URX neurons are also activated by CO_2 is unclear (Bretscher et al., 2011; Brandt et al., 2012). To test whether URX neurons regulate CO_2 response by directly responding to CO_2, we imaged

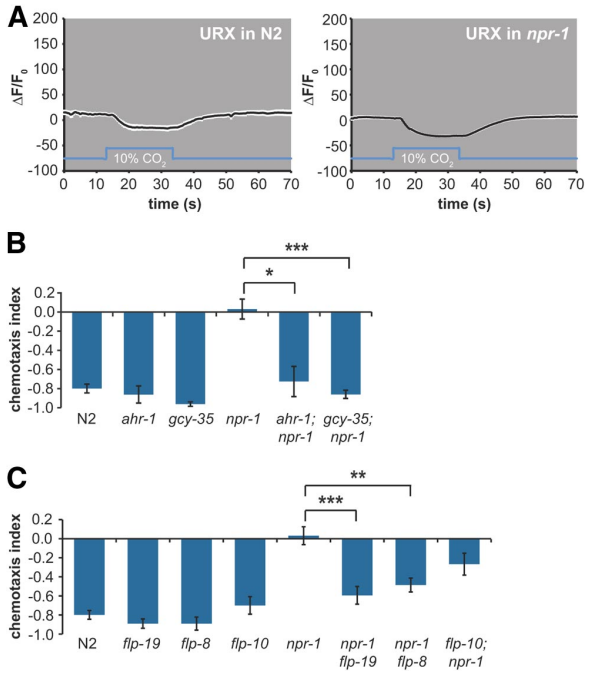

Figure 5. URX neurons mediate O_2-dependent regulation of CO_2 avoidance. ***A***, URX neurons do not respond to CO_2 in either N2 or *npr-1*(*lf*) animals under our imaging conditions. Calcium transients in URX neuron cell bodies were measured using G-CaMP3.0. Black lines indicate average calcium responses; white shading represents SEM. Blue lines below the traces indicate the timing of the CO_2 pulse. $n = 8$ or 9 animals for each genotype. To verify the lack of CO_2 response in URX neurons, we also imaged from N2 and *npr-1*(*lf*) animals containing an independently generated construct that expressed G-CaMP in URX (McGrath et al., 2009); these animals also did not display CO_2-evoked activity in URX (data not shown). ***B***, O_2 sensing by URX neurons is required for regulation of CO_2 avoidance. Mutation of *ahr-1* or *gcy-35* rescues the CO_2 response defect of *npr-1*(*lf*) mutants. $^*p < 0.05$ (Kruskal–Wallis test with Dunn's post-test). $^{***}p < 0.001$ (Kruskal–Wallis test with Dunn's post-test). $n = 4$–9 trials for each genotype. Error bars represent SEM. ***C***, Neuropeptide signaling regulates CO_2 avoidance. Mutation of the URX-expressed neuropeptide genes *flp-8* and *flp-19* significantly rescues the CO_2 response defect of *npr-1*(*lf*) mutants. $^{**}p < 0.01$, relative to the *npr-1*(*lf*) mutant (one-way ANOVA with Bonferroni post-test). $^{***}p < 0.001$, relative to the *npr-1*(*lf*) mutant (one-way ANOVA with Bonferroni post-test). $n = 6$–14 trials. Error bars represent SEM.

from the URX neurons of N2 and *npr-1*(*lf*) animals during CO_2 exposure using the calcium indicator G-CaMP3.0. We found that URX neurons are not activated by CO_2 (Fig. 5*A*). URX neurons did appear to show a slight decrease in calcium levels in response to CO_2, but whether this decrease is biologically relevant is not yet clear. These results indicate that URX neurons do not regulate CO_2 response as a result of CO_2-induced activation.

To test whether URX neurons instead regulate CO_2 response by responding to O_2, we examined the CO_2-evoked behavior of *aryl hydrocarbon receptor-1* (*ahr-1*) mutants. AHR-1 is a transcription factor that regulates aggregation behavior and that is required for normal expression of sGC O_2 receptors in URX neurons (Qin et al., 2006). We found that *ahr-1* mutants respond normally to CO_2 and that the *ahr-1* mutation rescues the CO_2 response defect of *npr-1*(*lf*) mutants (Fig. 5*B*). Thus, regulation of CO_2 avoidance by URX neurons of *npr-1*(*lf*) animals depends on their ability to sense O_2. Furthermore, mutation of the sGC gene *gcy-35*, which encodes an O_2 receptor that is expressed in URX and required for its O_2 response (Zimmer et al., 2009), also rescues the CO_2 response defect of *npr-1* mutants (Fig. 5*B*). Thus, GCY-35-mediated activation of URX neurons by ambient O_2 is required for regulation of CO_2 avoidance behavior. Together, these results demonstrate that CO_2 response is regulated by ambient O_2.

To investigate the mechanism by which URX neurons regulate CO_2 response in *npr-1* mutants, we examined the role of neuropeptide signaling in the regulation of CO_2 avoidance behavior. The URX neurons are known to express FMRFamide-related neuropeptide genes, including *flp-8*, *flp-10*, and *flp-19* (Li and Kim, 2008). To test whether these neuropeptide genes are required for the regulation of CO_2 response, we examined the CO_2-evoked behavior of neuropeptide mutants in the *npr-1*(*lf*) mutant background. We found that mutation of either *flp-8* or *flp-19*, but not *flp-10*, significantly rescued the CO_2 response defect of *npr-1* mutants (Fig. 5*C*). These results are consistent with the hypothesis that URX neurons modulate CO_2 response via a neuropeptide signaling pathway involving *flp-8* and *flp-19*. However, we cannot exclude the possibility that release of *flp-8* and *flp-19* from other neurons also contributes to the O_2-dependent regulation of CO_2 response.

npr-1(*lf*) and HW animals avoid CO_2 under low O_2 conditions

The URX neurons are activated when the ambient O_2 concentration increases from 10% to 21% (Zimmer et al., 2009; Busch et al., 2012). This response consists of both phasic and tonic components: a large initial increase in calcium transients is followed by a smaller sustained increase that continues until O_2 levels return to 10% (Busch et al., 2012). The fact that URX neurons remain active at high O_2 levels but are inactive at low O_2 levels led us to hypothesize that *npr-1*(*lf*) and HW animals might avoid CO_2 under low O_2 conditions, when URX neurons are inactive. We therefore examined the responses of *npr-1*(*lf*) and HW animals to CO_2 under low O_2 conditions by reducing the ambient O_2 concentration to 7% for the duration of the CO_2 chemotaxis assay. We found that, at 7% ambient O_2, both *npr-1*(*lf*) and HW animals displayed CO_2 avoidance behavior that was comparable with that of N2 animals (Fig. 6*A*). Thus, *npr-1*(*lf*) and HW animals are indeed capable of responding robustly to CO_2. However, CO_2 response in these animals is regulated by ambient O_2 such that CO_2 is repulsive at low O_2 concentrations and neutral at high O_2 concentrations.

The BAG neurons, which are activated by CO_2, are also activated by decreases in ambient O_2 from 21% to <10% (Zimmer et al., 2009). This raised the possibility that BAG neurons could cell-autonomously integrate responses to O_2 and CO_2, thus contributing to the O_2-dependent regulation of CO_2 response. To test this possibility, we examined the ability of animals that lack the soluble guanylate cyclase genes *gcy-31* and *gcy-33*, which are expressed in BAG neurons and are required for the O_2-evoked activity of BAG neurons (Zimmer et al., 2009), to respond to CO_2 at low ambient O_2. We found that *gcy-33; gcy-31* mutants responded normally to CO_2 at low ambient O_2 in both N2 and *npr-1*(*lf*) animals (Fig. 6*B*), indicating that the O_2-sensing ability of BAG is not required for the O_2-dependent regulation of CO_2 response. Consistent with these results, the BAG neurons were recently shown to play only a minor role in the chronic response to ambient O_2 (Busch et al., 2012). Thus, regulation of CO_2 response by ambient O_2 is not a result of cell-intrinsic signaling within BAG but instead requires a pair of designated O_2-sensing neurons.

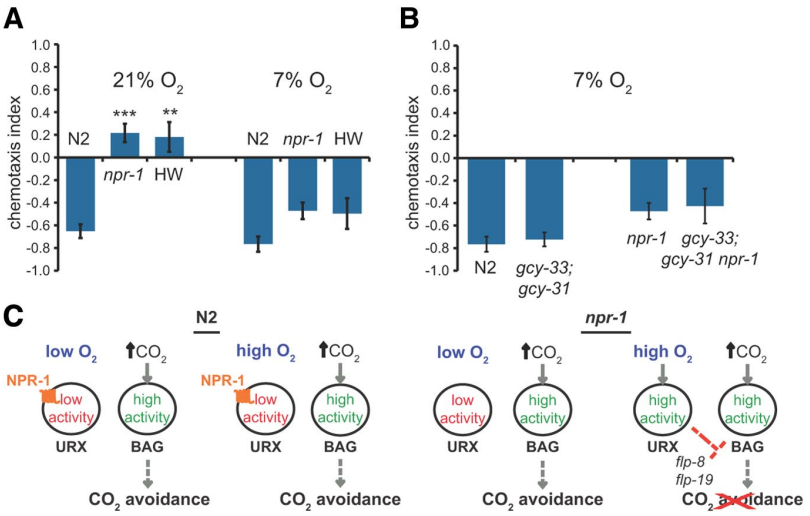

Figure 6. *npr-1*(*lf*) and HW animals avoid CO_2 under low O_2 conditions. ***A***, *npr-1*(*lf*) and HW animals do not respond to CO_2 at 21% ambient O_2 but avoid CO_2 at 7% ambient O_2. $^{**}p < 0.01$, relative to N2 control (Kruskal–Wallis test with Dunn's post-test). $^{***}p < 0.001$, relative to N2 control (Kruskal–Wallis test with Dunn's post-test). $n = 7$–26 trials for each genotype and condition. Error bars represent SEM. ***B***, CO_2 response at low ambient O_2 does not require O_2 sensing by BAG neurons. Animals that lack the soluble guanylate cyclase genes *gcy-31* and *gcy-33*, which are required for the O_2 response of BAG neurons (Zimmer et al., 2009), respond normally to CO_2 at 7% ambient O_2 in both the N2 and *npr-1*(*lf*) mutant backgrounds. The response of N2 animals is not significantly different from the response of *gcy-33; gcy-31* animals, and the response of *npr-1* animals is not significantly different from the response of *gcy-33; gcy-31 npr-1* animals (Kruskal–Wallis test with Dunn's post-test). $n = 8$–26 trials for each genotype. Error bars represent SEM. ***C***, A model for O_2-dependent regulation of CO_2 avoidance. Our results suggest that, in N2 animals, NPR-1 maintains URX in a low activity state, thus enabling CO_2 avoidance even at high ambient O_2. In *npr-1*(*lf*) mutant animals, reduced activity of URX at low ambient O_2 allows CO_2 avoidance, and increased activity of URX at high ambient O_2 inhibits CO_2 avoidance. Our results also suggest that CO_2 avoidance by URX neurons may be mediated by the URX-expressed neuropeptide genes *flp-8* and *flp-19*.

Discussion

Our results demonstrate that URX neurons control CO_2 response by coordinating the response to CO_2 with the response to ambient O_2. In *npr-1*(*lf*) animals, O_2-dependent activation of URX neurons determines CO_2 response such that CO_2 is repulsive at low ambient O_2 but neutral at high ambient O_2 (Fig. 6*C*). Moreover, our results are consistent with the hypothesis that URX neurons regulate the activity of the CO_2 circuit via a neuropeptide signaling pathway that involves the FMRFamide-related neuropeptide genes *flp-19* and *flp-8*. By contrast, in N2 animals, the URX neurons do not inhibit CO_2 avoidance at high ambient O_2 as a result of the presence of NPR-1 (Fig. 6*C*). NPR-1 does not constitutively silence the URX neurons of N2 animals because the URX neurons of N2 animals are activated by increases in ambient O_2 and ablation of URX in N2 animals alters O_2 response (Zimmer et al., 2009). However, our results suggest that NPR-1 may reduce URX neuron activity in N2 animals such that URX neurons no longer inhibit the CO_2 avoidance circuit. Alternatively, it is possible that NPR-1 activity is dynamically regulated by its neuropeptide ligands such that it is active under some conditions but not others, or that the URX neurons of N2 animals are sufficiently activated but are incapable of regulating CO_2 avoidance as a result of differences in neural connectivity or signaling between N2 and *npr-1*(*lf*) animals.

A recent survey of wild *C. elegans* strains revealed that the HW allele of *npr-1* is the natural variant, with the N2 allele having arisen during laboratory culturing (McGrath et al., 2009). HW animals were previously thought to be virtually insensitive to CO_2 (Hallem and Sternberg, 2008; McGrath et al., 2009), raising the question of whether CO_2 avoidance is exclusively a laboratory-derived behavior. Our results demonstrate that HW animals do indeed display robust CO_2 avoidance, but this behavior is restricted to low O_2 conditions. Wild *C. elegans* adults have been found in fallen rotting fruit and in the soil under rotting fruit, where O_2 levels are lower and CO_2 levels are higher than in the atmosphere (Felix and Duveau, 2012). Inside rotting fruit, *C. elegans* occupies microhabitats replete with bacteria, fungi, worms, insects, and other small invertebrates (Felix and Duveau, 2012). In this context, fluctuating levels of CO_2 and O_2 likely serve as important indicators of food availability, population density, and predator proximity (Bendesky et al., 2011; Milward et al., 2011; Scott, 2011). Suppression of CO_2 avoidance at high ambient O_2 may allow worms to migrate toward rotting fruit, which emits CO_2. Once inside the low O_2 environment of rotting fruit, CO_2 avoidance may allow worms to avoid cohabitating predators or overcrowding. Thus, O_2-dependent regulation of CO_2 avoidance is likely to be an ecologically relevant mechanism by which nematodes navigate gas gradients.

In addition to CO_2 response, a number of other chemosensory behaviors in *C. elegans* are subject to context-dependent changes in sensory valence (Sengupta, 2012). For example, olfactory and gustatory behavior exhibits experience-dependent plasticity, in which chemicals that are attractive to naive animals become neutral or repulsive after prolonged or repeated exposure in the absence of food (Sengupta, 2012). Olfactory plasticity occurs as a result of altered signaling in the AWC olfactory neurons (Tsunozaki et al., 2008), and salt plasticity occurs as a result of altered signaling in the ASE gustatory neurons and the downstream AIA and AIB interneurons (Tomioka et al., 2006; Adachi et al., 2010; Oda et al., 2011). Similarly, O_2 preference is modulated by prior O_2 exposure and the presence of bacterial food as a result of altered signaling in a distributed network of chemosensory neurons (Cheung et al., 2005; Chang et al., 2006). Our results suggest that CO_2 response is modulated by ambient O_2 via the activity of a pair of O_2-detecting neurons that interact with the CO_2 circuit downstream of CO_2 detection by BAG neurons (Fig. 6*C*). The neurons that act downstream of BAG and URX to control CO_2 response have not yet been identified. A number of interneurons receive synaptic input from both BAG and URX (White et al., 1986), and it will be interesting to determine whether any of them play a role in CO_2 avoidance.

CO_2-evoked behaviors in insects are also subject to context-dependent modulation. For example, the fruit fly *Drosophila melanogaster* is repelled by CO_2 when walking (Suh et al., 2004) but attracted to CO_2 in flight, a valence change that is modulated by octopamine signaling (Wasserman et al., 2013). In addition, both CO_2 repulsion by walking *D. melanogaster* and CO_2 attraction by mosquitoes can be suppressed by food odorants, which

directly alter the activity of the CO_2 receptor (Turner and Ray, 2009; Turner et al., 2011). Insects as well as many other animals, both free-living and parasitic, occupy microhabitats where environmental levels of O_2 and CO_2 vary greatly as a function of food or host availability, population density, and microorganism composition. Thus, it will be interesting to determine whether the control of CO_2 response by O_2-sensing neurons is a conserved feature of gas-sensing circuits.

References

Adachi T, Kunitomo H, Tomioka M, Ohno H, Okochi Y, Mori I, Iino Y (2010) Reversal of salt preference is directed by the insulin/PI3K and Gq/PKC signaling in *Caenorhabditis elegans.* Genetics 186:1309–1319. CrossRef Medline

Bargmann CI, Hartwieg E, Horvitz HR (1993) Odorant-selective genes and neurons mediate olfaction in *C. elegans.* Cell 74:515–527. CrossRef Medline

Bendesky A, Tsunozaki M, Rockman MV, Kruglyak L, Bargmann CI (2011) Catecholamine receptor polymorphisms affect decision-making in *C. elegans.* Nature 472:313–318. CrossRef Medline

Brandt JP, Aziz-Zaman S, Juozaityte V, Martinez-Velazquez LA, Petersen JG, Pocock R, Ringstad N (2012) A single gene target of an ETS-family transcription factor determines neuronal CO_2-chemosensitivity. PLoS One 7:e34014. CrossRef Medline

Brenner S (1974) The genetics of *Caenorhabditis elegans.* Genetics 77:71–94. Medline

Bretscher AJ, Busch KE, de Bono M (2008) A carbon dioxide avoidance behavior is integrated with responses to ambient oxygen and food in *Caenorhabditis elegans.* Proc Natl Acad Sci U S A 105:8044–8049. CrossRef Medline

Bretscher AJ, Kodama-Namba E, Busch KE, Murphy RJ, Soltesz Z, Laurent P, de Bono M (2011) Temperature, oxygen, and salt-sensing neurons in *C. elegans* are carbon dioxide sensors that control avoidance behavior. Neuron 69:1099–1113. CrossRef Medline

Buehlmann C, Hansson BS, Knaden M (2012) Path integration controls nest-plume following in desert ants. Curr Biol 22:645–649. CrossRef Medline

Busch KE, Laurent P, Soltesz Z, Murphy RJ, Faivre O, Hedwig B, Thomas M, Smith HL, de Bono M (2012) Tonic signaling from O_2 sensors sets neural circuit activity and behavioral state. Nat Neurosci 15:581–591. CrossRef Medline

Chaisson KE, Hallem EA (2012) Chemosensory behaviors of parasites. Trends Parasitol 28:427–436. CrossRef Medline

Chang AJ, Chronis N, Karow DS, Marletta MA, Bargmann CI (2006) A distributed chemosensory circuit for oxygen preference in *C. elegans.* PLoS Biol 4:e274. CrossRef Medline

Cheung BH, Arellano-Carbajal F, Rybicki I, de Bono M (2004) Soluble guanylate cyclases act in neurons exposed to the body fluid to promote *C. elegans* aggregation behavior. Curr Biol 14:1105–1111. CrossRef Medline

Cheung BH, Cohen M, Rogers C, Albayram O, de Bono M (2005) Experience-dependent modulation of *C. elegans* behavior by ambient oxygen. Curr Biol 15:905–917. CrossRef Medline

de Bono M, Bargmann CI (1998) Natural variation in a neuropeptide Y receptor homolog modifies social behavior and food response in *C. elegans.* Cell 94:679–689. CrossRef Medline

Dillman AR, Guillermin ML, Lee JH, Kim B, Sternberg PW, Hallem EA (2012) Olfaction shapes host-parasite interactions in parasitic nematodes. Proc Natl Acad Sci U S A 109:E2324–E2333. CrossRef Medline

Félix MA, Duveau F (2012) Population dynamics and habitat sharing of natural populations of *Caenorhabditis elegans* and *C. briggsae.* BMC Biol 10:59. CrossRef Medline

Glauser DA, Chen WC, Agin R, Macinnis BL, Hellman AB, Garrity PA, Tan MW, Goodman MB (2011) Heat avoidance is regulated by transient receptor potential (TRP) channels and a neuropeptide signaling pathway in *Caenorhabditis elegans.* Genetics 188:91–103. CrossRef Medline

Gray JM, Karow DS, Lu H, Chang AJ, Chang JS, Ellis RE, Marletta MA, Bargmann CI (2004) Oxygen sensation and social feeding mediated by a *C. elegans* guanylate cyclase homologue. Nature 430:317–322. CrossRef Medline

Guillermin ML, Castelletto ML, Hallem EA (2011) Differentiation of carbon dioxide-sensing neurons in *Caenorhabditis elegans* requires the ETS-5 transcription factor. Genetics 189:1327–1339. CrossRef Medline

Hallem EA, Sternberg PW (2008) Acute carbon dioxide avoidance in *Caenorhabditis elegans.* Proc Natl Acad Sci U S A 105:8038–8043. CrossRef Medline

Hallem EA, Dillman AR, Hong AV, Zhang Y, Yano JM, DeMarco SF, Sternberg PW (2011a) A sensory code for host seeking in parasitic nematodes. Curr Biol 21:377–383. CrossRef Medline

Hallem EA, Spencer WC, McWhirter RD, Zeller G, Henz SR, Ratsch G, Miller DM 3rd, Horvitz HR, Sternberg PW, Ringstad N (2011b) Receptor-type guanylate cyclase is required for carbon dioxide sensation by *Caenorhabditis elegans.* Proc Natl Acad Sci U S A 108:254–259. CrossRef Medline

Harris AL (2002) Hypoxia: a key regulatory factor in tumour growth. Nat Rev Cancer 2:38–47. CrossRef Medline

Hobert O. (2010) Neurogenesis in the nematode *Caenorhabditis elegans.* In: WormBook. www.WormBook.org. Accessed May 8th, 2013.

Hotez P, Hawdon J, Schad GA (1993) Hookworm larval infectivity, arrest and amphiparatenesis: the *Caenorhabditis elegans* Daf-c paradigm. Parasitol Today 9:23–26. CrossRef Medline

Langford NJ (2005) Carbon dioxide poisoning. Toxicol Rev 24:229–235. CrossRef Medline

Li C, Kim, K. (2008) Neuropeptides. In: WormBook, www.WormBook.org. Accessed May 8th, 2013.

Luo M, Sun L, Hu J (2009) Neural detection of gases—carbon dioxide, oxygen—in vertebrates and invertebrates. Curr Opin Neurobiol 19:354–361. CrossRef Medline

Macosko EZ, Pokala N, Feinberg EH, Chalasani SH, Butcher RA, Clardy J, Bargmann CI (2009) A hub-and-spoke circuit drives pheromone attraction and social behaviour in *C. elegans.* Nature 458:1171–1175. CrossRef Medline

McGrath PT, Rockman MV, Zimmer M, Jang H, Macosko EZ, Kruglyak L, Bargmann CI (2009) Quantitative mapping of a digenic behavioral trait implicates globin variation in *C. elegans* sensory behaviors. Neuron 61: 692–699. CrossRef Medline

Milward K, Busch KE, Murphy RJ, de Bono M, Olofsson B (2011) Neuronal and molecular substrates for optimal foraging in *Caenorhabditis elegans.* Proc Natl Acad Sci U S A 108:20672–20677. CrossRef Medline

Morton DB (2011) Behavioral responses to hypoxia and hyperoxia in *Drosophila* larvae: molecular and neuronal sensors. Fly (Austin) 5:119–125. CrossRef Medline

Nagai T, Yamada S, Tominaga T, Ichikawa M, Miyawaki A (2004) Expanded dynamic range of fluorescent indicators for Ca^{2+} by circularly permuted yellow fluorescent proteins. Proc Natl Acad Sci U S A 101: 10554–10559. CrossRef Medline

Oda S, Tomioka M, Iino Y (2011) Neuronal plasticity regulated by the insulin-like signaling pathway underlies salt chemotaxis learning in *Caenorhabditis elegans.* J Neurophysiol 106:301–308. CrossRef Medline

Persson A, Gross E, Laurent P, Busch KE, Bretes H, de Bono M (2009) Natural variation in a neural globin tunes oxygen sensing in wild *Caenorhabditis elegans.* Nature 458:1030–1033. CrossRef Medline

Qin H, Zhai Z, Powell-Coffman JA (2006) The *Caenorhabditis elegans* AHR-1 transcription complex controls expression of soluble guanylate cyclase genes in the URX neurons and regulates aggregation behavior. Dev Biol 298:606–615. CrossRef Medline

Reddy KC, Andersen EC, Kruglyak L, Kim DH (2009) A polymorphism in *npr-1* is a behavioral determinant of pathogen susceptibility in *C. elegans.* Science 323:382–384. CrossRef Medline

Rogers C, Persson A, Cheung B, de Bono M (2006) Behavioral motifs and neural pathways coordinating O_2 responses and aggregation in *C. elegans.* Curr Biol 16:649–659. CrossRef Medline

Satterlee JS, Sasakura H, Kuhara A, Berkeley M, Mori I, Sengupta P (2001) Specification of thermosensory neuron fate in *C. elegans* requires *ttx-1*, a homolog of *otd/Otx.* Neuron 31:943–956. CrossRef Medline

Scott K (2011) Out of thin air: sensory detection of oxygen and carbon dioxide. Neuron 69:194–202. CrossRef Medline

Sengupta P (2013) The belly rules the nose: feeding state-dependent modulation of peripheral chemosensory responses. Curr Opin Neurobiol 23: 68–75. CrossRef Medline

Suh GS, Wong AM, Hergarden AC, Wang JW, Simon AF, Benzer S, Axel R, Anderson DJ (2004) A single population of olfactory sensory neurons mediates an innate avoidance behaviour in *Drosophila.* Nature 431:854–859. CrossRef Medline

Tian L, Hires SA, Mao T, Huber D, Chiappe ME, Chalasani SH, Petreanu L, Akerboom J, McKinney SA, Schreiter ER, Bargmann CI, Jayaraman V, Svoboda K, Looger LL (2009) Imaging neural activity in worms, flies and mice with improved GCaMP calcium indicators. Nat Methods 6:875–881. CrossRef Medline

Tomioka M, Adachi T, Suzuki H, Kunitomo H, Schafer WR, Iino Y (2006) The insulin/PI 3-kinase pathway regulates salt chemotaxis learning in *Caenorhabditis elegans.* Neuron 51:613–625. CrossRef Medline

Tsunozaki M, Chalasani SH, Bargmann CI (2008) A behavioral switch: cGMP and PKC signaling in olfactory neurons reverses odor preference in *C. elegans.* Neuron 59:959–971. CrossRef Medline

Turner SL, Ray A (2009) Modification of CO_2 avoidance behaviour in *Drosophila* by inhibitory odorants. Nature 461:277–281. CrossRef Medline

Turner SL, Li N, Guda T, Githure J, Cardé RT, Ray A (2011) Ultra-prolonged activation of CO_2-sensing neurons disorients mosquitoes. Nature 474:87–91. CrossRef Medline

Uchida O, Nakano H, Koga M, Ohshima Y (2003) The *C. elegans che-1* gene encodes a zinc finger transcription factor required for specification of the ASE chemosensory neurons. Development 130:1215–1224. CrossRef Medline

Vigne P, Frelin C (2010) Hypoxia modifies the feeding preferences of *Drosophila*: consequences for diet dependent hypoxic survival. BMC Physiol 10:8. CrossRef Medline

Wasserman S, Salomon A, Frye MA (2013) *Drosophila* tracks carbon dioxide in flight. Curr Biol 23:301–306. CrossRef Medline

West JB (2004) The physiologic basis of high-altitude diseases. Ann Intern Med 141:789–800. CrossRef Medline

White JG, Southgate E, Thomson JN, Brenner S (1986) The structure of the nervous system of the nematode *Caenorhabditis elegans.* Philos Trans R Soc Lond B Biol Sci 314:1–340. CrossRef Medline

Wingrove JA, O'Farrell PH (1999) Nitric oxide contributes to behavioral, cellular, and developmental responses to low oxygen in *Drosophila.* Cell 98:105–114. CrossRef Medline

Zimmer M, Gray JM, Pokala N, Chang AJ, Karow DS, Marletta MA, Hudson ML, Morton DB, Chronis N, Bargmann CI (2009) Neurons detect increases and decreases in oxygen levels using distinct guanylate cyclases. Neuron 61:865–879. CrossRef Medline

Chapter 3

Feeding state sculpts a circuit for sensory valence

Introduction

To appropriately respond to sensory information in our environment, humans must constantly sense external changes and weigh these against their own internal needs. The integration of external stimuli with internal state establishes our framework for decision-making. Across diverse animal phyla, sensory valence, *i.e.* the measure of aversiveness or attractiveness that an animal attaches to a particular stimulus, is dynamic and intimately tied to internal state (Fontanini and Katz, 2008; Inagaki et al., 2014; Li and Liberles, 2015; Numan et al., 2006; Wasserman et al., 2013). For example, when humans are hungry, we perceive food-associated odors as attractive, but as our satiety increases, we perceive the same odors as aversive (O'Doherty et al., 2000; Smeets et al., 2006). How a single sensory stimulus drives dramatically different valence responses under distinct states, and how neural circuit function dynamically shifts as an animal fluidly transitions between these states, remain poorly understood.

Despite its relatively small nervous system, the free-living nematode *Caenorhabditis elegans* exhibits a wide range of sensory behaviors and responds to gustatory, olfactory, mechanosensory, and thermosensory stimuli (Bargmann, 2006; Goodman, 2006; Goodman et al., 2014; Hart and Chao, 2010; Rengarajan and Hallem, 2016). The sensory valence that *C. elegans* attaches to these stimuli can be altered by sex, experience, state, and environmental context (Carrillo et al., 2013; Fenk and de Bono, 2017; Ghosh et al., 2016; Laurent et al., 2015; Macosko et al., 2009; Ryan et al., 2014; Saeki et al., 2001; Satterlee et al., 2001), making it an appropriate model for studying how neural circuits are modulated to drive changes in sensory valence. How

the *C. elegans* nervous system adapts in response to these changing conditions to appropriately drive behavior is incompletely understood.

CO_2 is a suitable stimulus for understanding the mechanisms that determine sensory valence. For both *C. elegans* and the fruit fly *Drosophila melanogaster,* CO_2 can signal unfavorable environments by indicating social crowding or the presence of predators or can, alternately, signal favorable environments by indicating the presence of food or conspecifics (Carrillo and Hallem, 2014; Faucher et al., 2006; Wasserman et al., 2013). Although *C. elegans* adults grown in ambient laboratory conditions avoid CO_2, the valence of their response is flexible and can be either attractive or repulsive depending on the life stage, experience, environmental context, and internal state of the animal (Bretscher et al., 2008; Bretscher et al., 2011; Carrillo et al., 2013; Guillermin et al., in submission; Hallem et al., 2011; Hallem and Sternberg, 2008; Kodama-Namba et al., 2013).

In particular, feeding state, an internal state common to all organisms, has been implicated in modulating CO_2-response valence in *C. elegans* (Bretscher et al., 2008; Hallem and Sternberg, 2008), but how starvation drives this change in valence is not understood. By contrast to sleep-wake transitions which occur rapidly (Lee and Dan, 2012), the transition between fed and starved states is gradual and exists on a continuum as energy stores become depleted. Studying how food-deprivation dynamically modulates the valence of CO_2 can inform how neural circuits are continuously sculpted by gradually shifting behavioral states.

Here we show that feeding state regulates CO_2 response valence; although fed worms display robust CO_2 avoidance, as worms are food-deprived, their valence shifts

gradually to robust attraction. We characterized this shift and identified a core motif of the CO_2 circuit involving two pairs of neurons, AIY and RIG, that have opposing effects on behavior. RIG neurons are subject to transient modulation during the valence shift, but their activity in fed and starved states is identical. By contrast, the AIY neurons are probabilistic; CO_2 evokes multiple qualitatively different responses in AIY neurons, but feeding state dictates the proportion in which these responses are present. We demonstrate that both mechanical and gustatory components of food, conveyed by dopamine signaling and the presence of salt, contribute to feeding-state-dependent valence. Dopamine signaling coordinately enhances both RIG activation and AIY suppression, thereby sculpting the CO_2 microcircuit to promote CO_2 avoidance. Our results have novel implications for how valence-encoding circuits dynamically change as a function of behavioral state.

Results:

***C. elegans* shifts CO_2 response valence as a function of starvation**

To determine how starvation alters the chemotaxis behavior of worms, we deprived wild-type worms of food and assayed their chemotaxis response after increasing periods of food deprivation (Figure 1A). Whereas fed worms strongly avoided CO_2, indicated by their negative chemotaxis index (CI), food-deprived worms gradually lost their avoidance and responded neutrally to CO_2 by 90 minutes and demonstrated CO_2 attraction by 3 hours. We assayed CO_2 response in worms deprived of food for 6 hours and 9 hours and found that CO_2 attraction was still maintained.

Figure 1

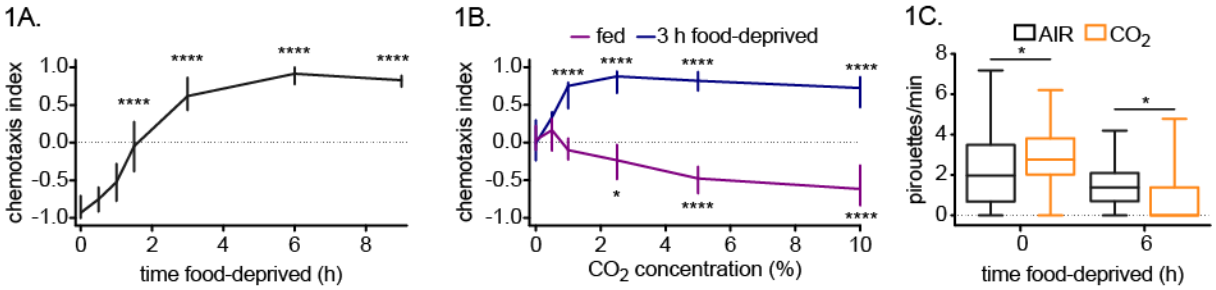

Starvation shifts CO_2 response valence from avoidance to attraction in *C. elegans*
(A) CO_2 response valence shifts from avoidance to attraction as worms are deprived of food for increasing periods of time (0, 0.5, 1, 1.5, 3, 6, or 9 hours). Curve shows median with interquartile range as errors. n=10-72 trials per condition. **** $p<0.0001$, Kruskal Wallis test, post-test compared to the 0-hour state with Dunn's correction. (B) Valence remains constant across CO_2 concentrations. Fed (purple) and 3 hour food-deprived (blue) worms were assayed with 0%, 0.5%, 1%, 2.5%, 5%, or 10% CO_2. n=10-24 trials per condition. *$p<0.05$, ****$p<0.0001$ 2-way ANOVA, post-test with Sidak's correction comparing each concentration to 0% within the same state. (C) Food-deprivation alters pirouette frequency of worms in response to CO_2. Box plots show the behavior 0-hour and 6-hour food-deprived worms in the presence of CO_2 (orange) or air (black). n=43-77 tracks per condition. *$p<0.05$, 2-way ANOVA, post-test with Sidak's correction comparing the CO_2 response to the air response within each state.

To understand whether the CO_2 response valence is determined solely by feeding state or by a combination of CO_2 concentration and feeding state, we assayed CO_2 response of fed and 3-hour food-deprived worms across a range of concentrations from 0% to 10%. We found that for both of these feeding states, valence remained constant across CO_2 concentrations, suggesting that valence is determined by feeding state and not by CO_2 concentration (Figure 1B). Starved worms had enhanced behavioral sensitivity to CO_2 and demonstrated CO_2 attraction to concentrations as low as 1%, whereas fed worms only showed CO_2 avoidance at concentrations of 2.5% or higher.

We then explored how the locomotor strategy of worms is affected by the presence of CO_2 during fed and food-deprived states. We tracked the locomotion of worms exposed to a stream of 15% CO_2 vs. an air control. We discovered that, depending on feeding state, CO_2 had opposing effects on the rate of sharp turning bouts, called pirouettes (Pierce-Shimomura et al., 1999). In fed worms, the presence of CO_2 caused worms to pirouette more whereas in starved worms the presence of CO_2 caused worms to pirouette less (Figure 1C). The CO_2-induced increase in pirouette frequency of fed worms corresponds to CO_2 avoidance in chemotaxis assays. By contrast, the decreased pirouette frequency of starved worms corresponds to CO_2 attraction. The correlation of pirouette frequency and CO_2 response valence suggests that pirouette frequency modulation is an important output of the neural circuit driving CO_2 sensory valence.

Two pairs of interneurons, AIY and RIG, act on different timescales to promote opposing valence states

We next investigated how feeding state sculpts the CO_2 circuit to effect these behavioral changes. We and others previously showed that the BAG neurons are primary CO_2 sensing neurons that are required for most CO_2-evoked behaviors (Bretscher et al., 2011; Carrillo et al., 2013; Hallem et al., 2011; Hallem and Sternberg, 2008; Kodama-Namba et al., 2013). To determine whether the CO_2 response of the BAG neurons is altered by starvation, we used calcium imaging to measure the activity of BAG in response to a 20-s pulse of 10% CO_2 in worms starved for variable periods of time. We found that the response of BAG remains constant across feeding states

(Figure S2A-D), suggesting that feeding state acts downstream from the calcium response of BAG.

The Hallem lab previously found that cultivating *C. elegans* in a high-CO_2 environment causes worms to be attracted to CO_2 (Guillermin et al., in submission). A set of 4 pairs of interneurons directly downstream from the BAG sensory neurons that regulate CO_2 valence (RIG, AIY and RIA neurons) and sensitivity (AIZ neurons) as a function of CO_2-cultivation environment were identified. To determine whether those neurons also alter the valence of CO_2 response as a function of food deprivation, we screened through strains with each pair of neurons either genetically ablated (Guillermin et al., in submission) or silenced (Calhoun et al., 2015). We assayed the CO_2 response of each strain as a function of food deprivation. Whereas ablating RIA neurons or silencing both AIB and AIZ neurons did not affect CO_2-response valence, ablating either RIG or AIY neurons altered CO_2-response valence compared to wild-type worms (Figure 2A). RIG-ablated animals tested when fed or food-deprived for 1.5-hours showed less CO_2 avoidance, suggesting that RIG normally acts to promote CO_2 avoidance early on during food-deprivation. By contrast, ablating the AIY neurons suppressed CO_2 attraction in worms food-deprived for 3 and 6 hours, suggesting that AIY normally functions to promote CO_2 attraction in worms deprived of food for longer periods.

We then imaged from RIG and AIY in fed and starved worms to determine whether their calcium responses to CO_2 are modulated by starvation. RIG neurons are robustly depolarized by CO_2 in fed worms, but worms that are food-deprived for 90 minutes, the time point at which wild-type worms do not respond behaviorally to CO_2,

have an attenuated RIG response to CO_2 (Figure 2B-C). This attenuation is only transient, as the RIG calcium response of worms that are food-deprived for 6 hours is indistinguishable from the calcium response of well-fed worms. Thus, the activity of RIG neurons is transiently modulated as worms transition between fed and starved states.

Figure 2

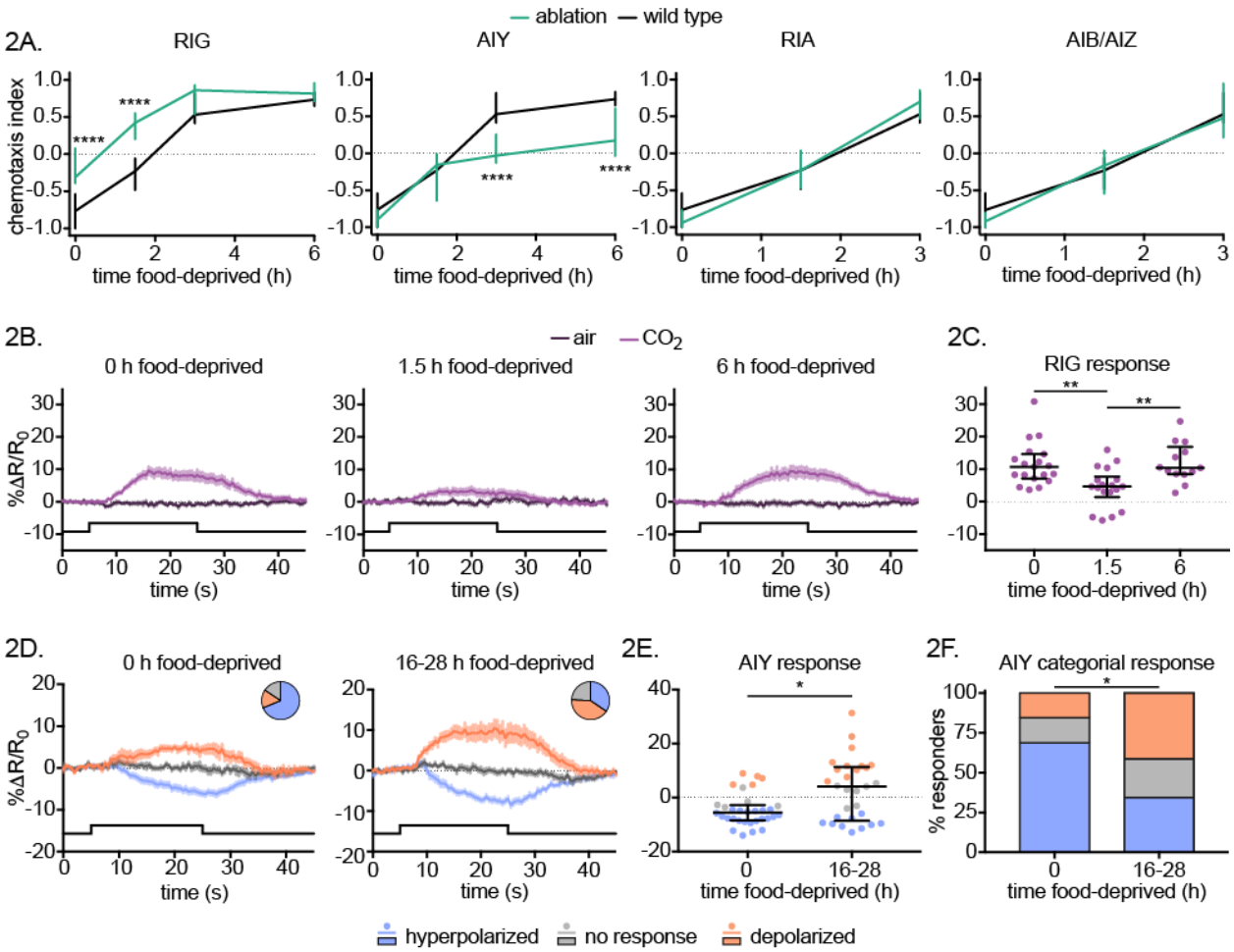

First-order interneurons in the CO_2 microcircuit promote opposing CO_2 responses (A) RIG and AIY interneurons have opposing effects on CO_2 valence and act on different time scales during starvation. Time courses for ablation lines for individual neurons –RIG, AIY, RIA– and tetanus toxin-silenced AIB and AIZ interneurons (green) vs. wild-type worms (black). Curves plot median values with interquartile ranges indicated as errors. n=6-18 trials for each condition. ****p<0.0001, 2-way ANOVA, post-test with Sidak's correction comparing wild type and mutant at a

given time point. (B) RIG neurons transiently less depolarized during the shift in CO_2 response valence. Curves plot mean values with SEMs of response to CO_2 (light purple) and air (darker purple). Black line indicates timing of gas pulse. n= 13-19 recordings per condition. (C) RIG response to CO_2 is attenuated in worms starved for 90 minutes but indistinguishable in fed and 6 hour food-deprived worms ($p>0.9999$). **$p<0.01$ Kruskal-Wallis test, post-test with Dunn's correction. Lines show the median and interquartile range. (D) AIY neurons show categorically different types of responses during both fed (age-matched) and starved (16-28 hours) states. Separate curves show summarized depolarized (orange), hyperpolarized (blue), and non-responses (gray). Pie charts depict the proportion for each type of response. n=29-32 recordings for each state. (E) AIY response to CO_2 increases with prolonged food-deprivation. *$p<0.05$ Mann-Whitney test. (F) The distribution of categorically different responses of AIY neurons shifts as a function of feeding state. *$p<0.05$ chi-squared test.

Taken together, our RIG-ablation behavior and RIG imaging results in fed worms suggest that the depolarization of RIG neurons in response to CO_2 is important for promoting CO_2 avoidance. Ablating RIG neurons abolishes this depolarization and corresponds to an attenuated CO_2 avoidance behaviorally. By contrast, in worms food-deprived for 6 hours, RIG neurons are also depolarized by CO_2 but ablating the RIG neurons did not alter CO_2 attraction behaviorally. Perhaps in starved worms, the CO_2 circuit can override the CO_2-evoked depolarization of RIG. For fed and 1.5-hour food-deprived worms transitioning from avoidance to attraction, suppression of the RIG CO_2-evoked calcium response is important for setting the time course of the shift in valence.

By contrast to the transient suppression we saw in RIG, when we imaged from AIY interneurons, we found that the responses were probabilistic. In both fed and starved worms, we saw 3 types of qualitatively different CO_2-evoked activity: hyperpolarizations, depolarizations and activity that was too small in magnitude to be considered a response (Figure 2D-F). Although these 3 types of responses were found in both fed and 16-28-hour food-deprived states, the proportion of these responses was

significantly modulated by feeding states. When we first examined CO_2-evoked AIY activity of worms food-deprived for 0, 1.5, or 3 hours we saw a small but non-significant shift away from hyperpolarizing responses toward depolarizations and non-responses (Figure S3), consistent with the behavior of AIY-ablated animals only modulating CO_2 response later in starvation (Figure 2A). To fully uncover the effect of starvation on the CO_2 response of AIY neurons, we food-deprived worms for longer periods, 16-28 hours, and imaged the response of AIY to CO_2. Whereas in fed worms the predominant AIY response was hyperpolarizing, in starved worms the proportion of hyperpolarizing and depolarizing responses was roughly equal.

Variability of the AIY response to CO_2 reflects behavioral robustness of CO_2 attraction

The Hallem lab previously investigated the CO_2 microcircuit in worms raised in higher CO_2 environments and discovered that they show robust attraction to CO_2 (Guillermin et al., in submission). We wanted to compare the attraction of fed worms raised at high CO_2 to the attraction of starved worms raised in ambient CO_2 conditions. When surveyed in population-based chemotaxis assays, both starved worms and CO_2-cultivated worms show robust attraction (Figure 3A). Although these responses were not quantitatively different, we noticed a qualitative difference that was not captured in the chemotaxis index (Figure 3B). At the end of a chemotaxis assay, starved worms distributed sparsely along a CO_2 gradient; most worms moved toward the CO_2 source, but they were thinly scattered. By contrast, CO_2-cultivated worms moved more

coherently toward the CO_2 source and, by the end of the assay, the majority of worms were densely clumped just below the location where CO_2 was delivered.

When we quantified the behavior of individual worms through worm tracking, we found that CO_2-cultivated worms showed a stronger bias toward CO_2 than starved worms (Figure 3C-D). Within two minutes of exposure to a stream of CO_2 or a control air stream, CO_2-cultivated worms moved closer to the CO_2 source than to the air source. By contrast, starved worms showed no difference in motion toward CO_2 and the control air stream. Furthermore, we calculated the percentage of time that worms spent moving toward gas, which we defined as within 60 degrees from the gas source, during the first 3 minutes of gas exposure. We found that CO_2-cultivated, but not starved worms, spent more time moving toward CO_2.

Figure 3

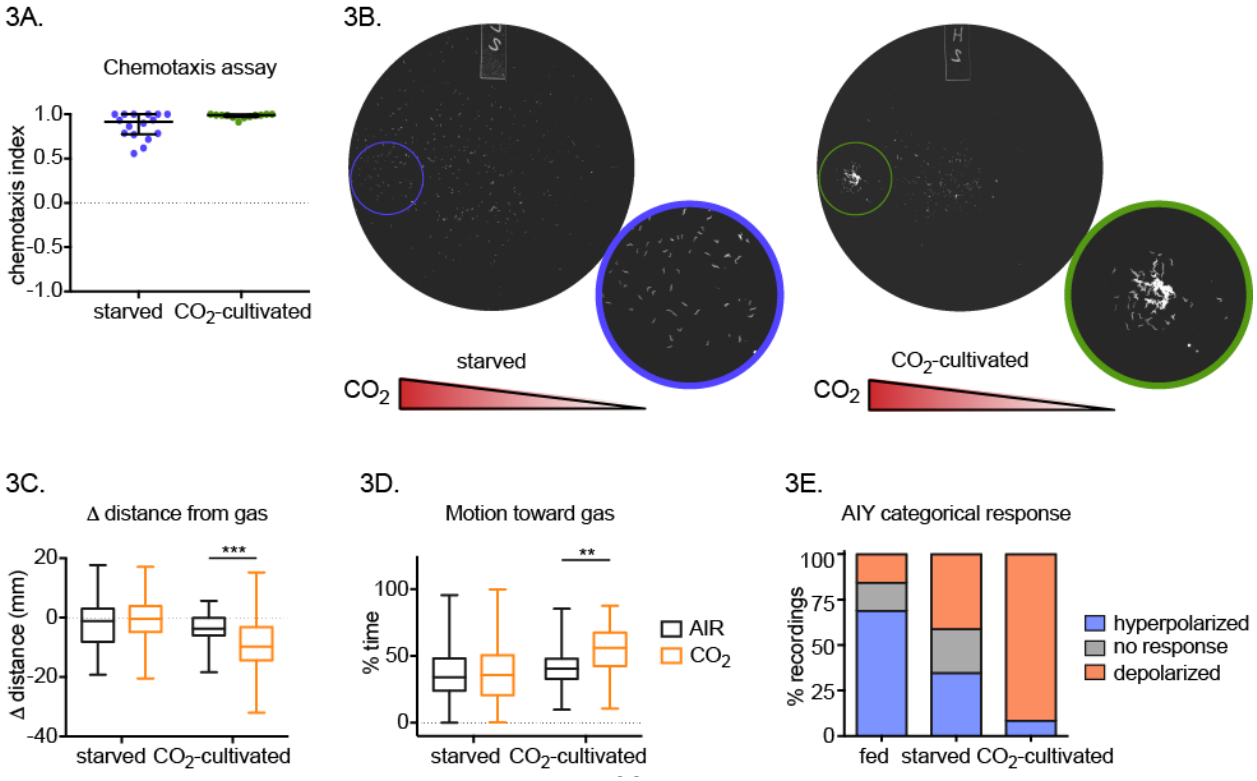

The AIY CO_2 response reflects the variability of behavior across starved worms
(A) Starved and CO_2-cultivated worms show comparable attraction in CO_2 preference assays. n=12-16 trials per condition. p=0.1519, Mann-Whitney test. (B) Starved (left) and CO_2-cultivated (right) worms distribute differently along a CO_2 gradient. Images show example plates at the end of chemotaxis assays. (C) CO_2-cultivated worms move closer toward a CO_2 source than starved worms. Box plots show response to CO_2 (orange) or air (black). n=48-86 trials per condition. ***p<0.001 two-way ANOVA, post-test with Sidak's correction comparing CO_2 and air responses. (D) The locomotion of high CO_2 cultivated worms is more biased toward CO_2 than starved worms. n=48-86 trials per condition. **p<0.01 two-way ANOVA, post-test with Sidak's correction. (E) The distribution of AIY CO_2 responses is altered by state. n=12-32 recordings per condition. p<0.0001, chi squared test for all groups.

The activity of AIY in these states is correlated with the enhanced behavioral robustness we see in CO_2-cultivated worms (Figure 3E). Whereas in starved worms, roughly equal numbers of worms show depolarizing and hyperpolarizing responses in AIY in response to CO_2, nearly all of the CO_2-cultivated worms had depolarizing responses in AIY, suggesting that the decreased variability of starved worms correlates with their enhanced CO_2-attraction.

Dopamine promotes CO_2 avoidance by enhancing RIG neuron activity and suppressing AIY neuron activity

After uncovering how food-deprivation modulates the activity of RIG and AIY, we next investigated the mechanisms by which feeding state sculpts the CO_2 circuit. Nervous systems often internally represent behavioral states with neuromodulators (Bargmann and Marder, 2013). In *C. elegans,* the biogenic amine dopamine is released in response to the mechanosensory detection of food (Chase and Koelle, 2007; Sawin et al., 2000). Dopamine is known to promote food-seeking behaviors, regulate

locomotion, and modulate avoidance behaviors, and is thus well suited to instruct the CO_2 circuit about behavioral state in order to modulate behavioral valence (Ezak and Ferkey, 2010; Ezcurra et al., 2011; Hills et al., 2004; Kimura et al., 2010; Omura et al., 2012; Sawin et al., 2000).

We assayed worms with all dopamine neurons ablated (*dat-1::ICE)* and found that they are constitutively attracted to CO_2 regardless of feeding state, suggesting that dopamine neurons normally act to promote CO_2 avoidance (Figure 4A). When we assayed worms lacking tyrosine hydroxylase (*cat-2 loss-of-function (lf)),* the enzyme required for the rate-limiting step of dopamine biosynthesis, they still avoided CO_2 in fed states but shifted faster to attraction. Mammalian cells are able to bypass tyrosine hydroxylase and produce dopamine through tyrosinase enzymes (Rios et al., 1999), raising the possibility that *cat-2(lf)* worms may still retain some level of dopamine production. The intermediate effect of *cat-2(lf)* worms is consistent with a dose-dependent effect of dopamine.

To confirm that dopamine released from dopaminergic neurons was driving CO_2 avoidance, we administered dopamine exogenously to worms for 30 minutes before assaying their CO_2 response. In wild-type worms, there was no difference between dopamine- and mock-treated worms (Figure 4C). By contrast, whereas mock-treated *dat-1::ICE* worms were attracted to CO_2, dopamine-treated *dat-1::ICE* worms showed robust CO_2 avoidance, demonstrating that the presence of exogenous dopamine rescues avoidance in worms with all dopamine neurons ablated. To test whether dopamine signaling also antagonizes CO_2 attraction in starved worms, we deprived wild-type worms of food for three hours in the presence of exogenous dopamine or

water, and found that dopamine-treated worms showed suppressed CO_2 attraction relative to worms receiving mock treatment (Figure 4D). Taken together, these experiments demonstrated that the biogenic amine dopamine is an important driver of CO_2-response valence; it promotes CO_2 avoidance in fed worms and antagonizes CO_2 attraction in starved worms.

Figure 4

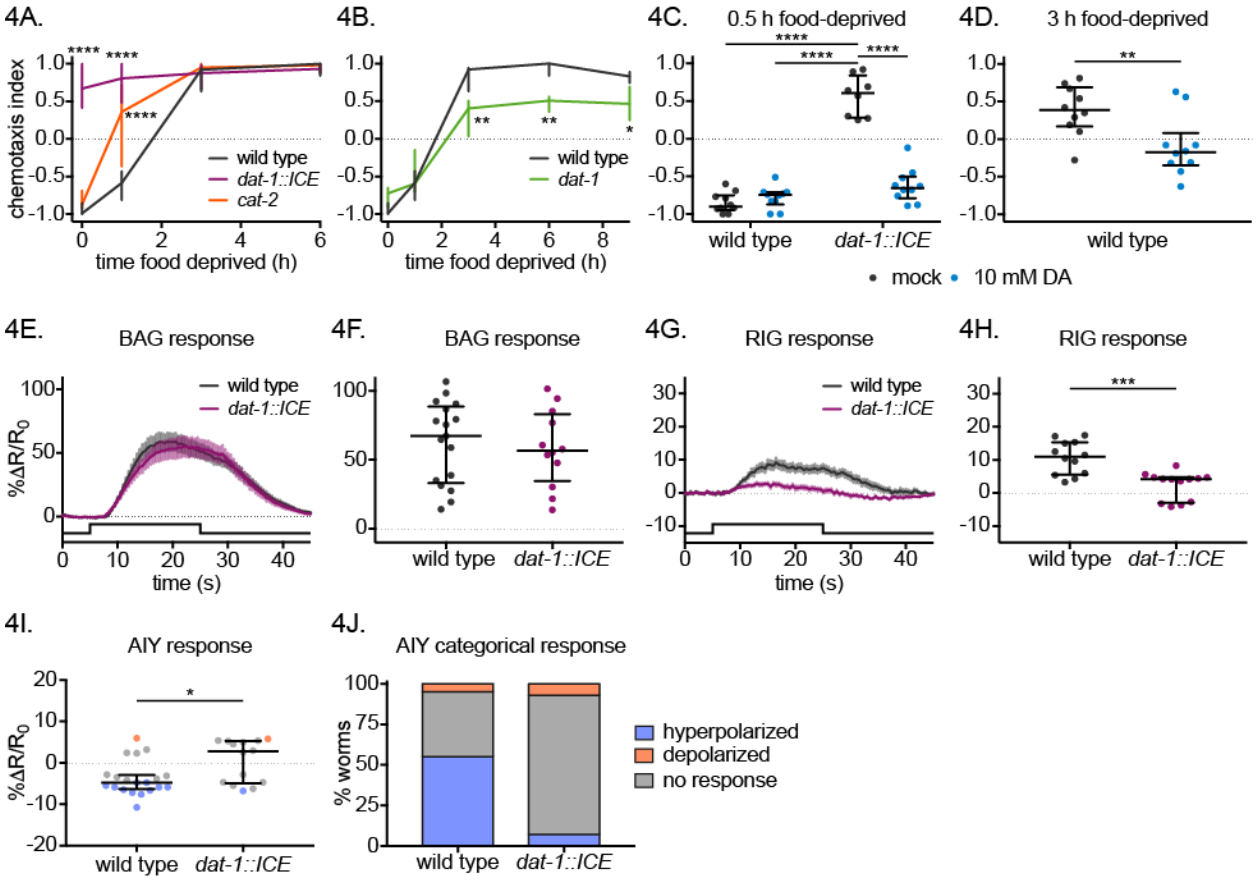

Dopaminergic signaling modulates the CO_2 microcircuit to promote CO_2 avoidance in fed worms (A) Dopamine promotes CO_2 avoidance. *dat-1::ICE* (purple), *cat-2* (orange), and wild-type worms (black) were food-deprived for 0, 1, 3, or 6 hours. Curves plot median values with interquartile ranges indicating errors. n=6-12 trials for each condition tested. ****p<0.0001 2-way ANOVA, post-test with Dunnett's correction comparing mutant to wild type for a given time point. (B) Increased dopamine

transmission attenuates CO_2 attraction of starved worms. *dat-1(lf)* (green) and wild-type worms (black) were food-deprived for 0, 1, 3, 6, or 9 hours. n=8-14 trials per condition. **p<0.01, *p<0.05 2-way ANOVA, post-test with Sidak's correction. (C) Exogenous dopamine treatment (blue) restores CO_2 avoidance in *dat-1::ICE* worms vs. mock-treated worms (black). Lines indicate median with errors as interquartile ranges. n = 8-10 trials per condition. ****p<0.0001 two-way ANOVA, post-test with Sidak's correction. (D) Exogenous dopamine treatment during starvation attenuates attraction. n=10 trials per condition. **p<0.01, unpaired t-test. (E-F) The BAG response to CO_2 is unchanged in worms lacking dopaminergic neurons. n=12-17 per strain. (E) Calcium response of wild-type (black) or *dat-1::ICE (*purple). Traces plot mean with SEMs as errors. (F) The quantified BAG response is indistinguishable in wild-type and *dat-1::ICE* worms. (p=0.6896, unpaired t-test). (G-H) The RIG response to CO_2 is attenuated in *dat-1::ICE* worms compared to wild type. n=12-13 trials per strain. ***p<0.001, unpaired t-test. (H-F) AIY neurons fail to show hyperpolarizations in *dat-1::ICE* worms compared to wild-type worms. n=14-16 trials per strain. *p<0.05 Mann-Whitney. (I) AIY responses categorized.

We next investigated whether dopamine modulates the activity of the CO_2 circuit. We imaged the calcium activity of the BAG sensory neurons in fed wild-type worms and *dat-1::ICE* worms. There was no difference in the BAG response between these two backgrounds, suggesting that dopamine signaling does not alter the CO_2-evoked activity of the BAG neurons (Figure 4E-F).

We next imaged the CO_2 responses of RIG and AIY interneurons of fed worms in either wild-type or *dat-1::ICE* backgrounds to determine if dopamine signaling modulates how these neurons respond to CO_2. Whereas in fed wild-type worms RIG showed a strong depolarization to CO_2, in the *dat-1::ICE* background, RIG neurons showed a significantly attenuated response to CO_2, suggesting that dopamine normally acts to enhance RIG's depolarizing response to CO_2 (Figure 4G-H).

Finally, we performed the same experiments for AIY interneurons. Whereas AIY neurons in the wild-type background were primarily hyperpolarized by CO_2, in the *dat-*

1::ICE background the majority of AIY neurons did not show a response to CO_2, suggesting that normally dopamine promotes a hyperpolarizing response in AIY neurons (Figure 4I-J). These results suggest that dopamine acts downstream of the BAG calcium response and results in an enhanced depolarizing response in RIG and a higher proportion of hyperpolarizing responses in AIY.

Salt and dopamine interact to redundantly promote CO_2 avoidance

After determining that dopamine alters CO_2 response behavior, we next investigated whether other sensory modalities involved in food-sensing, besides mechanosensation, also alter CO_2 response valence. An important gustatory component of food for *C. elegans* is salt. We assayed the CO_2-response behavior of fed wild-type and *dat-1::ICE* worms on standard chemotaxis plates and chemotaxis plates with added salt. In the presence of salt, wild-type worms showed slightly enhanced avoidance. For *dat-1::ICE* worms, the presence of salt had a more pronounced effect and was sufficient to restore CO_2 avoidance (Figure 5A). To control for osmotic changes, we added sorbitol to chemotaxis plates to achieve the same osmolarity. Sorbitol has been previously used in other *C. elegans* salt studies to control for osmolarity (Saeki et al., 2001). By contrast to salt, adding sorbitol had no effect on the behavior of either wild-type or *dat-1::ICE* worms, confirming that the salt specifically enhances avoidance of wild-type worms and rescues CO_2 avoidance in *dat-1::ICE* worms. Thus, we determined that salt and dopamine, two independent components of food-sensing, act redundantly to promote CO_2 avoidance in fed worms.

Since the ASE neurons are the primary salt-sensing neurons (Bargmann and Horvitz, 1991; Kaufman et al., 2005), we thought that salt-dependent modulation of CO_2 response would involve the ASE neurons. When we tested ASE-ablated worms in both the wild-type and *dat-1::ICE* backgrounds, all worms demonstrated robust CO_2 avoidance and we did not see any effect of salt context on behavior (Figure 5B). Since we had initially tested worms with a relatively strong concentration of CO_2, 15%, we wondered if the high concentration of CO_2 was masking a smaller effect of salt context. We tested worms at 2.5% CO_2 and found that salt did not alter the behavior of ASE-ablated worms in either the wild-type or *dat-1:ICE* backgrounds, confirming that salt is sensed through ASE to affect behavior (Figure 5C).

Figure 5

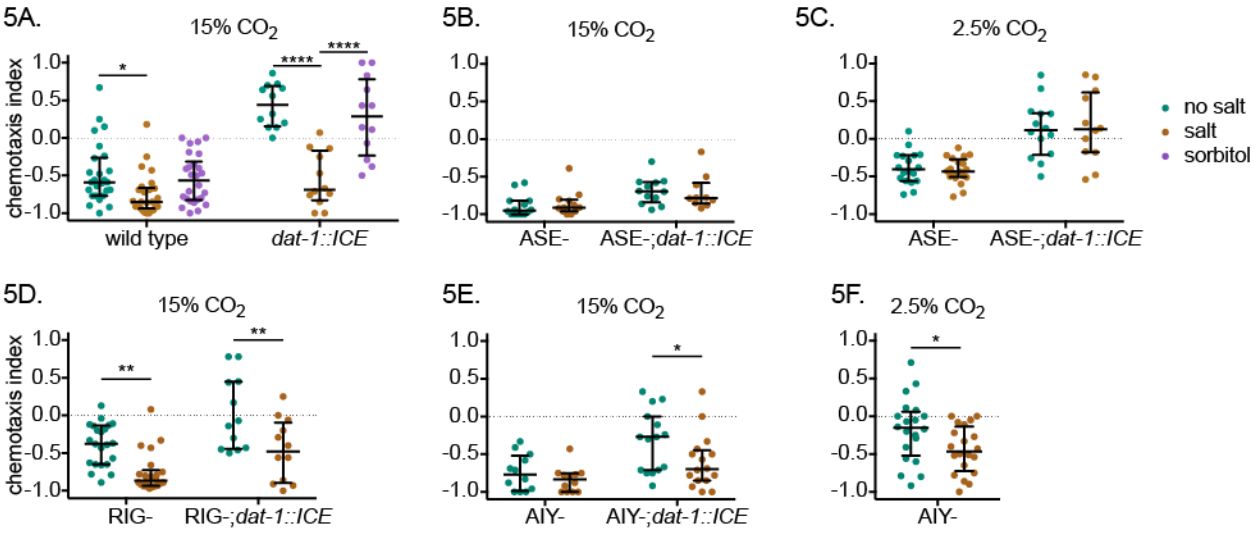

Salt context and dopaminergic signaling interact to determine CO_2 response valence (A) Salt context determines CO_2 valence in worms lacking dopamine. Wild-type and *dat-1::ICE* worms were tested in conditions with no salt (green) or salt (yellow) or sorbitol (purple). Lines show medians with interquartile ranges. n= 12-26 trials per condition. ****p<0.0001, *p<0.05, 2-way ANOVA post-test with Tukey's correction. (B-C)

The salt-sensing ASE neurons are required for salt- and dopaminergic enhancement of CO_2 avoidance for (B) 15%CO_2, n=10-14 trials per condition (p_{strain}=0.0013, $p_{context}$=0.8755, $p_{interaction}$=0.5902, 2-way ANOVA) and (C) 2.5% CO_2, n= 12-20 trials per condition. (p_{strain}<0.0001, $p_{context}$=0.9904, $p_{interaction}$=0.6419, 2-way ANOVA) (D) Salt enhances avoidance of RIG-ablated worms to 15%CO_2 in both wild-type and *dat-1::ICE* backgrounds. n=12-22 trials per condition. **p<0.01, 2-way ANOVA post-test with Sidak's correction. (E) Salt enhances avoidance of AIY-ablated worms to 15% CO_2 in *dat-1::ICE* but not *dat-1::ICE* backgrounds. n=12-16 trials per condition. *p<0.05, two-way ANOVA post-test with Sidak's correction. (F) In response to 2.5%CO_2, salt enhances avoidance of AIY-ablated worms in the wild-type background. n=20 trials per condition. *p<0.05, unpaired t-test.

We next wondered whether salt context was acting through the RIG and AIY neurons. We hypothesized that if salt were primarily acting through RIG or AIY to promote avoidance, then in RIG-ablated or AIY-ablated worms, we would see no effect of salt context on behavior. We tested RIG-ablated and AIY-ablated worms in wild-type and *dat-1::ICE* backgrounds. For the RIG-ablated worms, the presence of salt enhanced CO_2 avoidance in both wild-type and *dat-1::ICE* backgrounds (Figure 5D). For AIY-ablated worms, the presence of salt enhanced avoidance in the *dat-1::ICE* background but not in the wild-type background (Figure 5D). Since worms with AIY neurons ablated in the wild-type background showed strong avoidance to the concentration of CO_2 we tested (15%), we tested worms at a lower concentration of CO_2 in an attempt to unmask a salt-dependent effect on behavior. However, in response to 2.5% CO_2, the presence of salt enhanced CO_2 avoidance in wild-type worms (Figure 5E). Taken together, our results suggest that another interneuron or group of interneurons whose activity is differentially modulated by salt-context may regulate the context-dependent modulation of CO_2 response valence, as neither RIG nor AIY neurons are required to see salt-dependent effects on behavior.

Discussion

We have demonstrated a mechanism by which feeding state sculpts a neural circuit to alter the valence of the chemosensory cue CO_2. We found that while fed worms raised in ambient CO_2 concentrations avoid CO_2, after only 3 hours of food-deprivation, worms become attracted to CO_2. This shift in valence likely reflects an internal risk-benefit analysis. Freely proliferating populations of *C. elegans* are found in rotting fruits, where concentrations of CO_2 are high, suggesting that CO_2 may indicate the presence of food (Felix and Duveau, 2012). Despite this, fed worms grown in laboratory conditions avoid CO_2, perhaps to elude CO_2-emitting predators. By contrast, the CO_2-response valence of starved worms may shift as worms prioritize food-seeking behavior over predator evasion. Similar risk-taking strategies emerge during starvation in mammals and other animals when food seeking becomes a top priority (Filosa et al., 2016; Padilla et al., 2016). Increased risk-taking behavior has also been documented in hungry humans, who are willing to gamble money under lower chances of winning than sated humans (Symmonds et al., 2010). We have investigated a core circuit motif involved in this valence change, and we show that dopamine signaling sculpts the neural circuit to promote CO_2 avoidance in fed worms (Figure 6).

Figure 6

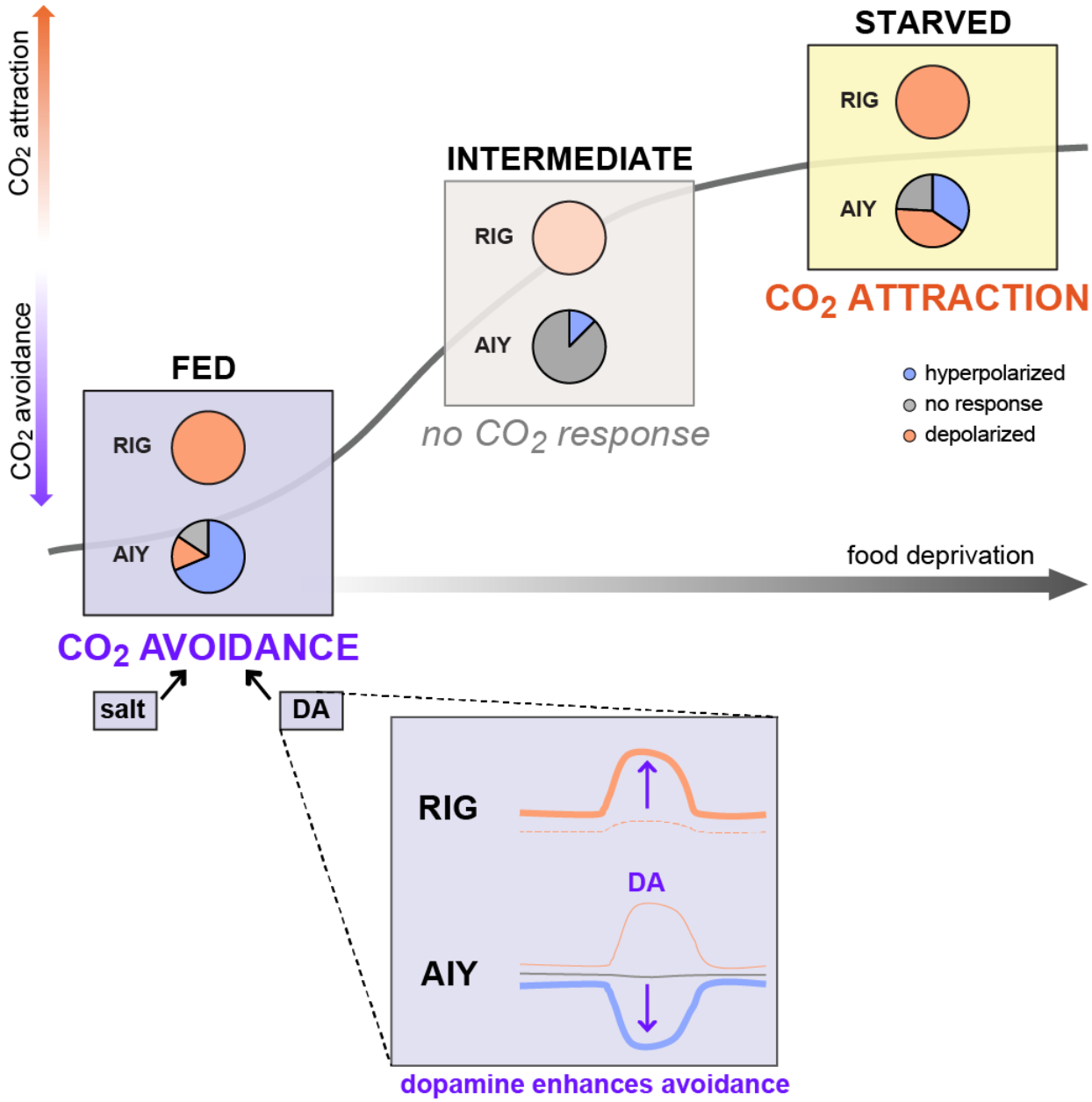

A model depicting how feeding-state regulates CO_2-response valence. The gray curve in the background is a schematic showing CO_2-response valence as a function of food-deprivation based on Figure 1a. Each box along the curve shows RIG and AIY activity in fed (purple), 90-minute starved (gray), and 6 hour (RIG) or 16-28 hour (AIY) food-deprived worms (yellow). Pie charts for AIY interneurons are from data in Figures 2D

and S3. RIG circles qualitatively show the CO_2-evoked depolarization (fed, starved) and suppression of activity (intermediate) from Figure 2B. In the fed state, dopamine (DA) and salt coordinately promote CO_2 avoidance. The dopamine inset schematically represents how dopamine modulates activity of RIG and AIY neurons in order to promote CO_2 based on conclusions from Figure 4.

Modulation of the CO_2 circuit during starvation:

To identify neurons regulating CO_2 response valence as a function of feeding state, we first looked at the BAG sensory neurons. Throughout starvation, the BAG calcium response to CO_2 remained relatively constant, suggesting that CO_2 valence arises downstream of the BAG calcium response, consistent with our previous study of CO_2 response in ambient- and CO_2-cultivated worms (Guillermin et al., in submission). A previous *C. elegans* study demonstrated that state- and sex- dependent changes in behavioral prioritization for food preference can occur at the sensory neuron level (Ryan et al., 2014). CO_2, in contrast to food, is a particularly complex stimulus because it carries implications with mixed valence. Thus, the sensory valence of CO_2 at a given time may emerge from a complex computation that is encoded by the coordinated activity of multiple neurons. We decided to focus primarily on the modulation of RIG and AIY since ablating either of these neurons had dramatic effects on CO_2-response valence. However, it is possible that other neurons we did not probe may also have important roles in regulating CO_2-response valence.

Food-deprivation causes transient circuit changes:

Many studies have probed state-dependent changes in neural circuits at end points of behavioral states (Fenk and de Bono, 2017; Ko et al., 2015; Krashes et al., 2009). The transition from fed to starved states during food deprivation represents a continuous spectrum, suggesting that the activity of neural circuits driving state-

dependent behaviors may shift over a continuum as well. In our study, by imaging the CO_2 circuit over the course of food deprivation, we have discovered that neural circuits can be reversibly modulated. RIG neurons were depolarized by CO_2 indistinguishably in fed worms and 6-hour food-deprived worms. However, RIG-ablated worms had impaired avoidance behavior and accelerated attraction, implicating RIG in the shift from avoidance to attraction. We uncovered a suppressed RIG CO_2 response in worms that were food-deprived for 90 minutes, which may set the time course for the shift in valence. This transient suppression suggests that neural circuit activity reflects intermediate behavioral states, and studying the activity of neural circuits at either extreme of a behavioral spectrum may fail to capture important changes that drive transitions. That RIG activity promotes an avoidance state but has no effect on CO_2 attraction in 6-hour food-deprived worms suggests that, in starved worms, the CO_2 circuit can override the CO_2-evoked depolarization of RIG to still produce attraction.

Food deprivation increases variability of AIY neuron activity

In contrast to the transient modulation of RIG neurons, AIY neurons demonstrated a probabilistic CO_2-evoked response, and the distribution of qualitatively different calcium responses was determined by feeding state. AIY response in fed worms was primarily hyperpolarizing, whereas in starved worms the AIY response was more variable with roughly equal numbers of responses classified as depolarizations and hyperpolarizations. These results suggest that AIY activity promotes CO_2 attraction. AIY activity has been shown to suppress pirouette frequency during unstimulated movement (Li et al., 2014), consistent with our findings in worm tracking experiments. In fed worms, which primarily have CO_2-evoked hyperpolarizations in AIY,

CO_2 increases pirouette frequency. By contrast, in starved worms, where a greater proportion of AIY neurons are depolarized than hyperpolarized, the presence of CO_2 increases pirouette frequency. Thus, CO_2-evoked changes in AIY activity may contribute to modulation of pirouette frequency in fed and starved states.

We found that although starved worms demonstrate CO_2 attraction on the population level, their attraction was less robust than the CO_2 attraction of worms raised in a high CO_2 environment. This difference is correlated with the CO_2-evoked response of AIY neurons, which was much more variable for starved worms than for worms cultivated in high CO_2 environments. We hypothesize that starvation represents a period of environmental uncertainty. Behavioral variability among a population of genetically similar individuals might represent an evolutionarily advantageous mechanism of selection at the population level. By having some individuals in a population maintain their CO_2 avoidance even after prolonged food-deprivation, *C. elegans* may optimize food seeking while still hedging against being captured by predators. Such a strategy, called bet-hedging, allows risk to be spread out over the population to promote fitness of a particular genotype (Gillespie and Langley, 1976; Philippi and Seger, 1989; Slatkin, 1974). Bet-hedging is a universal strategy for evolutionary fitness employed under uncertain periods by organisms such as yeast, plants, insects, fish and mammals (Hopper, 1999; Kain et al., 2015; Levy et al., 2012; Nevoux et al., 2010; Venable, 2007). Humans, for example, use bet-hedging in farming. By planting a variety of crops, rather than a single most profitable crop, the farmer can still make a profit even during unpredictable fluctuations in environment or crop demand.

A previous study found that whereas olfactory responses of the *C. elegans* sensory neuron AWC were reliable, odor-evoked responses of AIB, an interneuron directly downstream from AWC, could be either reliable or probabilistic, depending on the network state of a circuit motif (Gordus et al., 2015). Here we found that the response of AIY to CO_2 is similarly variable in starved worms, despite the reliability of CO_2-evoked responses from the BAG sensory neurons. Our study links neuronal variability to behavioral state, and we provide an ecological relevance –bet hedging during starvation– for why probabilistic neural responses occur. The variability of response in AIY neurons may be a neural correlate for population-based risk spreading for optimizing foraging and minimizing predation.

Dopaminergic modulation of RIG and AIY

We found that the lack of dopaminergic neurons caused constitutive CO_2 attraction regardless of feeding state by modulating the CO_2 response of RIG and AIY in opposite directions. The lack of dopaminergic neurons caused a suppression of the RIG depolarization to CO_2 and caused the AIY CO_2 response to shift from largely hyperpolarizing to no response. The loss of any single dopaminergic receptor was not sufficient to cause CO_2 attraction, suggesting that multiple receptors redundantly promote CO_2 avoidance.

Whether dopamine binds receptors on AIY or RIG to directly modulate their activity, or whether it binds dopamine receptors on neurons upstream of AIY and RIG remains unclear. Although the AIY neurons do not receive direct synaptic input from the dopaminergic neurons, they have been shown to express the dopamine receptor DOP-5

(Bentley et al., 2016). A recent study found that 82.3% of neurons known to express dopamine receptors do not receive direct synaptic input from the dopaminergic neurons, suggesting that extrasynaptic signaling is an important mediator of dopamine transmission (Bentley et al., 2016).

By contrast, RIG neurons receive strong synaptic input from the dopaminergic ADE neurons (Varshney et al., 2011; White et al., 1986), raising the likelihood of direct dopaminergic modulation of RIG. No dopamine receptors are known to be expressed in RIG neurons, however the characterization of dopamine receptor expression is not comprehensive, leaving open the possibility that dopaminergic receptors expressed in RIG have yet to be identified.

The effects of dopaminergic modulation on the core circuit were primarily described during the fed state and early on during food deprivation. Although we have focused on elucidating how dopamine signaling modulates the CO_2 circuit during the fed state where its effect is most pronounced, we demonstrated that excess dopamine disrupts CO_2 attraction in worms food-deprived for 3 or more hours (Figure 4B, 4D), suggesting that dopamine signaling acts beyond the fed state. Although dopamine is released during the presence of food, previous studies have demonstrated that dopamine inhibits release and downstream signaling of the starvation-associated biogenic amine octopamine (Suo et al., 2009); perhaps our results implicate a role for octopamine in worms deprived of food for longer periods.

Salt and dopamine redundantly encode food

Finally, we demonstrated that dopamine signaling, a signal for the mechanosensation of food, and the presence of salt, a gustatory component of food, interact to promote CO_2 avoidance. Abolishing either of these signals alone was not sufficient to eliminate CO_2 avoidance. These findings suggest that the presence of food and the fed state are complex and encoded by multiple sensory modalities. Similarly, in humans, multiple modalities of food sensing, for example the smell of strawberries and taste of sugar, synergistically combine to increase food reward (de Araujo et al., 2003). Thus, similar mechanisms of sensory integration create a complex, multisensory representation of food in humans as well. Our results indicate that neither the RIG nor AIY neurons was required to show salt-dependent differences in CO_2 response, suggesting that other neurons outside of the CO_2 circuit motif that we examined integrate information about salt context.

Taken together, our results provide novel mechanisms for how neural circuits integrate internal state with current environment in order to encode an ecologically appropriate sensory valence. Similar to humans, worms become less risk averse as they starve, and they correspondingly prioritize foraging over predator avoidance. The behavior of starved worms reflects a bet-hedging strategy that allows worms to spread risk by maintaining multiple types of CO_2-response valence, and we identified a neuronal correlate for this behavioral variability. By contrast, the redundant encoding of multiple sensory components of food in promoting CO_2 avoidance may encode enhanced risk aversion in well-fed worms. When starvation risk is low, neural circuits may primarily utilize a strategy of CO_2 avoidance.

All animals navigate through uncertain and rapidly fluctuating environments. Animal survival requires that neural circuits maintain a current representation of internal and external context. Our results provide fundamental insights into dynamic mechanisms of neural circuits underlying state- and context-dependent behaviors and likely have implications for higher-level nervous systems.

Methods:

Animals:

C. elegans worms were reared on nematode growth media (NGM) plates seeded with the bacteria *E. coli* OP50 strain. Except for CO_2-cultivated worms, all worms were raised at ambient temperature (~22°C) and CO_2 (~0.038%). Some strains were raised at 15°C, but were moved to room temperature at least 12 hours prior to experiments in order to prevent any effects of temperature shifts on behavior. CO_2-cultivated worms were raised as previously described (Guillermin et al., in submission). Young adult worms were placed in a Tritech Research DigiTherm® at 22°C and 2.5%CO_2, and three days later their progeny were tested in behavioral assays or calcium imaging experiments.

Table 1: Strain list

Strain Number	Genotype	Description
N2	[wild isolate strain]	Bristol isolate
EAH284	*bruEx138[Pttx-3::814caspase3; Pttx-3::813caspase3; myo-2::dsRed]*	AIY ablation (Guillermin et al., in submission)

EAH268	*bruEx160[twk-3::814caspase3; twk-3::813caspase3; myo-2::dsRed]*	RIG ablation (Guillermin et al., in submission)
IV316	*ueEx194[odr-2b3a::TeTx::GFP; elt-2::SL2::GFP]*	AIB and AIZ silenced by tetanus toxin (Calhoun et al., 2014)
PS6028	*syEx1134[twk-3::CAM #1.1]*	RIG neurons expressing cameleon
EAH319	*bruEx171[Pglr-3::814caspase3; Pglr-3::813caspase3; myo-2::dsRed]*	RIA ablation (Guillermin et al., in submission)
IK1405	*njEx568[ttx-3::YC3.60, ges-1::NLS-RFP]*	AIY neurons expressing cameleon (Kuhara and Mori, 2006)
AX2073	*lin-15(n765ts); dbEx[flp-17::YC3.60, lin-15(+)]*	BAG neurons expressing cameleon (Bretscher et al., 2011)
EAH240	otIs181 [dat-1::mCherry + ttx-3::mCherry]; *akEx387[lin-15(+), dat-1::GFP, dat-1::ICE]*	Dopaminergic neuron ablation with integrated mCherry reporter
MT15620	*cat-2(n4547)*	Loss-of-function of tyrosine hydroxylase gene (Omura et al., 2012)
RM2702	*dat-1(ok157)*	Loss-of-function of dopamine transporter
VM636	*lin-15(n765ts); akEx387[lin-15(+), dat-1::GFP, dat-1::ICE]*	*dat-1::ICE* without integrated mCherry
LX636	*dop-1(vs101)*	*dop-1(lf)* 4x outcrossed to N2
LX702	*dop-2(vs105)*	*dop-2(lf)* 4x outcrossed to N2
LX703	*dop-3(vs106)*	*dop-3(lf)* 4x outcrossed to N2
FG58	*dop-4(tm1392)*	*dop-4(lf)* 5x outcrossed to N2
CX13111	*dop-5(ok568)*	*dop-5(lf)* 3x outcrossed to N2
EAH337	*dop-6(ok2090)*	*dop-6(lf)* 3x outcrossed to N2
MT13952	*lgc-53(n4330)*	*lgc-53(lf)* (Ringstad et al., 2009)
EAH334	lin-15(n765ts); otIs181 [dat-1::mCherry + ttx-3::mCherry]; akEx387[lin-15(+), dat-1::GFP, dat-1::ICE]; dbEx[flp-17::YC3.60, lin-15(+)]	BAG neurons expressing cameleon in *dat-1::ICE* background
EAH339	*otIs181 [dat-1::mCherry + ttx-3::mCherry]; akEx387[lin-15(+), dat-1::GFP, dat-1::ICE];syEx1134[twk-*	RIG neurons expressing cameleon in the *dat-1::ICE* background

	3::CAM #1.1]	
EAH338	*otIs181 [dat-1::mCherry + ttx-3::mCherry]; akEx387[lin-15(+), dat-1::GFP, dat-1::ICE];njEx568[ttx-3::YC3.60, ges-1::NLS-RFP]*	AIY neurons expressing cameleon in the *dat-1::ICE* background
EAH293	Ex[gcy-5/7::NzCsp3, gcy-5/7::CzCsp3, gcy-5/7::GFP, elt-2::GFP]	ASE-ablation (Shingai et al., 2014)
EAH332	otIs181 [dat-1::mCherry + ttx-3::mCherry]; *akEx387[lin-15(+), dat-1::GFP, dat-1::ICE];* Ex[gcy-5/7::NzCsp3, gcy-5/7::CzCsp3, gcy-5/7::GFP, elt-2::GFP]	ASE ablation in *dat-1::ICE* background
EAH331	otIs181 [dat-1::mCherry + ttx-3::mCherry]; *akEx387[lin-15(+), dat-1::GFP, dat-1::ICE]; bruEx160[twk-3::814caspase3; twk-3::813caspase3; myo-2::dsRed]*	RIG ablation in dat-1::ICE background
EAH333	otIs181 [dat-1::mCherry + ttx-3::mCherry]; *akEx387[lin-15(+), dat-1::GFP, dat-1::ICE];bruEx138[Pttx-3::814caspase3; Pttx-3::813caspase3; myo-2::dsRed]*	AIY ablation in dat-1::ICE background

Population-based behavioral assays:

Chemotaxis assays:

Except as otherwise noted, chemotaxis assays were performed similarly to previously described (Carrillo et al., 2013). Roughly 100-500 young adult worms were washed off seeded nematode growth media (NGM) plates into a 65 mm Syracuse watch glass. Worms were washed 3 times with 3 ml of M9 buffer and were allowed to settle at the bottom of the dish. After supernatant removal, worms were transferred to a 1.5 cm x1.5 cm piece of Whatman filter paper. The filter paper was flipped onto the center of a 9 cm circular chemotaxis or NGM plate for testing. The plate was covered with a modified lid fabricated to fit two ¼-inch (outer diameter) PVC tubes, inserted on

opposite sides along the lid diameter, each 3 cm away from the center. Two gases, CO_2 and an air control, were delivered to either side of the plate through the tubing to establish a CO_2 gradient across the dish. The CO_2 gas was a custom mixture of CO_2, O_2, and N_2. The air control for a given experiment had the same O_2 background, but had 0% CO_2 and N_2 balanced the lack of CO_2. The O_2 background was either 10% (Figures 1A, 3A, 4A-D, S4B, S5) or 21% (Figures 1B, 2A, 3B-D, 4E-J, 5A-F, S4A). No difference was observed between these backgrounds on behavior. A Harvard Apparatus syringe pump was used to control gas delivery at a rate of 2 ml/min. Assays were run for 20 minutes except for Figure 1B assays, which were run for 10 minutes. At the end of each assay, experiments were scored by counting the number of worms in the 2-cm circular scoring regions directly under the CO_2 and air control sources. In certain experiments (Figures 1B, 4C-D, 5 A-F), we expanded the scoring regions (referred to as "large scoring regions") to include the regions defined as circular segments beginning 1.5 cm away from the center of the plate. The results were quantified as chemotaxis index (CI), which was calculated as follows:

$$CI = \frac{\#\ worms\ in\ CO_2\ region - \#\ worms\ in\ air\ control\ region}{\#\ worms\ in\ CO_2\ region + \#\ worms\ in\ air\ control\ region}$$

To check for directional bias from room vibrations, assays were run in pairs and the CO_2 and air control gases were oriented in opposite directions for the two plates. If the difference in CIs between these assays was greater than or equal to 0.9, it was concluded that directional bias was strongly influencing behavior and those trials were discarded from analysis. Assay pairs were also discarded if, for at least one assay in the pair, fewer than 7 worms total were counted in either scoring region. Since AIY-ablated animals moved poorly in chemotaxis assays, if there was no directional bias within a

pair of assays but only one of the assays had fewer than 7 worms move, the assay with at least 7 worms scored was included in analysis.

Starvation assays:

For chemotaxis assays in starved worms, worms were food-deprived on 9-cm NGM plates. Plates were made with 2% agar to limit worms from burrowing into the agar during the period of food deprivation. To prevent worms from crawling off the plate during starvation, we dipped an annular-shaped ring of Whatman filter paper with an outer diameter of 7 cm and width of 0.75 cm into a 20-mM copper chloride ($CuCl_2$) solution and transferred the ring onto the 2% NGM plate. Fed worms were washed off growing plates with M9 buffer into a Syracuse watch glass, washed 3 times in M9, and then transferred with Whatman paper to the center of the starvation plate (within the $CuCl_2$-soaked ring). Worms were left on the plates during the period of food deprivation. Immediately prior to behavioral testing, the $CuCl_2$-soaked filter paper was removed and worms were washed off the plate and then washed 3 times with M9 before being transferred to an assay plate as described earlier.

Exogenous dopamine assays:

A fresh stock solution of 1M dopamine-HCl in distilled water was prepared each day. The stock solution was wrapped in aluminum foil and stored in a 4°C incubator to minimize oxidation of dopamine. To make dopamine-treated plates for worm incubation, 200 μl of the stock solution was added to each 9 cm 2% NGM plate to make a final concentration of 10 mM dopamine for the plate. For mock-treatment plates, 200 μl of distilled water was added to 2% NGM plates. The treatment solution was spread on the plates, and then the plates were closed and loosely covered with aluminum foil to dry.

Within 15 minutes, worms were washed off food, washed 3 times as previously described, and then added to the plates for the duration of food deprivation. For testing, 200μl of the dopamine stock solution or distilled water was added to each chemotaxis plate, spread and dried as described. Within 15 minutes, worms were washed off the incubation plates and transferred with 1.5 cm by 1.5 cm Whatman filter paper onto the testing plates. Assays were run as previously described except that aluminum foil was loosely placed over the assays plates for the duration of the assay to limit light exposure.

Salt context assays:

Assays tested behavior of fed worms on chemotaxis-based plates. The "no salt" condition used chemotaxis plates with no modifications. The "salt" condition used chemotaxis plates with 50 mM NaCl. The "sorbitol" condition balanced the osmolarity of the salt plates with sorbitol and thus consisted of chemotaxis plates with 100 mM sorbitol.

Worm Tracking

Fed worms were placed on homogenously spread OP50 plates for at least one hour prior to testing. Food-deprived worms were washed as described and incubated on 2% NGM plates without $CuCl_2$ for 6 hours. To confirm that the conditions used for worm tracking produced avoidance and attraction in chemotaxis assays, chemotaxis assays were performed under these same conditions (Figure S1).

For testing, fed worms were first transferred to an NGM plate with no food, and were allowed to crawl around the plate for one minute to remove residual food on their

cuticles. Worms were then transferred to a fresh 2% NGM (Figure 1C) or chemotaxis plate (Figure 3B-C) for testing. Food-deprived worms were picked directly off of the starving plate onto the testing plate but were given at least one minute to recover from worm picking prior to tracking. Tracking plates were prepared by making a single small hole to fit 1/8" (OD) PVC tubing on the side of a plate. PVC tubing was inserted through both the lid and the plate sides, and gas was delivered at a rate of 2 ml/min via a Harvard Apparatus syringe pump. In each experiment either 15% CO_2 (with a 21% O_2 background) or the air control was inserted into the hole to establish a gradient with highest concentration of the gas at the end of the tube.

Video acquisition were acquired at 2 frames per second and recording began the moment that the testing plate was positioned under a Mightex CMOS camera (BTE-B050-U). The gas tube was inserted into the plate within the first 60 frames of the video. For analysis, the frames prior to insertion of the gas tube were discarded.

The open source Worm Tracker and Track Analyzer (Ramot et al., 2008) were used to track worms and compute speed and pirouette frequency. Only tracks that were at least two minutes long were used for analysis, which ensured that no worms were tracked more than once. The Track Analyzer code was modified to calculate the direction of worm locomotion with respect to the gas source and to calculate worm distance from the CO_2 source. To monitor whether locomotion was biased by the presence of gas, two new parameters were created. The first parameter was the change in displacement of a worm from the gas source. It was calculated by subtracting the distance of the worm from the CO_2 source at the beginning of a track from the distance of the worm from the CO_2 source exactly two minutes into the track.

A negative value indicates that the worm moved closer to the gas source whereas a positive value indicates that the worm moved farther away from the gas source. The second parameter computed the percent of time that a worm spent moving toward a gas source. Given that at any point in time the worm could move directly toward the gas source or as much as 180 degrees away from it, we defined motion toward the gas source as movement within 60 degrees of the gas source. Thus, a given frame where the worm moved either ≤ 60 degrees or ≥ -60 degrees from the gas source was considered motion toward the gas. To compute the percent of time a worm moved toward the gas source within a track, the following formula was used:

$$\%\ Motion\ toward\ gas = \frac{(\#frames\ direction \geq 60) + (\#frames\ direction \leq 60)}{\#frames\ in\ track} * 100$$

<u>Calcium Imaging:</u>

Worms were imaged as previously described (Hallem et al, 2011, Carrillo et al, 2013). Briefly, transgenic worms expressing the genetically-encoded FRET-based calcium indicator cameleon YC3.60 in the neuron of interest were placed on a 2% agarose pad made with 10 mM HEPES solution. Worms were glued onto the pad with Meridian Surgi-Lock glue. A chamber was fabricated from a 10-mm petri dish with two holes on opposite sides of the dish. The chamber was secured onto the coverslip with beeswax. Two gas tanks were fitted with pneumatic valves controlled by a ValveBank TTL-generator. Flow meters delivered gas at a rate of 0.73-0.78 L/min. The two gas tubes were attached with a Y attachment fitted with a pipette tip. The pipette tip was inserted into one side of the chamber and the end was placed within 2 mm of the worm's nose.

A custom program controlled gas delivery. The first gas, a control air pulse, was delivered for 20s, then the test gas was delivered for 20s, and finally the air control was again delivered for 40 seconds. In CO_2 trials, the test gas was either 15% CO_2 (for AIY recordings) or 10% CO_2 (BAG and RIG recordings) in a background of 21%O_2. For air trials, the test gas was the same as the air control gas (21% O_2). Images were acquired in two separate channels for YFP and CFP at 2 frames per second with a CCD camera and commercial AxioVision software. For analysis, regions of interest (ROIs) were selected for the soma of the neuron of interest (BAG, RIG) or for the process (AIY, zone 2 (Colon-Ramos et al., 2007)) and also for a background region. Average intensity for YFP and CFP of the background ROI was subtracted from the average intensity for YFP and CFP of the neuron/process, respectively. The YFP values were adjusted to correct for CFP signal bleed through, and then the YFP to CFP ratio (YFP/CFP) was calculated. The data was linearly baseline-adjusted using the air periods before and after the gas pulse as the baseline. Then the average ratio during the baseline periods (R_0) was subtracted from the adjusted YFP/CFP (R) and the resulting value was normalized to the average baseline. The value was multiplied by 100 to get $\%\Delta R/R_0$. Recordings were excluded from analysis if the YFP/CFP ratio during the baseline periods was not flat.

To quantify responses, the response period was defined as the 30-second period that began at the moment when the test gas was delivered. The most extreme response was calculated as the value of $\% \Delta R/R_0$ during the response period that had the greatest absolute value. For AIY imaging, each recording was categorized as a hyperpolarization, depolarization or non-response. To determine the threshold for each

of these categories, data from the air control experiments were used. For each condition tested, the mean of the maximum and minimum for each air control recording was calculated. Thresholds for responses were set as three standard deviations above the average maximum air response or 3 standard deviations below the average minimum air response. Thus, for CO_2 trials, if the most extreme value was positive and greater than our threshold, the recording was classified as a depolarization. Recordings from CO_2 trials with negative most extreme values that were less than the minimum threshold were categorized as hyperpolarizations. The remaining recordings whose most extreme value fell in between the thresholds for depolarizations and hyperpolarizations were categorized as non-responses.

Worm preparation for calcium imaging

Young adult worms were screened for YC3.60 expression in the neuron of interest. To optimize the dynamic range of calcium activity, worms with dim YC3.60 were selected for recordings that measured activity of the soma. For recordings that measured activity in processes, brighter expression of YC3.60 was required to optimize the signal to noise ratio.

Worms food-deprived for up to 6 hours were starved similarly to worms in chemotaxis assays. Fluorescent, YC3.60-expressing worms were picked off seeded NGM plates onto unseeded NGM plates. Worms were allowed to crawl around the plate for one minute to clear any food on the worm cuticle. Worms were then picked to the center of a 2% NGM plate lined with a $CuCl_2$-dipped annular Whatman filter paper where they were left for the period of food deprivation.

Worms food-deprived for prolonged periods (16-28 hours) prior to imaging were starved in M9 buffer rather than on 2% NGM plates to limit the number of worms lost from burrowing or crawling off the plate. Worms were washed 3 times with M9 buffer as described and starved in a 14-cm glass petri dish filled with approximately 60 mL of M9 buffer. The petri dish was left on a shaker platform for the period of food deprivation to prevent worm hypoxia during starvation. To control for the increased age of these worms, the fed control used worms that were matched in age to the starved worms.

Statistical Analysis:

All statistics were computed using GraphPad Prism (version 7.0a) software. For one-way ANOVA tests and two group comparisons, the data was first evaluated for normality using the D'Agostino and Pearson test. If the data passed the normality test, a parametric test was used, otherwise a non-parametric test (Kruskal-Wallis test for one-way ANOVAs and Mann-Whitney rank-based test for two-group comparisons).

Supplementary figures

Figure S1

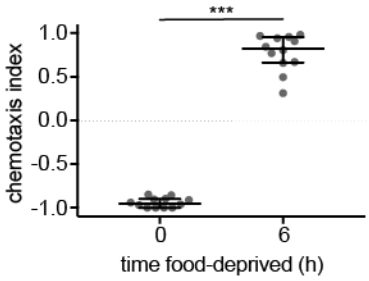

Conditions used for worm tracking produce both CO_2 avoidance and attraction. n=12 trials for each condition. ***p<0.001, unpaired t-test.

Figure S2

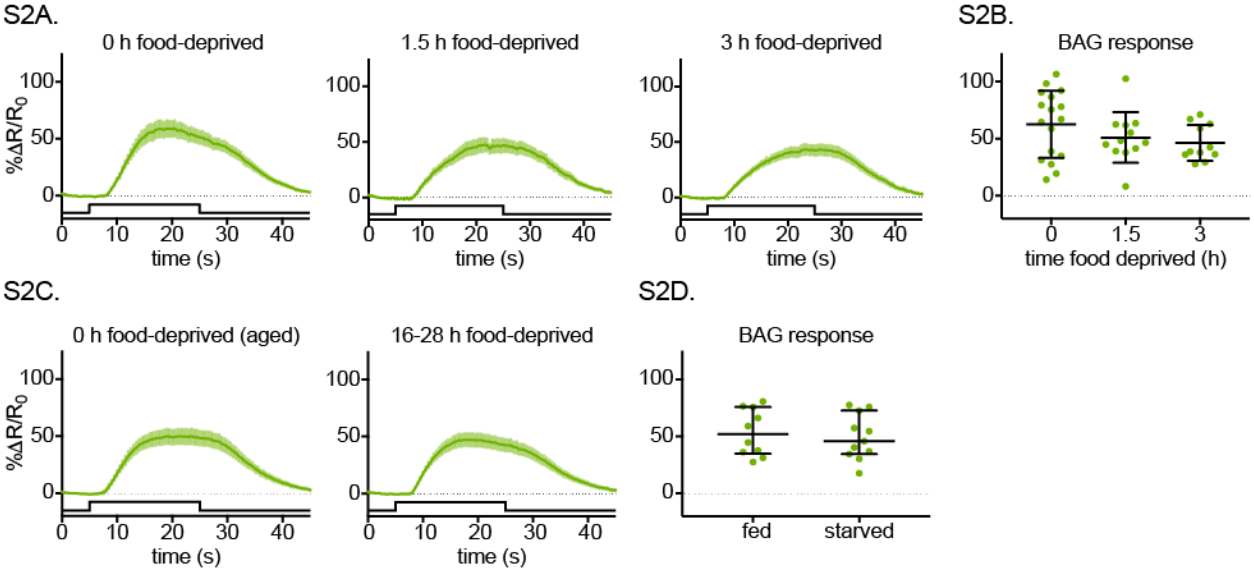

The BAG neuron response to CO_2 remains constant throughout starvation. (A-B) Activity of BAG in worms food-deprived for 0, 1.5 and 3 hours. n=11-17 recordings per condition. (A) Curves represent mean values and SEMs. (B) BAG responses quantified across states. p=0.1966, one-way ANOVA. (C-D) Worms food-deprived for 16-28 hours show the same CO_2 response as fed worms, matched in age. n=10-11 trials per condition. (C) Curve represents mean with SEM as errors. (D) BAG most extreme response quantified. p=0.6454, unpaired t-test.

Figure S3

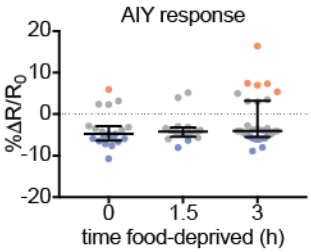

The AIY CO_2 response remains relatively constant in worms food-deprived for 0, 1.5, and 3 hours. Responses were analyzed and sorted as described in (2E). n=16-30 recordings per condition. p=0.3450, Kruskal-Wallis test.

Figure S4

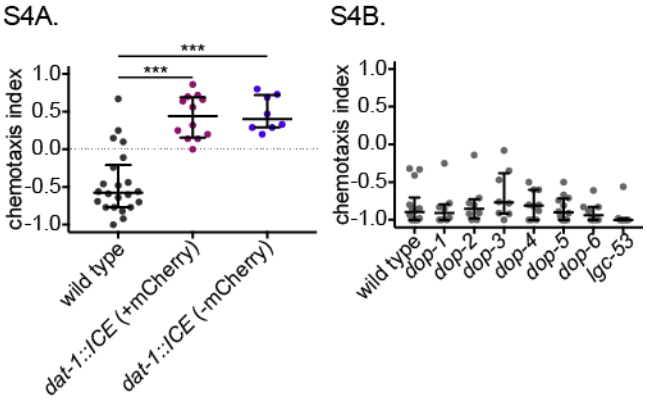

Dopamine promotes CO_2 avoidance (A) The integrated *ttx-3/dat-1::mCherry* reporter is not required for CO_2 attraction in *dat-1::ICE* worms. n=8-22 trials per strain. ***p<0.001, Kruskal-Wallis test, post-test with Dunn's correction. (B) No single dopamine receptor is required for CO_2 avoidance in fed worms. n=8-14 trials per strain. p=0.2479, Kruskal-Wallis test.

Figure S5

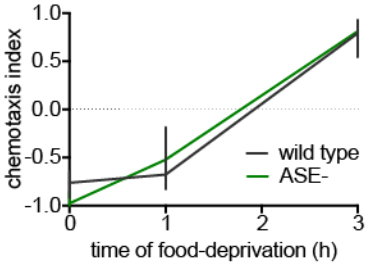

Ablating the ASE neurons does not alter the shift of CO_2 response during food deprivation. ASE-ablated worms (green), N2 (black). n=10-16 trials for each condition. (p_{strain} =0.7278, p_{state}<0.0001, $p_{interaction}$= 0.1077, 2-way ANOVA)

References

Bargmann, C.I. (2006). Chemosensation in *C. elegans.* WormBook, 1-29.

Bargmann, C.I., and Horvitz, H.R. (1991). Chemosensory neurons with overlapping functions direct chemotaxis to multiple chemicals in *C. elegans*. Neuron *7*, 729-742.

Bargmann, C.I., and Marder, E. (2013). From the connectome to brain function. Nat Methods *10*, 483-490.

Bentley, B., Branicky, R., Barnes, C.L., Chew, Y.L., Yemini, E., Bullmore, E.T., Vertes, P.E., and Schafer, W.R. (2016). The Multilayer Connectome of *Caenorhabditis elegans*. PLoS computational biology *12*, e1005283.

Bretscher, A.J., Busch, K.E., and de Bono, M. (2008). A carbon dioxide avoidance behavior is integrated with responses to ambient oxygen and food in *Caenorhabditis elegans.* Proc Natl Acad Sci U S A *105*, 8044-8049.

Bretscher, A.J., Kodama-Namba, E., Busch, K.E., Murphy, R.J., Soltesz, Z., Laurent, P., and de Bono, M. (2011). Temperature, oxygen, and salt-sensing neurons in *C. elegans* are carbon dioxide sensors that control avoidance behavior. Neuron *69*, 1099-1113.

Calhoun, A.J., Chalasani, S.H., and Sharpee, T.O. (2014). Maximally informative foraging by *Caenorhabditis elegans*. Elife *3*.

Calhoun, A.J., Tong, A., Pokala, N., Fitzpatrick, J.A., Sharpee, T.O., and Chalasani, S.H. (2015). Neural Mechanisms for Evaluating Environmental Variability in *Caenorhabditis elegans*. Neuron *86*, 428-441.

Carrillo, M.A., Guillermin, M.L., Rengarajan, S., Okubo, R.P., and Hallem, E.A. (2013). O_2-sensing neurons control CO_2 response in *C. elegans*. J Neurosci *33*, 9675-9683.

Carrillo, M.A., and Hallem, E.A. (2014). Gas Sensing in Nematodes. Molecular neurobiology.

Chase, D.L., and Koelle, M.R. (2007). Biogenic amine neurotransmitters in *C. elegans*. WormBook, 1-15.

Colon-Ramos, D.A., Margeta, M.A., and Shen, K. (2007). Glia promote local synaptogenesis through UNC-6 (netrin) signaling in *C. elegans.* Science *318*, 103-106.

de Araujo, I.E., Rolls, E.T., Kringelbach, M.L., McGlone, F., and Phillips, N. (2003). Taste-olfactory convergence, and the representation of the pleasantness of flavour, in the human brain. Eur J Neurosci *18*, 2059-2068.

Ezak, M.J., and Ferkey, D.M. (2010). The *C. elegans* D2-like dopamine receptor DOP-3 decreases behavioral sensitivity to the olfactory stimulus 1-octanol. PLoS One *5*, e9487.

Ezcurra, M., Tanizawa, Y., Swoboda, P., and Schafer, W.R. (2011). Food sensitizes *C. elegans* avoidance behaviours through acute dopamine signalling. EMBO J *30*, 1110-1122.

Faucher, C., Forstreuter, M., Hilker, M., and de Bruyne, M. (2006). Behavioral responses of Drosophila to biogenic levels of carbon dioxide depend on life-stage, sex and olfactory context. J Exp Biol *209*, 2739-2748.

Felix, M.A., and Duveau, F. (2012). Population dynamics and habitat sharing of natural populations of *Caenorhabditis elegans* and *C. briggsae*. BMC Biol *10*, 59.

Fenk, L.A., and de Bono, M. (2017). Memory of recent oxygen experience switches pheromone valence in *Caenorhabditis elegans.* Proc Natl Acad Sci U S A *114*, 4195-4200.

Filosa, A., Barker, A.J., Dal Maschio, M., and Baier, H. (2016). Feeding State Modulates Behavioral Choice and Processing of Prey Stimuli in the Zebrafish Tectum. Neuron *90*, 596-608.

Fontanini, A., and Katz, D.B. (2008). Behavioral states, network states, and sensory response variability. J Neurophysiol *100*, 1160-1168.

Ghosh, D.D., Sanders, T., Hong, S., McCurdy, L.Y., Chase, D.L., Cohen, N., Koelle, M.R., and Nitabach, M.N. (2016). Neural Architecture of Hunger-Dependent Multisensory Decision Making in *C. elegans*. Neuron *92*, 1049-1062.

Gillespie, J., and Langley, C. (1976). Multilocus behavior in random environments. I. Random Levene models. Genetics *82*, 123-137.

Goodman, M.B. (2006). Mechanosensation. WormBook, 1-14.

Goodman, M.B., Klein, M., Lasse, S., Luo, L., Mori, I., Samuel, A., Sengupta, P., and Wang, D. (2014). Thermotaxis navigation behavior. WormBook, 1-10.

Gordus, A., Pokala, N., Levy, S., Flavell, S.W., and Bargmann, C.I. (2015). Feedback from network states generates variability in a probabilistic olfactory circuit. Cell *161*, 215-227.

Guillermin, M.L., Carrillo, M.A., and Hallem, E.A. (in submission). A single set of interneurons drives opposite behaviors in *C. elegans.*

Hallem, E.A., Dillman, A.R., Hong, A.V., Zhang, Y., Yano, J.M., DeMarco, S.F., and Sternberg, P.W. (2011). A sensory code for host seeking in parasitic nematodes. Curr Biol *21*, 377-383.

Hallem, E.A., and Sternberg, P.W. (2008). Acute carbon dioxide avoidance in *Caenorhabditis elegans.* Proc Natl Acad Sci U S A *105*, 8038-8043.

Hart, A.C., and Chao, M.Y. (2010). From Odors to Behaviors in *Caenorhabditis elegans*. In The Neurobiology of Olfaction, A. Menini, ed. (Boca Raton (FL)).

Hills, T., Brockie, P.J., and Maricq, A.V. (2004). Dopamine and glutamate control area-restricted search behavior in *Caenorhabditis elegans.* J Neurosci *24*, 1217-1225.

Hopper, K.R. (1999). Risk-spreading and bet-hedging in insect population biology. Annual review of entomology *44*, 535-560.

Inagaki, H.K., Panse, K.M., and Anderson, D.J. (2014). Independent, reciprocal neuromodulatory control of sweet and bitter taste sensitivity during starvation in Drosophila. Neuron *84*, 806-820.

Kain, J.S., Zhang, S., Akhund-Zade, J., Samuel, A.D., Klein, M., and de Bivort, B.L. (2015). Variability in thermal and phototactic preferences in Drosophila may reflect an adaptive bet-hedging strategy. Evolution *69*, 3171-3185.

Kaufman, A., Keinan, A., Meilijson, I., Kupiec, M., and Ruppin, E. (2005). Quantitative analysis of genetic and neuronal multi-perturbation experiments. PLoS computational biology *1*, e64.

Kimura, K.D., Fujita, K., and Katsura, I. (2010). Enhancement of odor avoidance regulated by dopamine signaling in *Caenorhabditis elegans*. J Neurosci *30*, 16365-16375.

Ko, K.I., Root, C.M., Lindsay, S.A., Zaninovich, O.A., Shepherd, A.K., Wasserman, S.A., Kim, S.M., and Wang, J.W. (2015). Starvation promotes concerted modulation of appetitive olfactory behavior via parallel neuromodulatory circuits. Elife *4*.

Kodama-Namba, E., Fenk, L.A., Bretscher, A.J., Gross, E., Busch, K.E., and de Bono, M. (2013). Cross-modulation of homeostatic responses to temperature, oxygen and carbon dioxide in *C. elegans.* PLoS Genet *9*, e1004011.

Krashes, M.J., DasGupta, S., Vreede, A., White, B., Armstrong, J.D., and Waddell, S. (2009). A neural circuit mechanism integrating motivational state with memory expression in Drosophila. Cell *139*, 416-427.

Kuhara, A., and Mori, I. (2006). Molecular physiology of the neural circuit for calcineurin-dependent associative learning in *Caenorhabditis elegans.* J Neurosci *26*, 9355-9364.

Laurent, P., Soltesz, Z., Nelson, G.M., Chen, C., Arellano-Carbajal, F., Levy, E., and de Bono, M. (2015). Decoding a neural circuit controlling global animal state in *C. elegans.* Elife *4*.

Lee, S.H., and Dan, Y. (2012). Neuromodulation of brain states. Neuron *76*, 209-222.

Levy, S.F., Ziv, N., and Siegal, M.L. (2012). Bet hedging in yeast by heterogeneous, age-correlated expression of a stress protectant. PLoS Biol *10*, e1001325.

Li, Q., and Liberles, S.D. (2015). Aversion and Attraction through Olfaction. Current Biology *25*, R120-R129.

Li, Z., Liu, J., Zheng, M., and Xu, X.Z. (2014). Encoding of both analog- and digital-like behavioral outputs by one *C. elegans* interneuron. Cell *159*, 751-765.

Macosko, E.Z., Pokala, N., Feinberg, E.H., Chalasani, S.H., Butcher, R.A., Clardy, J., and Bargmann, C.I. (2009). A hub-and-spoke circuit drives pheromone attraction and social behaviour in *C. elegans.* Nature *458*, 1171-1175.

Nevoux, M., Forcada, J., Barbraud, C., Croxall, J., and Weimerskirchi, H. (2010). Bet-hedging response to environmental variability, an intraspecific comparison. Ecology *91*, 2416-2427.

Numan, M., Fleming, A.S., and Levy, F. (2006). Maternal Behavior. Knobil and Neill's Physiology of Reproduction, Vols 1 and 2, 3rd Editon, 1921-1993.

O'Doherty, J., Rolls, E.T., Francis, S., Bowtell, R., McGlone, F., Kobal, G., Renner, B., and Ahne, G. (2000). Sensory-specific satiety-related olfactory activation of the human orbitofrontal cortex. Neuroreport *11*, 893-897.

Omura, D.T., Clark, D.A., Samuel, A.D., and Horvitz, H.R. (2012). Dopamine signaling is essential for precise rates of locomotion by *C. elegans*. PLoS One *7*, e38649.

Padilla, S.L., Qiu, J., Soden, M.E., Sanz, E., Nestor, C.C., Barker, F.D., Quintana, A., Zweifel, L.S., Ronnekleiv, O.K., Kelly, M.J.*, et al.* (2016). Agouti-related peptide neural circuits mediate adaptive behaviors in the starved state. Nat Neurosci *19*, 734-741.

Philippi, T., and Seger, J. (1989). Hedging one's evolutionary bets, revisited. Trends Ecol Evol *4*, 41-44.

Pierce-Shimomura, J.T., Morse, T.M., and Lockery, S.R. (1999). The fundamental role of pirouettes in Caenorhabditis elegans chemotaxis. J Neurosci *19*, 9557-9569.

Ramot, D., Johnson, B.E., Berry, T.L., Jr., Carnell, L., and Goodman, M.B. (2008). The Parallel Worm Tracker: a platform for measuring average speed and drug-induced paralysis in nematodes. PLoS One *3*, e2208.

Rengarajan, S., and Hallem, E.A. (2016). Olfactory circuits and behaviors of nematodes. Curr Opin Neurobiol *41*, 136-148.

Ringstad, N., Abe, N., and Horvitz, H.R. (2009). Ligand-gated chloride channels are receptors for biogenic amines in *C. elegans*. Science *325*, 96-100.

Rios, M., Habecker, B., Sasaoka, T., Eisenhofer, G., Tian, H., Landis, S., Chikaraishi, D., and Roffler-Tarlov, S. (1999). Catecholamine synthesis is mediated by tyrosinase in the absence of tyrosine hydroxylase. J Neurosci *19*, 3519-3526.

Ryan, D.A., Miller, R.M., Lee, K., Neal, S.J., Fagan, K.A., Sengupta, P., and Portman, D.S. (2014). Sex, age, and hunger regulate behavioral prioritization through dynamic modulation of chemoreceptor expression. Curr Biol *24*, 2509-2517.

Saeki, S., Yamamoto, M., and Iino, Y. (2001). Plasticity of chemotaxis revealed by paired presentation of a chemoattractant and starvation in the nematode *Caenorhabditis elegans.* J Exp Biol *204*, 1757-1764.

Satterlee, J.S., Sasakura, H., Kuhara, A., Berkeley, M., Mori, I., and Sengupta, P. (2001). Specification of thermosensory neuron fate in *C. elegans* requires ttx-1, a homolog of otd/Otx. Neuron *31*, 943-956.

Sawin, E.R., Ranganathan, R., and Horvitz, H.R. (2000). *C. elegans* locomotory rate is modulated by the environment through a dopaminergic pathway and by experience through a serotonergic pathway. Neuron *26*, 619-631.

Shingai, R., Ichijo, H., Wakabayashi, T., Tanaka, H., and Ogurusu, T. (2014). Chemotaxis behavior toward an odor is regulated by constant sodium chloride stimulus in *Caenorhabditis elegans*. Neurosci Res *81-82*, 51-54.

Slatkin, M. (1974). Hedging one's evolutionary bets. Nature *250*, 704-705.

Smeets, P.A., de Graaf, C., Stafleu, A., van Osch, M.J., Nievelstein, R.A., and van der Grond, J. (2006). Effect of satiety on brain activation during chocolate tasting in men and women. Am J Clin Nutr *83*, 1297-1305.

Suo, S., Culotti, J.G., and Van Tol, H.H. (2009). Dopamine counteracts octopamine signalling in a neural circuit mediating food response in *C. elegans*. EMBO J *28*, 2437-2448.

Symmonds, M., Emmanuel, J.J., Drew, M.E., Batterham, R.L., and Dolan, R.J. (2010). Metabolic state alters economic decision making under risk in humans. PLoS One *5*, e11090.

Varshney, L.R., Chen, B.L., Paniagua, E., Hall, D.H., and Chklovskii, D.B. (2011). Structural properties of the *Caenorhabditis elegans* neuronal network. PLoS computational biology *7*, e1001066.

Venable, D.L. (2007). Bet hedging in a guild of desert annuals. Ecology *88*, 1086-1090.

Wasserman, S., Salomon, A., and Frye, M.A. (2013). Drosophila tracks carbon dioxide in flight. Curr Biol *23*, 301-306.

White, J.G., Southgate, E., Thomson, J.N., and Brenner, S. (1986). The structure of the nervous system of the nematode *Caenorhabditis elegans*. Philos Trans R Soc Lond B Biol Sci *314*, 1-340.

Chapter 4

Conclusions and future directions

Conclusions:

We have shown that, for the nematode *C. elegans,* the chemosensory stimulus CO_2 is a complex cue that can represent multiple outcomes of mixed valence. Behavioral state, context and experience are all important factors that determine whether CO_2 might signify the presence of food, conspecifics or predators. Correspondingly, the *C. elegans* nervous system must dynamically integrate information about these factors and sculpt the CO_2 microcircuit. We demonstrate that food deprivation shifts the circuit from promoting avoidance to attraction. Unlike other conditions in which worms are attracted to CO_2 (e.g. worms raised in high CO_2 environments), starvation represents a particularly uncertain period. Worms must forage at the expense of predation. Consistently, we find that CO_2 attraction in starved worms is variable. We have identified a neuronal correlate for this behavioral variability. We propose that probabilistic neural activity underlies a bet-hedging population-based behavioral strategy. Having some worms avoid CO_2 while the majority is attracted to it spreads risk over the population and optimizes survival. We also demonstrate that transient changes in neural circuits promote transitions between states. Finally, we demonstrate that multiple food-associated signals act redundantly to promote CO_2 avoidance.

Follow-up experiments:

A neuronal correlate for bet-hedging

To follow up on our model that the probabilistic signaling of AIY neurons promotes behavioral variability, future experiments will image the activity of AIY neurons

in worms moving freely in a CO_2 gradient. If our hypothesis is correct, we predict that, in starved worms moving toward a CO_2 source, AIY neurons would be depolarized whereas in worms moving away from a CO_2 source AIY neurons would be hyperpolarized. Complementing these studies with optogenetic activation of AIY neurons of freely moving worms, a strategy successfully shown to influence other chemotaxis behaviors (Kocabas et al., 2012), could support a link between AIY variability and behavioral variability. Activating the AIY neurons in a population of starved worms exposed to a CO_2 gradient would increase coherence of the AIY signal across animals, and possibly abolish the behavioral variability in CO_2 response that we saw in starved worms. Taken together, these studies could establish a causal link between neuronal variability and behavioral variability in starved worms.

Valence encoded outside of the core circuit motif

We focused on understanding a core circuit motif, which consisted of the RIG and AIY interneurons. RIG acted earlier during the course of food-deprivation to promote CO_2 avoidance whereas AIY acted later on to promote attraction. Although worms with ablation of the AIY neurons showed attenuated attraction, they were still capable of showing attraction, suggesting that there are other neurons besides RIG and AIY that encode valence in fed and starved worms. Prior work in our lab has shown that RIA encodes valence in fed and CO_2-cultivated worms (Guillermin et al., in submission). However, these experiments used a much lower concentration of CO_2, 1%, to assess the effects of RIA. In our study, we chose to use a higher screening concentration, 10%, to isolate neurons that have larger effects on valence. Preliminary work in our lab has demonstrated that another pair of interneurons, the AIA neurons,

promotes CO_2 attraction in food-deprived worms (Yankura et al., in preparation). Worms with AIA neurons ablated fail to shift to CO_2 attraction during food-deprivation. Interestingly, ablating the AIA interneurons does not abolish CO_2 attraction in CO_2-cultivated worms, suggesting that feeding-state encodes valence with a distinct but overlapping set of neurons than CO_2-cultivation environment. The AIA neurons have previously been shown to regulate avoidance of multiple noxious stimuli, and they release an insulin-like peptide, INS-1. Thus, AIA neurons are a likely candidate for modulating valence as a function of feeding state (Chalasani et al., 2010; Cho et al., 2016; Oda et al., 2011; Shinkai et al., 2011). Our preliminary calcium imaging experiments suggest that in fed worms AIA neurons are depolarized by CO_2, consistent with a prior study (Fenk and de Bono, 2015), whereas in starved worms AIA neurons hyperpolarize in response to CO_2, consistent with a model that AIA activity promotes CO_2 avoidance.

Characterizing the locomotor strategy of state-dependent sensory valence

After investigating additional valence-encoding interneurons, we will delve deeper into our worm-tracking data to investigate the types of locomotor strategies underlying CO_2-response valence across different conditions. Previous studies of chemosensation in *C. elegans* have identified two behavioral strategies that worms employ to navigate toward and away from attractive and aversive stimuli, respectively. The biased random walk model states that the absolute direction of worm motion is random, but worms regulate their turning rate and forward locomotion based on whether they perceive increases or decreases in the concentration of chemosensory stimuli. When moving toward an attractive stimulus, worms increase their forward motion and

suppress their pirouettes to continue motion in the same direction (Pierce-Shimomura et al., 1999). When moving away from an attractive stimulus, worms suppress their forward locomotion and increase their pirouette frequency to change their direction. By contrast, in the weathervane strategy, worms actively turn toward attractive chemicals (Iino and Yoshida, 2009). Future studies will determine whether CO_2-response valence uses either or both of these strategies.

We have shown that worms are capable of producing qualitatively different types of CO_2 attraction based on feeding state and CO_2-cultivation environment. A previous study demonstrated that different circuits in fed and starved states encode octanol avoidance (Chao et al., 2004). It is possible that different circuits might give rise to distinct strategies for the same response valence of a given stimulus. We will next determine if CO_2-cultivated and starved worms encode distinct strategies for CO_2 attraction.

Elucidating a circuit mechanisms for salt-dependent modulation of valence

We demonstrated that CO_2 response is modulated by the presence of salt. Future studies will investigate other interneurons in the CO_2 circuit that may encode salt context and modulate CO_2 response. We predict that such neurons would show different CO_2-evoked calcium dynamics when imaged in the absence vs. the presence of salt. Behaviorally, we hypothesize that ablating a neuron required for salt-dependent changes in CO_2 response would abolish salt-dependent changes on behavior, similar to the phenotype of ASE-ablated worms. However, it is also possible that many interneurons could encode salt context redundantly such that no single interneuron would be required. Our behavior results with AIY and RIG suggest that neither neuron

is required for salt-dependent changes in CO_2-response valence; however, we cannot rule out that either neuron plays a contributory role in encoding salt context. We have preliminarily imaged the activity of AIY in different salt contexts, and there does not appear to be a difference in CO_2-evoked activity between these conditions. However, our current imaging conditions may not be optimized to highlight such differences. Future experiments will expand our search to other neurons implicated in the salt circuit, including AIA, AIB and AIZ interneurons (Luo et al., 2014; Tomioka et al., 2006).

Redundant sensory stimuli may coordinate CO_2 avoidance

Given that salt and dopamine, two signals associated with the fed state, redundantly promote CO_2 avoidance, it is likely that other sensory modalities may also encode CO_2-response valence. A previous study implicated the sensory neurons AFD, AWC and ASE in regulating foraging strategy in *C. elegans* (Cohen et al., 2009). These three pairs of neurons converge on the interneuron AIY to regulate its neuropeptide signaling. Given that salt context has a profound effect on the behavior of worms lacking dopamine signaling, it is possible that olfactory and thermal cues, could also interact with dopamine signaling to determine CO_2-response valence. Previous work has shown that temperature (Kodama-Namba et al., 2013) and odors (Carrillo, unpublished) have small, modulatory effects on CO_2 avoidance. However, neither sensory modality has been shown to cause a complete change in CO_2 valence. Future experiments will investigate the role of these different, nutrition-associated sensory stimuli on the behavior of *dat-1::ICE* worms to untangle how multisensory integration informs CO_2-response valence.

As animals navigate through rapidly changing environments, neural circuits must be dynamically sculpted by current behavioral state to integrate multisensory information and drive appropriate behaviors. We provide neuronal correlates underlying behavioral state-dependent changes in valence of the chemosensory stimulus CO_2. These risk-benefit calculations, especially under periods of uncertainty such as starvation, are central to decision-making across all animals, and our results provide fundamental insights into the modulation of neural circuits.

References

Chalasani, S.H., Kato, S., Albrecht, D.R., Nakagawa, T., Abbott, L.F., and Bargmann, C.I. (2010). Neuropeptide feedback modifies odor-evoked dynamics in *Caenorhabditis elegans* olfactory neurons. Nat Neurosci *13*, 615-621.

Chao, M.Y., Komatsu, H., Fukuto, H.S., Dionne, H.M., and Hart, A.C. (2004). Feeding status and serotonin rapidly and reversibly modulate a *Caenorhabditis elegans* chemosensory circuit. Proc Natl Acad Sci U S A *101*, 15512-15517.

Cho, C.E., Brueggemann, C., L'Etoile, N.D., and Bargmann, C.I. (2016). Parallel encoding of sensory history and behavioral preference during *Caenorhabditis elegans* olfactory learning. Elife *5*.

Cohen, M., Reale, V., Olofsson, B., Knights, A., Evans, P., and de Bono, M. (2009). Coordinated regulation of foraging and metabolism in *C. elegans* by RFamide neuropeptide signaling. Cell Metab *9*, 375-385.

Fenk, L.A., and de Bono, M. (2015). Environmental CO_2 inhibits *Caenorhabditis elegans* egg-laying by modulating olfactory neurons and evokes widespread changes in neural activity. Proc Natl Acad Sci U S A *112*, E3525-3534.

Guillermin, M.L., Carrillo, M.A., and Hallem, E.A. (in submission). A single set of interneurons drives opposite behaviors in *C. elegans.*

Iino, Y., and Yoshida, K. (2009). Parallel use of two behavioral mechanisms for chemotaxis in *Caenorhabditis elegans*. J Neurosci *29*, 5370-5380.

Kocabas, A., Shen, C.H., Guo, Z.V., and Ramanathan, S. (2012). Controlling interneuron activity in *Caenorhabditis elegans* to evoke chemotactic behaviour. Nature *490*, 273-277.

Kodama-Namba, E., Fenk, L.A., Bretscher, A.J., Gross, E., Busch, K.E., and de Bono, M. (2013). Cross-modulation of homeostatic responses to temperature, oxygen and carbon dioxide in *C. elegans.* PLoS Genet *9*, e1004011.

Luo, L., Wen, Q., Ren, J., Hendricks, M., Gershow, M., Qin, Y., Greenwood, J., Soucy, E.R., Klein, M., Smith-Parker, H.K.*, et al.* (2014). Dynamic encoding of perception, memory, and movement in a *C. elegans* chemotaxis circuit. Neuron *82*, 1115-1128.

Oda, S., Tomioka, M., and Iino, Y. (2011). Neuronal plasticity regulated by the insulin-like signaling pathway underlies salt chemotaxis learning in *Caenorhabditis elegans*. J Neurophysiol *106*, 301-308.

Pierce-Shimomura, J.T., Morse, T.M., and Lockery, S.R. (1999). The fundamental role of pirouettes in *Caenorhabditis elegans* chemotaxis. J Neurosci *19*, 9557-9569.

Shinkai, Y., Yamamoto, Y., Fujiwara, M., Tabata, T., Murayama, T., Hirotsu, T., Ikeda, D.D., Tsunozaki, M., Iino, Y., Bargmann, C.I.*, et al.* (2011). Behavioral choice between conflicting alternatives is regulated by a receptor guanylyl cyclase, GCY-28, and a receptor tyrosine kinase, SCD-2, in AIA interneurons of *Caenorhabditis elegans*. J Neurosci *31*, 3007-3015.

Tomioka, M., Adachi, T., Suzuki, H., Kunitomo, H., Schafer, W.R., and Iino, Y. (2006). The insulin/PI 3-kinase pathway regulates salt chemotaxis learning in *Caenorhabditis elegans*. Neuron *51*, 613-625.